A Framework For Optimal Biomass-Based Polygeneration Facility Product Allocation

By

Norman Edward Sammons, Jr.

A dissertation submitted to the Graduate Faculty of
Auburn University
in partial fulfillment of the
requirements for the Degree of
Doctor of Philosophy

Auburn, Alabama
December 18, 2009

Keywords: Chemical engineering, process design, biorefinery,
optimization, polygeneration

Copyright 2009 by Norman Edward Sammons, Jr.

Approved by

Mario R. Eden, Chair, Associate Professor of Chemical Engineering
Christopher B. Roberts, Professor of Chemical Engineering
Gopal Krishnagopalan, Professor of Chemical Engineering
Joe B. Hanna, Professor of Aviation and Supply Chain Management

Abstract

Polygeneration facilities, such as the integrated biorefinery, have the opportunity to provide a strong, self-dependent, sustainable alternative for the production of bulk and fine chemicals, e.g. polymers, fiber composites and pharmaceuticals as well as energy, liquid fuels and hydrogen. Although most of the fundamental processing steps involved in these polygeneration facilities are well-known, there is a need for a methodology capable of evaluating the integrated processes in order to identify the optimal set of products and the best route for producing them. The complexity of the product allocation problem for such processing facilities demands a process systems engineering approach utilizing process integration and mathematical optimization techniques to ensure a targeted approach and serve as an interface between simulation work and experimental efforts. The objective of this work is to assist potential and existing polygeneration facilities in evaluating the profitability of different possible production routes and product portfolios while maximizing stakeholder value through global optimization of the supply chain. To meet these ends, a mathematical optimization based framework has been developed, which enables the inclusion of profitability measures and other techno-economic metrics along with process insights obtained from experimental as well as modeling and simulation studies.

Acknowledgements

The project undertaken for this research thesis has involved collaboration not only between academia and industry, but among a vast number of educational disciplines. Due to the broad interdisciplinary nature of this project, many people in many walks of life contributed to the success of the project, and I would like to recognize and thank all of them. First I would like to thank my research committee, Prof. Mario Eden, Prof. Chris Roberts, Prof. Joseph Hanna, and Prof. Gopal Krishnagopalan for their guidance and constructive feedback during the completion of this project. I would also like to thank the expertise of co-authors during my publications and presentations in relation to the project, particularly Prof. Harry Cullinan and Dr. Burak Aksoy. I would especially like to thank Andrew Odjo for his contribution of using novel problem-solving techniques within the project and his uncanny ability to explain complex mathematical algorithms so easily. I would like to thank my coworkers in the North American Mobility Program from Texas A&M University for their assistance in product design, product selection, process synthesis, and process design in respect to biorefining: David Bilhartz, John Pack, and Harsimran Jakhar. I would also like to acknowledge Prof. Paul Stuart, my advisor at Ecole Polytechnique Montreal (EPM) for his guidance and hospitality, as well as my coworkers at EPM for our mutual learning experiences: Virginie Chambost, Tatiana Rafione, Jeremie Cohen, Jose Melendez, Carl Tchoryk, Cindy Wong, Eemeli Hytonen, and Matty Janssen. Finally, I would like to thank all of my office mates and collaborators, both past and present: Dr. Fadwa Eljack, Dr. Jeff Seay,

PE, Rose Marie Cummings Hanks, Jennifer Wilder Kline, Kristin McGlocklin, Charlie Solvason, Nishanth Chemmangattuvalappil, Susilpa Bommareddy, and Wei Yuan for their ability to provide alternative viewpoints needed to tackle the problem from all angles. To each of you – My sincerest thanks.

Table of Contents

List of Tables

List of Figures

Chapter 1

Introduction

Integrated biorefineries, which constitute a subset of a larger class of chemical processing plants known as polygeneration facilities, have shown incredible potential as an alternative to fossil-based feedstocks necessary for the production of chemicals, fuels, pharmaceuticals, and energy. The growing abundance of biorefinery-based chemical process technology has yielded great promise in the use of biomass feedstocks for chemical production that is sustainable on both economic and environmental levels. However, this technological abundance has led to a vast number of process options and possible products, and rules of thumb are insufficient in making decisions on which technologies to pursue in order to enter the polygeneration arena. Thus, a need for a systematic framework exists, in which decision makers in academia and industry will have the tools necessary to evaluate the economic potential of implementing these novel technologies, as well as the relative environmental impact that the uses of these technologies may impart or subtract from the environment.

The methodology developed in this work systematically assists users in determining optimal product portfolios as well as ways in which chemical processes may be improved in order to increase economic sustainability while reducing negative environmental impact. An initial superstructure is first developed that lists the possible product options or feedstock possibilities, as well as the processes necessary to convert feedstocks into salable products.

Simulation models are then developed based on the different feasible process options in the initial superstructure. Through the use of computer-aided molecular design, environmental and safety hazards are abated through the design and use of more benign solvents that perform similarly to existing solvent systems. Mass integration ensures that minimal mass resources are released into the environment by finding the most efficient ways to recover raw materials and finished product, while heat integration focuses on matching heat exchange requirements that will minimize the need for external utility heating and cooling. These optimized simulation models then provide the data necessary to measure the economic potential and environmental impact of the chemical processes involved, and the result is a library of integrated simulation models along with corresponding data and performance metrics.

This library of models and corresponding database of metrics is combined with mathematical optimization to determine the candidate solutions that achieve the highest measure of profitability. Environmental impact is also measured and noted for each candidate for use as a screening tool, as the incorporation of this impact into the profit-based optimization may lead to trivial solutions. If a candidate solution has satisfied both economic and environmental criteria, then the final process design has been determined. However, if any of the criteria are violated, then the economic constraints may be relaxed, or the process is scrutinized to determine if the relative environmental impact can be lowered through minor process modifications. Current results have shown that this framework confirms the results attained through intuition or by hand for limited chemical process systems, and several case studies on potential biorefineries illustrate how optimization is used to solve this problem.

Chapter 2 outlines the fundamental precepts in the fields of process design and synthesis, structural optimization, process integration, economic decision making, environmental impact assessment, and supply chain management necessary to solve the problem on how novel biorefinery technologies may be utilized in a polygeneration facility to maximize added value. This chapter also details what is lacking in state of the art research concerning economic valuation for the purpose of process selection and design and how systematic analysis via optimization may be utilized effectively to evaluate novel polygeneration technologies. Chapter 3 illustrates the methodology in constructing polygeneration allocation problems, as well as the systematic procedures necessary for the solution of this class of problems. Chapter 4 details the use of this methodology in specific case study examples in terms of problem formulation and significant results. Chapter 5 highlights the conclusions developed through the usage of the framework, as well as a detailed plan of action to pursue in order to strengthen and expand this methodology.

Chapter 2

Theoretical Background

2.1 Introduction

The purpose of this research project is to develop a framework for the optimal allocation of available resources within polygeneration facilities in order to realize optimal added value while evaluating and reducing environmental impact. Polygeneration facilities are responsible for converting versatile feedstocks into multiple outputs including electricity, power, and chemical products. As such, fundamentals of process design and synthesis are crucial in order to enumerate the possible pathways and products as well as the capital equipment necessary to maximize the potential added value of the processes. Mathematical optimization is then necessary to measure pre-defined objectives subject to physical and practical constraints. These designed processes must then be refined using heat and mass integration in order to maximize resource usage and minimize utility usage along with environmental impact. Economic valuation must be taken into consideration in order to measure the profitability and added value that these possible polygeneration biorefineries will impart to any given product portfolio. While profitability is indeed critical for a chemical facility to sustain operation, environmental impact must also be estimated for each possible polygeneration plant design. A supply chain management perspective is also needed to ensure that optimality is reached not only for the focal firm, but for upstream and downstream supply chain members, resulting in economic and environmental synergy. This

perspective is also necessary to evaluate the potential of polygeneration products to serve as platform chemicals for additional value-added chemical products. The end result of this project is a methodology that can be applied in a flexible fashion to critique and improve upon new polygeneration and biorefining technologies and reach decisions that meet both shareholder and stakeholder objectives for all relevant members of the supply chain.

2.2 Polygeneration

Polygeneration is defined as the integrated production of three or more outputs, in the form of tangibles such as liquid fuels and chemicals, or intangibles such as electricity, heat, or other services, produced from one or more natural resources (POLYSMART, 2008). Polygeneration may be viewed as an extension upon traditional cogeneration facilities in which power and heat in the form of process steam are generated within the same facility. Cogeneration is the production of two products or services, while polygeneration can be broken down into subcategories of trigeneration and quadgeneration in which three or four products and services may be developed from the same feedstock. In addition to producing electricity and heat, trigeneration and quadgeneration facilities may also produce one or two additional products respectively, such as methanol, dimethyl ether, Fischer-Tropsch liquids, and syngas to be used as town gas for nearby residential and commercial users (Williams, 2000). By pursuing a polygeneration strategy, lower capital costs and lower product/energy costs will be realized in comparison to building separate cogeneration and chemical product facilities (Williams, 2000).

The concept of polygeneration may also be expanded to include other pathways that may provide a wide variety of chemicals, fuels, and services. An alternative form of

trigeneration results in the production of heat via process steam, power from on-site turbines, and refrigeration by supplying heat to absorption or adsorption chillers. Gasification systems provide similar heat and refrigeration capabilities through the production of syngas while producing residual fly ash to be used in construction. Similarly, biogas systems utilize biological pathways to produce nitrogen-based fertilizers as well as methane-rich biogas that can be used in heat and power generation. Bioethanol polygeneration systems result in the coproduction of ethanol and process steam, as well as a solid byproduct known as distiller's dry grains with solubles, or DDGS. Polygeneration-based services include the desalination and purification of water and the production of CO_2 for use in nearby greenhouses to encourage plant growth (POLYSMART, 2008). While many of these polygeneration concepts demonstrate a great deal of potential in maximizing value from natural resource utilization, the vast number of possible polygeneration options and the lack of a systematic methodology to evaluate the added benefits, incurred costs, and environmental impacts of these options may lead to the pursuit of sub-optimal process and product decisions.

2.3 Process Design and Synthesis

The goal of chemical engineering is to add value by developing, optimizing, and utilizing processes and products aimed at converting raw or intermediate materials and energy into useful materials that fulfill a societal need (Douglas, 1988). Product design refers to the formulation of an innovative chemical or mixture, or realization of an existing chemical or chemical mixture that has desired properties and performance while solving a societal problem (Seider, Seader et al., 2004). The development of chemical processes designed to produce these products is more commonly known as process design, which is the

generation of process ideas and subsequent translation into equipment and methods necessary to add chemical value (Douglas, 1988). In preliminary process design, a conceptual flowsheet is developed for a particular chemical process (Biegler, Grossmann et al., 1997). Conceptual process design can be divided into five main decision levels (Douglas, 1988):

- Batch versus continuous
- Input-output structure of the flowsheet
- Recycle and reactor structure of the flowsheet
- Separation system synthesis
- Heat exchanger networks

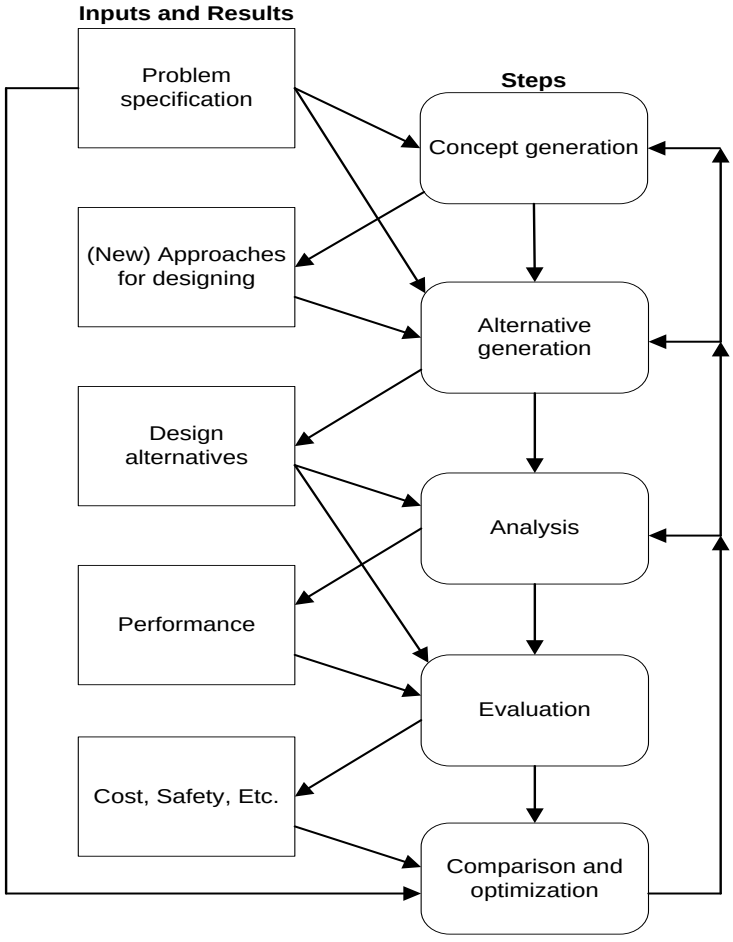

Figure 2.1 – The steps of process synthesis (Biegler, Grossmann et al., 1997).

Whereas the preliminary process design step will result in an abstract description of the chemical process, process synthesis involves refining the abstract ideas into a more concrete process description. The steps of process synthesis are illustrated in Figure 2.1. The first step of process synthesis is to generate the main overall concepts on which to base the refined process design, which includes specifying an overall design strategy and deciding whether or not to develop proprietary processes, utilize turnkey solutions, or a combination of both. Next, the generation of alternative reaction pathways, while maintaining the same general chemistry determined by the initial process design stage, involves scanning sources of alternative design ideas, brainstorming to develop original design processes, and questioning these alternatives in order to find the best process design ideas, which can be illustrated in the form of a synthesis tree as in the top branch of Figure 2.2 (Biegler, Grossmann et al., 1997; Seider, Seader et al., 2004).

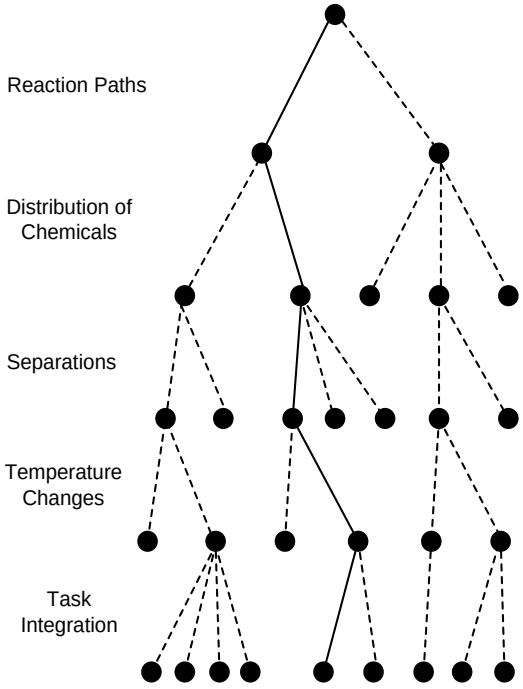

Figure 2.2 – Example of synthesis tree and design selection (Seider, Seader et al., 2004).

The subsequent analysis step establishes how each alternative idea performs, and this requires construction of base case simulation models of the most attractive alternatives in order to develop mass and energy balances and flowrate, temperature, and pressure data. The evaluation step is used to determine the economic value of each simulated process idea, as well as measure the environmental impact and process flexibility of the generated alternatives. Finally, these alternative process ideas are optimized and integrated in order to hone these designs, and these optimized processes are compared amongst each other (Biegler, Grossmann et al., 1997). The strongest process designs are then given further consideration, and the process synthesis step begins anew with fewer options and more attention to detail and task integration. The synthesis tree in Figure 2.2 illustrates the synthesis steps from the generation of alternative reaction paths, through the development of the base case designs and respective optimizations, to the selection of the optimal design (Seider, Seader et al., 2004).

2.4 Structural Optimization

Optimization is defined as a problem-solving methodology in which the most effective solution of a mathematical representation of a chemical process or system is determined, and this optimal solution is subject to system constraints. This is done by maximizing or minimizing an objective function, which is a numerical indicator of the positive or negative system qualities respectively (Biegler, Grossmann et al., 1997). This objective function is an implicit or explicit function of problem variables, and/or decision variables, and values of this objective function are obtained via manipulation of these variables. Although trial and error may result in the discovery of the optimal solution,

systematic methods have been developed that reduce the complexity and time necessary to solve these problems. Mathematical programming is the act of converting the process or system in question into an objective function and constraints in order to be solved through computational methods (Biegler, Grossmann et al., 1997).

2.4.1 General optimization

The four main classes of optimization problems are linear problems (LP's), nonlinear problems (NLP's), mixed integer linear problems (MILP's), and mixed integer nonlinear problems (MINLP's). Throughout this text, examples of optimization problems will be illustrated for discussion purposes, and optimization problems as a whole typically have one or more objective functions to be maximized or minimized, and these problems are subject to one or more classes of constraints. While these problems will appear as a combination of expressions, equations, and inequalities, each individual optimization problem will hereby be referred to as a Problem, followed by the chapter number and the order of appearance of the problem in the chapter. Linear problems (LPs) refer to the type of optimization problems in which the objective function and constraints are all linear, and these problems take the general form of Problem P2.1 (Biegler, Grossmann et al., 1997):

$$Minimize\ Z = c^T x \tag{P2.1}$$

$$s.t.\ Ax \leqq a$$

$$x \geq 0$$

where Z is the objective function, c^T represents the vector of coefficients that correspond to the decision variables x in the objective function, A corresponds to the vector of coefficients corresponding to x in the constraints, and a represents the vector of constraint values. The

sign in the constraint equation indicates that constraints can be inequalities and/or equalities. Linear problems are solved by the simplex algorithm, which is based on the fact that the globally optimal solution lies on a vertex of the solution space as defined by the linear constraints (Biegler, Grossmann et al., 1997).

Mixed integer linear problems (MILPs) also have a linear objective function and linear constraints, but these problems have a higher degree of complexity due to the introduction of binary variables. Binary variables have values of 0 or 1 only and take on the form in Problem P2.2 (Biegler, Grossmann et al., 1997):

$$Minimize\, Z = \ a^T y + \ c^T x \qquad \text{(P2.2)}$$

$$s.t. By + Ax \ \leqq b$$

$$y \ \in \{0,1\}^t$$

$$x \geq 0$$

where y represents a vector of t binary variables. A brute-force method would involve solving each LP for every combination of binary variables, but this is computationally expensive since there are 2^t possible combinations. A more effective way to solve this class of problem is known as the branch-and-bound technique. The problem is first relaxed, or reformulated so that the variables in y are no longer binary, but continuous between 0 and 1. At this point, y variables that contain non-integer values are then set one at a time to 0 or 1, and the resulting subproblems are now known as nodes. The relaxed LP is once again solved to determine which objective value contains a lower value, and the process continues until there is no further improvement in the objective function (Biegler, Grossmann et al., 1997).

Nonlinear problems (NLPs) involve objective functions and constraints that may be linear and/or nonlinear, and this class of problems is generally represented by Problem P2.3 (Biegler, Grossmann et al., 1997):

$$Minimize\ f(x) \tag{P2.3}$$

$$s.t.\ h(x) = 0$$

$$g(x) \leq 0$$

$$x \geq 0$$

where *f(x)*, *g(x)*, and *h(x)* may be linear and/or nonlinear functions. The two main methods used for solving nonlinear problems are successive quadratic programming (SQP) and the reduced gradient method. In the SQP method, values of *x* are chosen, and a step value is added to *x* before each iteration until a feasible, minimal solution is found. This method involves determining the Lagrange function, or Lagrangian, of the objective function, which takes the following form:

$$L(x, \mu, \lambda) = f(x) + g(x)^T \mu + h(x)^T \lambda \tag{2.1}$$

where *f(x)* is the original objective function, *g(x)* and *h(x)* represent the set of inequality and equality constraints respectively, and μ and λ are known as shadow prices, which are the changes in the objective function by relaxing its respective constraints by one unit. The Hessian, or second partial derivative matrix, of the Lagrangian of the problem, is then used to develop a series of quadratic problems that result in fewer calculations and faster solution of the problem in comparison with the reduced gradient method. In the reduced gradient method, iterative sequences of subproblems with linearized constraints are solved, and this method is most efficient for problems with a large number of linear constraints and the availability of analytical derivatives of nonlinear functions. While these tools are indeed

powerful in solving NLPs, neither one can guarantee that the local solution they find is indeed the global solution unless the problem is completely convex and differentiable (Biegler, Grossmann et al., 1997).

The class of problems that is most difficult to solve combines binary variables with nonlinear functions in mixed integer nonlinear problems, which by definition are NP-hard, or not able to be solved in polynomial time, and thus very computationally expensive. Problem P2.4 illustrates the general format of MINLP's (Biegler, Grossmann et al., 1997):

$$Minimize\ Z = c^T y + f(x) \tag{P2.4}$$

$$s.t.\ h(x) = 0$$

$$g(x) \leq 0$$

$$Ax = a$$

$$By + Cx \leq d$$

$$Ey \leq e$$

$$x \in X = \{x \mid x \in R^n, x^L \leq x \leq x^U\}$$

$$y \in \{0,1\}^t$$

where x is a member of the set of real numbers but also bounded by lower and upper limits in the form of x^L and x^U respectively. The branch and bound method used for MILP's may also be used for MINLP's, but the major drawback is that the NLP subproblems are more computationally expensive than the LP subproblems found in MILP's.

The two major methods to solve MINLP's are Outer-Approximiation (OA) and Generalized Benders Decomposition (GBD). Figure 2.3 demonstrates the general strategy that is executed in both of these methods. In the OA method, an alternating sequence of NLP subproblems and MILP master problems are solved in which the NLP subproblems are

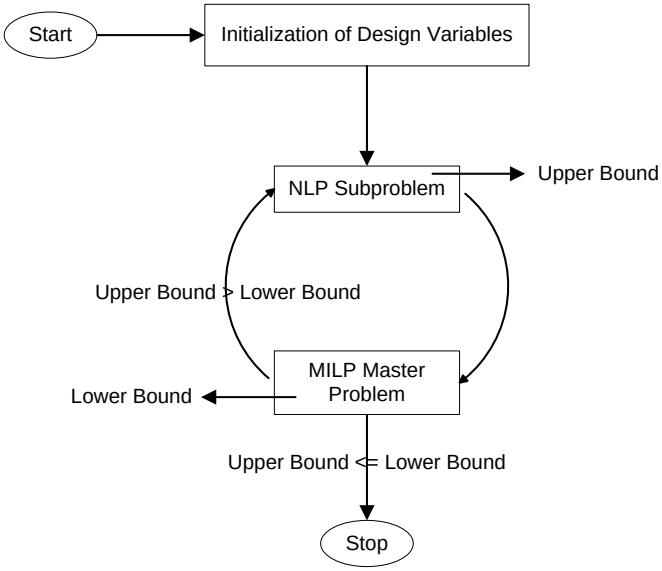

Figure 2.3 – Flowsheet of strategy used for MINLP optimization (Diwekar, 2003).

solved for a fixed choice of binary variables as determined by the linear approximation given by the master problem. To reduce the computational expense associated with the NLP subproblems, the equality constraints are relaxed into inequalities. The master problem accumulates all of the linear approximations of previous iterations in order to determine increasingly better approximations of the overall MINLP problem, and the iterations terminate when no lower bound can be found below the current best upper bound. The Generalized Benders decomposition follows a similar strategy, with the only difference being that the linearization of the MINLP is replaced with the largest Lagrangian approximation obtained from the NLP subproblems (Biegler, Grossmann et al., 1997).

2.4.2 Genetic algorithms

Genetic algorithms (GA's) refer to a probabilistic combinatorial method used to solve optimization problems (Diwekar, 2003). GA's are search algorithms based on evolution and natural selection in which the best solutions, both whole and in part, are combined in a

random yet structured fashion in order to discover increasingly effective solutions. Each possible solution to an optimization problem is known as a chromosome, and these chromosomes are composed of genes, which are representations of binary decision variable values. Chromosomes are grouped into sets of solutions known as populations, and generations refer to the group of populations that are generated after each full cycle of the algorithm (Diwekar, 2003). Chromosomes also store information such as termination criteria, overall ranking compared to other solutions in all generations, and its objective value when the chromosome is applied to the objective function of the optimization problem (Michalewicz, 1996). It should be noted here that a variation of genetic algorithm known as genetic programming, in which the chromosomes are not fixed in length, uses dendriform code in order to determine the length of the chromosome, resulting in increased problem solving flexibility (Wang, Li et al., 2008).

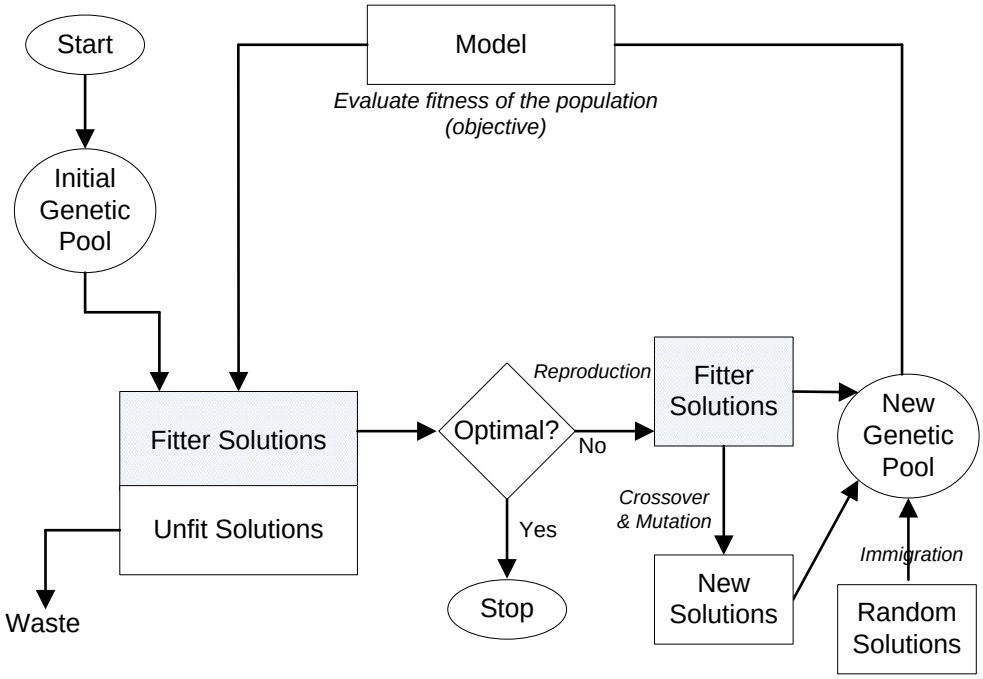

Figure 2.4 – Strategy pursued in genetic algorithm approach to optimization (Diwekar, 2003).

According to Figure 2.4, the first step of the genetic algorithm method is the development of the initial generation of solution sets, which can be created randomly or heuristically. Future generations may then be produced via a randomized selection procedure, which is composed of four possible operations. Reproduction is the process in which chromosomes are copied according to their desirable performance on the objective function, or fitness, and higher fitness of the string improves its chances of being carried on into the next generation. Crossover refers to the process in which two parent solution strings randomly exchange parts to generate two child solution strings in the next generation, and if the parts being exchanged result in higher desired performance levels, then this will focus the algorithmic search to chromosomes in the same general search space. Mutation is the random selection and changing of a gene in a chromosome, and immigration is an alternative to mutation in which new solution strings of high fitness and little similarity to existing solutions are added into future generations (Diwekar, 2003). These genetic functions may also be combined with one another in order to expedite the process of uncovering the optimal solution, and one example of a hybrid genetic function combines crossover with mutation, in which the offspring chromosomes bear an inexact yet structural relationship to two parent chromosomes, exploiting the portions of the parent chromosomes resulting in optimal fitness (Michalewicz, 1996). Termination of the genetic algorithm may be triggered by fixing the total number of generations to be evaluated, or by discovering an approximate solution in which no noticeable improvement occurs in subsequent generations (Diwekar, 2003).

2.4.3 Generalized Disjunctive Programming

Logical disjunctions sometimes play a significant role in defining constraints for optimization problems as well as defining the impact of decisions on objective functions. Disjunctions involving continuous variables must be treated in a different way than traditional optimization problems. Generalized disjunctive programming refers to the usage of logic-based disjunctions in optimization and the solution of those problems, and these problems take on the form (Türkay and Grossmann, 1996):

$$minimize\ Z = \sum_i c_i + f(x) \tag{P2.5}$$

$$s.t. \quad g(x) \leq 0$$

$$\begin{bmatrix} Y_i \\ A_i x \leq b_i \\ c_i = \gamma_i \end{bmatrix} \vee \begin{bmatrix} -Y_i \\ B^i x = 0 \\ c_i = 0 \end{bmatrix} \qquad i \in D$$

$$\Omega(Y) = True$$

$$x \in R^n, \qquad c \geq 0, \qquad Y \in \{True, False\}^m$$

where c_i is a continuous variable used to represent fixed costs associated with existing units, Y_i are Boolean true/false variables associated with the existence of process units, D is the set of logical disjunctive terms, and $\Omega(Y)$ is the combined group of Boolean variables. If a given Y_i is true, then corresponding process unit i exists, constraints $h_i(x) \leq 0$ become active, and the fixed charge of the unit c_i takes on the value of γ_i. If Y_i is false, then the unit does not exist, and a subset of the continuous variables x and fixed charge c_i are set to zero (Türkay and Grossmann, 1996).

For smaller disjunctive programming problems, the disjunctions in Problem P2.5 are converted into mixed-integer variables through the use of Big-M constraints, which are given as follows (Biegler, Grossmann et al., 1997):

$$A_i x \leq b_i + M_i(1 - y_i) \qquad i \in D \tag{P2.6}$$

$$\sum_{i \in D} y_i = 1$$

$$y_i = 0,1 \qquad i \in D$$

While the second and third constraints of this equation reinforce that the decision variables y_i are binary and that only one will be active for each disjunctive term, the first set of constraints utilizes a large value of M, which will make the inequality redundant and the constraint inactive if y_i is 0 and will only enforce the inequality if y_i is 1. The use of big-M constraints is indeed a simple way to handle GDP problems, but large values of M will cause weak relaxations for the objective function when the y_i variables are treated as continuous instead of binary (Biegler, Grossmann et al., 1997).

Larger problems will require a tighter relaxation of the objective function in order to find an optimal solution, and this relaxation comes about through convex hull formulation. Instead of converting the disjunctive terms into big-M constraints, the continuous variables x are disaggregated into as many new variables z_i as there are terms for the disjunctions. The following format illustrates this use of convex hull formulation (Biegler, Grossmann et al., 1997):

$$x = \sum_{i \in D} z_i \tag{P2.7}$$

$$A_i z_i \leq b_i y_i$$

$$\sum_{i \in D} y_i = 1$$

$$0 \leq z_i \leq U y_i$$

$$y_i = 0,1 \qquad i \in D$$

The first constraint splits up the continuous variables into disaggregated variables corresponding to disjunctive terms. The second constraint restates the disjunctive constraints into constraints that only deal with disaggregated and binary variables, and the fourth constraint applies only if $y_i = 0$ does not imply $z_i = 0$. This reformulation results in a much tighter LP relaxation, but at the expense of a much larger number of variables and constraints (Biegler, Grossmann et al., 1997).

In the case of nonlinear constraints and/or a nonlinear objective function, both the big-M and convex hull methods may not solve the problem within a reasonable amount of computing time. Similar to the difference in solving MILP's and MINLP's, nonlinearities require much more powerful solution methods. As stated above, Outer Approximation and Generalized Benders Decomposition have shown to be quite useful in solving regular MINLP problems, and logic-based variations of these two methods are commonly used to solve disjunctive MINLP problems (Türkay and Grossmann, 1996). A similar iterative approach of solving a master problem and subproblems is also utilized in disjunctive problems. In Logic-Based Outer Approximation, the disjunctive problem is reformulated as an MILP master problem by linearizing the objective function and constraints, and logic relations are converted into integer inequalities in the process. NLP subproblems are formed by fixing the Boolean variables predicted by the master problem, and the upper and lower bounds calculated by the master problem and subproblems are compared to determine if the solution has been found. If the solution has not been found, the values from the NLP subproblem are fed into the master problem, and the cycle begins anew (Türkay and Grossmann, 1996). This method is used in software known as LOGMIP, which solves optimization problems involving disjunctions and binary variables (Vecchietti and

Grossmann, 1999). Again, the difference between Logic-Based Outer Approximation and Generalized Benders Decomposition is that the Lagrangian is used in GBD instead of linearization (Türkay and Grossmann, 1996).

2.5 Process Integration

Process designs are optimized through process integration, which is a holistic approach to process design in which the entire chemical process is addressed before specifying the details of the process. This mindset is counterintuitive to traditional engineering problem-solving and practice where engineers instinctively use a bottom-up approach in which the details of the process are handled before making large-scale decisions dealing with the system as a whole (El-Halwagi and Spriggs, 1998). Process integration does not deal with local optimization of each unit operation of a process, but focuses on overall optimization of the process even if local unit operations are suboptimal.

The process integration approach is fundamentally different from traditional engineering problem-solving in many ways. First, the problem must be constructed as it pertains to the entire process, and then the overall system problem is broken down into subproblems that will define the focus of the engineer and dictate the skills and tools necessary to solve the problem. Next, the development and pursuit of quantitative performance targets will guide the problem solving process so that only design pathways that achieve the specified targets will be considered as part of the optimal solution. Solution fragments are then developed that represent feasible solutions in which performance targets are met, and these fragments are finally pieced together to form integrated solutions. These integrated solutions are composed of various combinations of solution fragments and are

individually critiqued until the optimal integrated solution is determined (El-Halwagi and Spriggs, 1998).

2.5.1 Energy Integration

Energy integration, also referred to as heat integration, is defined as a systematic methodology in which energy targets are identified for the purpose of optimizing energy recovery and utility systems (El-Halwagi, 2006). Heat integration involves the minimization of operating and/or capital costs for heating and cooling systems by utilizing proven mathematical techniques to maximize the amount of energy transferred between process streams while minimizing or even negating the use of external heating and cooling utilities. This optimization is achieved through the synthesis of heat exchange networks (HEN's), in which one or more heat exchangers are used to match hot streams with cold streams for the purpose of the efficient exchange of energy. The synthesis of HEN's will assist the process designer in answering the following questions (El-Halwagi, 2006):

- Which heating/cooling utilities should be used, if any?
- What is the optimal heat load removed or added by these utilities?
- How should the hot and cold process streams be matched?
- What is the optimal system configuration in terms of arrangement, stream splitting, and stream mixing?

To perform heat integration in an effective manner, it is first necessary to identify the process streams with heating and cooling needs in terms of input temperature, target temperature, mass flowrate, and heat capacity. Streams that require cooling are then categorized as hot streams, while streams in need of heat are labeled as cold streams. At this

point, various techniques may be utilized to pursue heat integration. The graphical technique involves constructing hot and cold composite streams that represent all of the process streams in need of heat exchange, and plotting these streams against each other. A minimum temperature difference must be determined in order to assure optimal heat exchange without the need for oversized heat exchangers, and this temperature difference may not be violated with any heat exchanger match. Once these composite streams are graphed in terms of temperature versus amount of heat to be exchanged, as done in Figure 2.5, one can determine the theoretical pinch point at which the minimum temperature difference is realized.

The thermal pinch occurs at the point where the minimum difference between the hot and cold composite streams is the minimum temperature difference. In Figure 2.5, the cold stream temperature scale, denoted by *t*, is merely the hot stream temperature minus the minimum temperature difference, in which case the pinch point occurs when the hot and cold

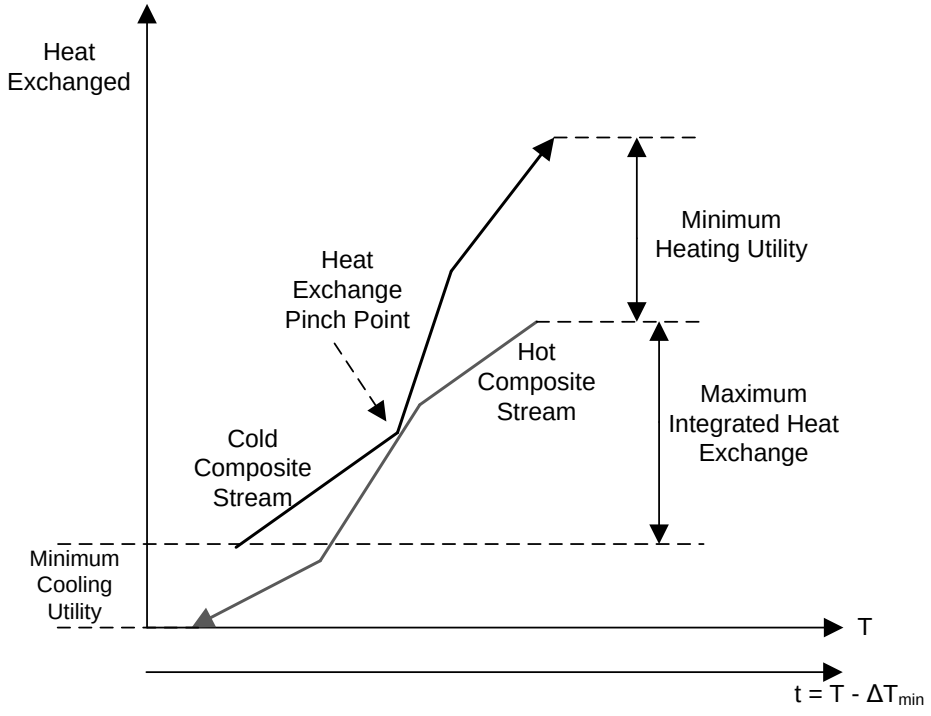

Figure 2.5 - Hot and cold composite diagram example (El-Halwagi, 2006).

streams meet graphically (El-Halwagi, 2006). The problem should then be divided at the pinch point into subproblems for the regions above and below the pinch point, and these subnetworks should be designed by starting at the pinch and moving away (Linnhoff, Townsend et al., 1994). After identifying the pinch, the HEN can be designed based on three rules which will result in minimal external utility cost (Linnhoff, Townsend et al., 1994; El-Halwagi, 2006):

- Heat may not be transferred across the pinch, as this results in a twofold penalty in both heating and cooling utilities.
- External cooling utilities may not be used above the pinch since there are excess cold process streams available for cooling in this region for little or no cost. This can also be considered to be the heat sink region since heat flows into the area above the pinch.
- External heating utilities may not be used below the pinch since there are excess hot process streams available for heating in this region for little or no cost. This can also be considered the heat source region since it supplies heat to the area above the pinch.

Another tool used in designing HEN's involves constructing a temperature interval diagram to be used in combination with a table of exchangeable heat loads in order to form a heat cascade diagram. Figure 2.6 illustrates the heat integration versions of a temperature interval diagram, while Figure 2.7 demonstrates the heat cascade diagram. First, a Temperature Interval Diagram (TID) is constructed where the hot streams and cold streams are drawn in the form of vertical arrows, and the placement of these arrows depends on its corresponding temperature in relation to the other arrows in the system. Horizontal intervals are constructed that denote the corresponding temperatures of the heads and tails of each

arrow, as shown in Figure 2.6 (El-Halwagi and Manousiouthakis, 1989). A Table of Exchangeable Loads (TEL) is then established which will determine the amount of energy exchanged among the process streams at each temperature interval, and these loads are calculated through the use of energy balance equations. Since negative heat flow is thermodynamically impossible, the absolute value of the most negative heat flow in the heat cascade diagram must be added to the first interval, which corresponds to the minimum heating utility requirement. The point in which zero heat is transferred between intervals corresponds to the pinch point, and the heat leaving the final interval represents the minimum cooling utility required (El-Halwagi, 2006).

The Temperature Interval Diagram shown in Figure 2.6 may be used to develop an optimization program to solve the HEN synthesis network problem. The optimization problem uses these temperature intervals defined in the diagram, and possibly additional interval ranges, to determine possible areas for process streams and utility streams to

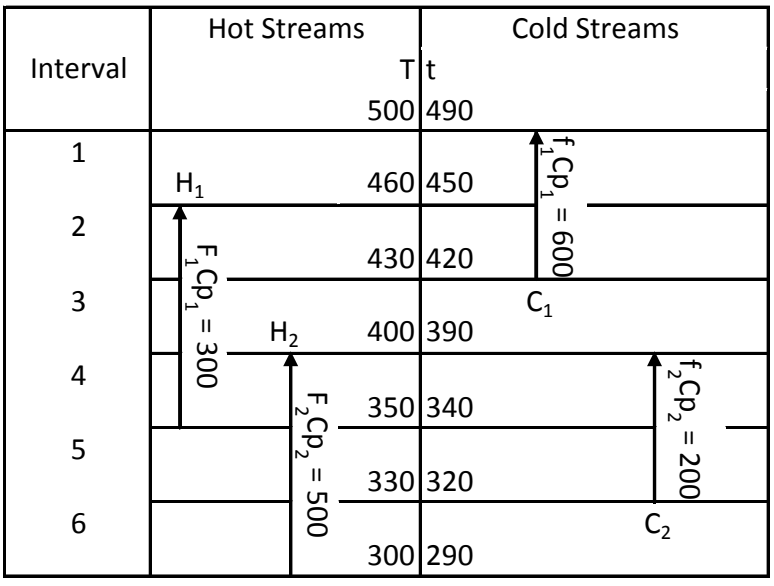

Figure 2.6 – Example of a Temperature Interval Diagram (El-Halwagi, 2006).

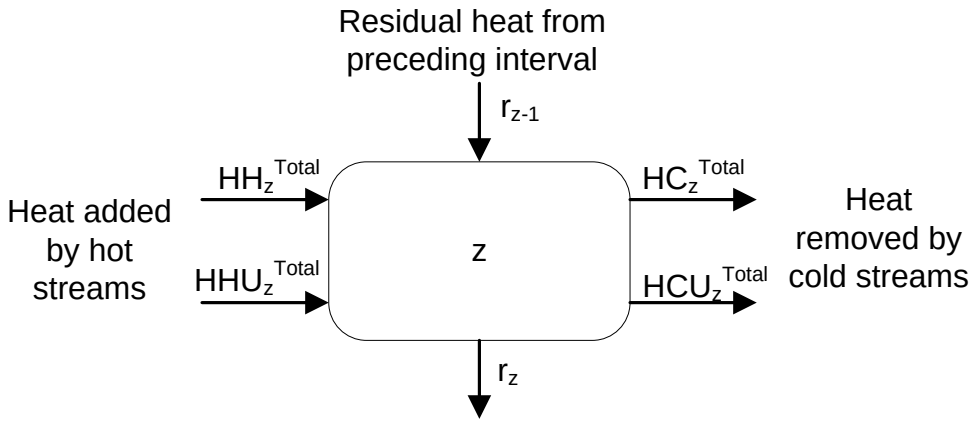

Figure 2.7 – Illustration of single level of heat cascade diagram (El-Halwagi, 2006).

exchange heat. An objective function must be determined, and in this example, the objective function is the minimization of cost of heating and cooling utility:

$$Minimize \sum_{u=N_H+1}^{N_H+N_{HU}} CH_u \times FU_u + \sum_{v=N_C+1}^{N_C+N_{CU}} CC_v \times fU_v \qquad \text{(P2.8a)}$$

where u and v represent the indices of hot and cold process/utility streams respectively, CH_u and CC_v represent the cost of hot and cold utilities per mass, and FU_u and fU_v represent the mass flow rate of hot and cold utilities (El-Halwagi, 2006). This objective function is subject to heat balance constraints:

$$HH_z^{Total} - HC_z^{Total} = HHU_z^{Total} - HCU_z^{Total} + r_{z-1} - r_z,\ z = 1,2,\dots,n_{int} \qquad \text{(P2.8b)}$$

where HH_z^{Total} and HC_z^{Total} represent the total hot and cold process streams that exist in each interval z, HHU_z^{Total} and HCU_z^{Total} represent the total hot and cold utility streams that exist in each interval z, and r_{z-1} and r_z represent the residual heat leaving and entering interval z as shown in Figure 2.12 (El-Halwagi, 2006). This optimization problem is also subject to constraints on non-negativity, thermodynamic feasibility, definitions of heating loads and

cooling capacities, and temperature scales based on minimum approach temperature, which are not shown for simplicity (El-Halwagi, 2006).

Because of the possible complexity of using this type of optimization to design heat exchange networks, these synthesis problems may be split into two main categories. Sequential synthesis involves dividing the problem into subproblems based on pinch points and/or temperature intervals, while simultaneous synthesis solves the problem without this decomposition. Sequential synthesis may be further classified by the type of objective function that is optimized: minimum utility usage or cost, minimum number of exchange units, or minimum capital cost as a function of total heat exchanger area. Sequential HEN synthesis problems can be solved either by evolutionary methods or mathematical programming, while simultaneous synthesis mainly relies on the latter, particularly mixed-integer nonlinear programming (Furman and Sahinidis, 2002).

Another vital tool in heat integration involves screening different external utilities that can be used once all the process streams have been utilized to meet heating and cooling demands. A grand composite curve (GCC), as shown in Figure 2.8, can be constructed directly from the heat cascade diagram, starting from the minimum heating utility going into the first interval and transcending all the way down to the minimum cooling utility in the last interval. The triangles on the GCC represent areas of heat integration in which process streams are used to satisfy heating and cooling demands, and the enthalpy gap between the y-axis of the GCC and the dotted line of the triangles are satisfied through external cooling and heating utilities. As stated before, heating is used above the pinch while cooling is used below the pinch, and the least expensive utilities in terms of cost per unit of energy should be used for the largest enthalpy gaps (El-Halwagi, 2006).

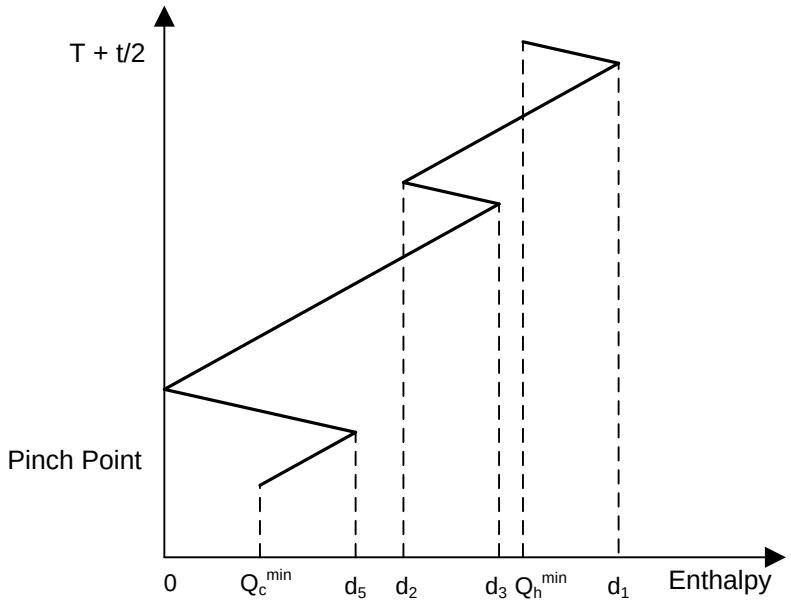

Figure 2.8 – Construction of grand composite curve (El-Halwagi, 2006).

Various issues add to the complexity of heat integration, such as scenarios in which a threshold temperature difference greater than ΔT_{min} exists. This threshold temperature difference, or ΔT_{thr}, eliminates either heating or cooling while avoiding constraints at the pinch, which may result in problem slack and, consequently, multiple optimal designs. Stream splitting may also need to be taken into consideration if there are not enough hot or cold streams to provide matches that satisfy the problem or if the heat capacity of a stream is not sufficient to satisfy heating and cooling requirements in a maximum energy recovery system. Forbidden and imposed matches may be required for safety or practicality reasons, which will result in additional usage of heating and cooling utilities above and beyond the optimal unrestricted problem (Linnhoff, Townsend et al., 1994). Finally, there may be isothermal process streams in which latent heat is transferred as a result of a phase change, such as in refrigeration and separation. There are methods available to take the latent heat

transfer into consideration for both isothermal and nonisothermal process streams when designing heat exchanger networks (Ponce-Ortega, Jimenez-Gutierrez et al., 2008).

Certain tradeoffs must be made in consideration to designing HEN's. For example, reducing the minimum allowable temperature difference will result in less external heating and cooling utility, but will result in larger heat exchanger areas due to decreased driving force. There is also a tradeoff between energy and capital in which the increase in the number of heat exchanger matches will increase energy recovery at the cost of more heat exchangers. In the case of matching different external utilities, the increase in options, such as variable temperature utilities, leads to an increase in network complexity, which will incur lower energy costs at the expense of increased capital investment. While energy usage reduction is important in the field of heat integration, one must consider the systematic impact of HEN's on an overall economic objective such as total annualized cost or profitability over plant life, and not just energy cost alone or design productivity (Hesselmann, 1984; Linnhoff, Townsend et al., 1994).

Many methods are available in which heat exchange networks can be designed and optimized. Superstructures are sometimes generated to illustrate all feasible possibilities, and these possibilities are then systematically explored in order to determine which configuration or network results in optimal operation (Floudas, Ciric et al., 1986; Colmenares and Seider, 1987; Asante and Zhu, 1996; Konukman, Camurdan et al., 1999; Wang, Qian et al., 1999; Kovabvc-Kralj, Glavibvc et al., 2000). Disjunctive programming has been used as an alternative formulation of traditional mathematical programming in which logical constraints are reformulated into an MINLP in order to devise the optimal heat exchanger network (Grossmann, Yeomans et al., 1998).

In addition to superstructure generation and disjunctive programming, evolutionary search methods are often used to design heat exchanger networks, specifically in sequential synthesis problems. Genetic algorithms have been used to design effective heat exchange networks in which the objective function may be minimized in terms of capital cost, utility cost, or a combination of the two. In this particular usage of genetic algorithm, chromosomes are composed of possible heat exchanger matches, splitting of streams, and/or activation of external heating and cooling utilities (Androulakis and Venkatasubramanian, 1991; Lewin, Wang et al., 1998; Wang, Qian et al., 1999; Yu, Fang et al., 2000). One specific example of a genetic algorithm is differential evolution, which is another form of evolutionary search in which the chromosomes indicate and store the location of splits and matches between hot and cold streams, as well as outlet temperatures and heat loads. Similar to other genetic algorithms, mutation and recombination algorithms are then used to produce the next generation of chromosomes until the optimal solution is found, and this method has shown improvement in case study problems over existing methodologies (Yerramsetty and Murty, 2008).

One example of how targeting and heat exchanger network design may be executed with computational assistance is through a software package known as HX-Net, created by Aspen Technology (2006). This simulation software is used to synthesize heat exchange networks by using the aforementioned algebraic and optimization-based targeting methods. Ultimately, options are identified in terms of suggested heat exchange networks in order to assist the user in understanding and reducing the gap between current and optimal operation. The user may also select whether to optimize energy recovery, number of units, total exchanger area, or total annualized fixed cost and may compare different options to each

other both for new plant designs as well as retrofit designs. The use of this design tool helps ensure that a new or revamped plant will achieve optimal energy recovery and usage.

2.5.2 Mass Integration

Mass integration is defined as the problem-solving methodology in which a global understanding of mass flow within a given process is used in identifying performance targets, optimizing mass generation, and allocating species of mass throughout the process (El-Halwagi, 1997). Mass integration has the twofold goal of pollution prevention and resource conservation since it can be used to reduce contaminants in effluent streams as well as facilitate recycling and reusing valuable raw or intermediate materials. While the motivation for heat integration lies in controlling rising energy costs, mass integration has grown in importance due to increased focus on environmental impact and raw material recovery.

Mass integration is analogous to heat integration in many ways. Instead of heat being transferred from a hot stream to a cold stream, mass is transferred from rich to lean composite streams. The driving force in mass integration is the minimum allowable composition difference, in comparison to the minimum temperature difference in heat exchange (El-Halwagi, 2006). Many of the graphical, algebraic, and optimization-based methods used for heat integration can also be used with slight modification to design mass exchange networks, or MEN's.

Waste reduction in a process can be achieved by following four strategies, which are ranked in order of increasing effectiveness: disposal, end-of-pipe treatment, recycle and reuse, and source reduction. Mass integration, specifically in terms of pollution prevention,

focuses on the recycle/reuse and source reduction strategies before employing disposal and end-of-pipe treatment (El-Halwagi, 1997).

The first key component of this holistic approach is process synthesis, which involves determining the system elements needed and the interconnectivity necessary between the elements in order to attain specific objectives. The next component is process analysis, which is the determination of detailed characteristics such as flowrates, temperature, and pressure of specific streams, using heuristics, mathematical models, and process simulation software. The last key component of mass integration is process optimization, which determines the best value of an objective function such as process cost, gross profit, net present value, and waste flowrates subject to constraints on process capacity, mass and energy balances, and thermodynamic requirements (El-Halwagi, 1997).

The development of mass-exchange networks (MENs) involves matching waste streams rich in a targeted pollutant to mass separating agents (MSAs) that are lean in the targeted pollutant. The process synthesis technique known as the targeting approach is commonly used for developing MENs, and the two targets involved in this approach are minimum cost of MSAs and minimum number of process units (El-Halwagi, 1997). The two targets can also be perceived as respectively representing the variable cost and fixed cost of possible mass integration solution systems. Similar to the quandary in the fields of operations and supply chain management in which total cost must be optimized through minimization of variable cost and fixed cost, these two targets in the targeting approach are often contradictory in the sense that a reduction in one cost dimension almost invariably means an increase in the other (Wisner, Leong et al., 2005).

The graphical approach to synthesizing MENs involves plotting the concentration and mass exchanged of rich streams and lean streams, and developing composite rich and lean streams by superimposing streams to add the mass in overlapping regions of streams. The pinch point of the diagram is determined by vertically moving the composite lean stream to a point where it is completely above the composite rich stream, and this point represents the area over which mass should not be transferred in order to avoid inefficiencies in the form of unnecessary mass exchange. As seen in Figure 2.9, there are three regions of interest in mass pinch diagrams, with the integrated mass exchange area bearing the most weight in mass integration. In this area, the composite rich and lean streams overlap, which allows mass exchange to take place internally between waste streams and MSA streams. Above the integrated mass exchange area, the lean stream represents excess capacity of process MSA streams, which can be eliminated by reducing the flowrate or mass percentage of targeted

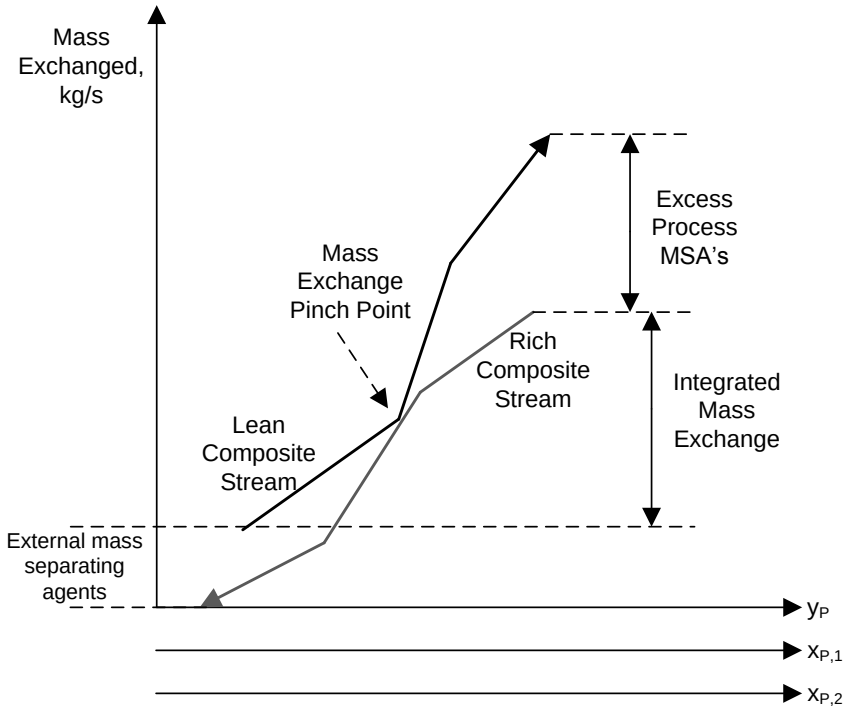

Figure 2.9 – General pinch diagram (El-Halwagi and Manousiouthakis, 1989).

pollutant in process MSA streams (El-Halwagi, 1997). Below the integrated mass exchange area, the rich stream represents the mass to be removed by external MSA systems, which incur much higher fixed and/or variable costs than process MSA streams.

The graphical techniques listed above may be replaced with an algebraic technique that yields similar results to graphical pinch methods. This is directly comparable to the use of temperature interval diagrams to create heat cascade diagrams that illustrate the amount of heat entering or leaving each temperature interval (El-Halwagi, 2006). First, a Composition-Interval Diagram (CID) is constructed where the waste streams and lean streams are drawn in the form of vertical arrows, and the placement of these arrows depends on its corresponding composition in relation to the other arrows in the system. Horizontal intervals are constructed

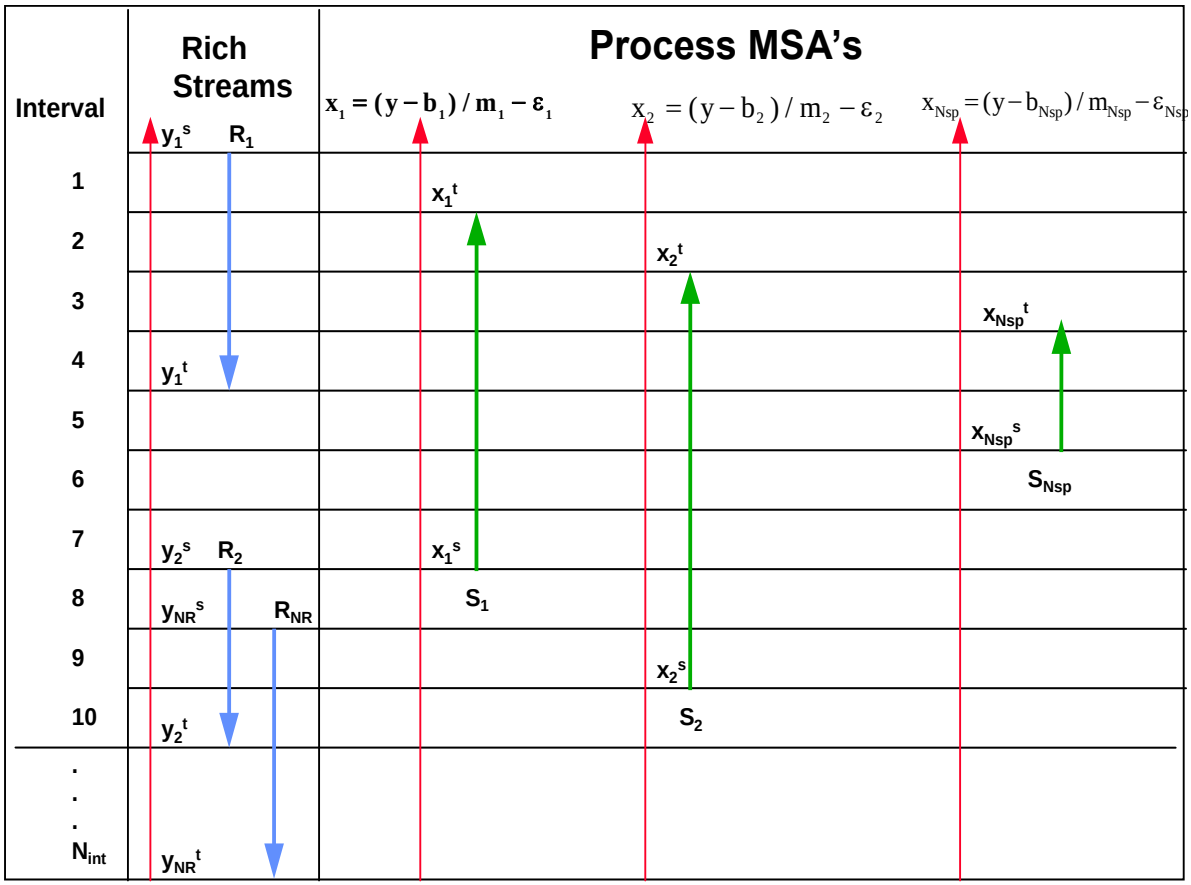

Figure 2.10 – Compostion Interval Diagram (El-Halwagi and Manousiouthakis, 1989).

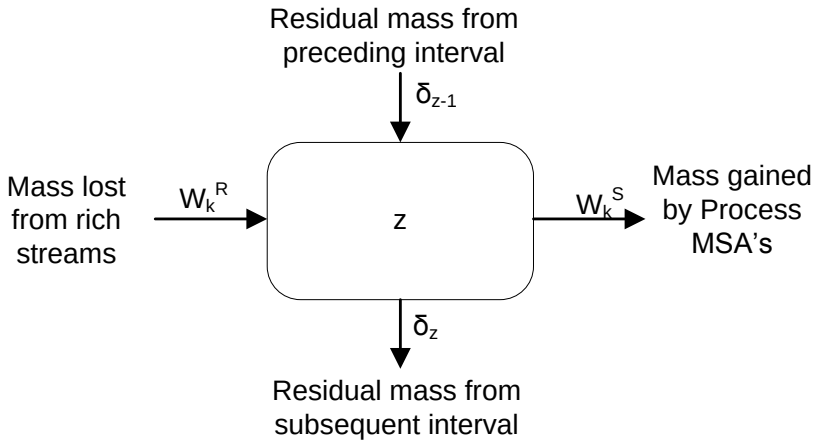

Figure 2.11 – Single level of mass cascade diagram (El-Halwagi, 2006).

that denote the corresponding compositions of the heads and tails of each arrow, as shown in Figure 2.10 (El-Halwagi and Manousiouthakis, 1989).

A Table of Exchangeable Loads (TEL) is then established which will determine the mass of pollutant exchanged among the process streams at each composition interval, and these loads are calculated through the use of mass-balance equations. By combining the use of the CID and the TEL, a cascade diagram, as seen in Figure 2.11, can then be constructed which illustrates the pollutant mass entering and leaving an interval, and this is again calculated through the use of a material balance (El-Halwagi, 2006). From the cascade diagram, the pinch point can be located in a similar fashion to the location of the pinch through graphical methods, and at this point, the mass exchange network may be synthesized by dissecting the problem into above-pinch and below-pinch subproblems in order to avoid mass transfer across the pinch point (El-Halwagi, 1997).

In addition to graphical and algebraic techniques for mass integration, mathematical optimization may also be used in order to minimize material usage and external pollution treatment while maximizing recovery. The basic objective function in Problem P2.9 to be

minimized is the total cost of MSA's, and it should be noted that process MSA's typically have negligible costs while external MSA's have significant regeneration costs.

$$\min \sum_{j=1}^{N_S} C_j L_j \tag{P2.9}$$

$$s.t. \quad \delta_k - \delta_{k-1} + \sum_{j \ passes \ through \ interval \ k} L_j w_{j,k}^s = W_k^R, \quad k = 1,2,\dots,N_{int}$$

$$L_j \geq 0, \quad j = 1,2,\dots,N_S$$

$$L_j \leq L_j^C, \quad j = 1,2,\dots,N_S$$

$$\delta_0 = 0, \quad \delta_{N_{int}} = 0, \qquad \delta_k \geq 0, \quad k = 1,2,\dots,N_{int} - 1$$

In the objective function, C_j represents the cost of the j^{th} MSA while L_j is the flowrate of the j^{th} MSA. The first constraint in this program represents a mass balance around each composition interval where δ_{k-1} and δ_k are the residual masses of the key pollutant entering and leaving the *k*th interval respectively. The second and third constraints ensure that the flowrate of each mass separating agent is between zero and the total available quantity of that lean stream. The fourth and fifth constraints ensure that the overall material balance is satisfied by ensuring that the initial and terminal residuals are zero, while the final constraint ensures either a positive or zero flow of the key pollutant in each interval (El-Halwagi, 1997).

However, solution of this optimization problem is only the stepping stone to determining a comprehensive mass integration solution. The outlet compositions of MSA streams may be optimized, as the initial problem only deals with the maximum possible outlet composition and may overlook an optimal cost solution that involves decreasing this outlet composition. A subsequent optimization problem involves only minor modifications in

which substreams are utilized to represent different maximum outlet compositions (El-Halwagi, 1997):

$$\min \sum_{j=1}^{N_S} C_j \sum_{d_j=1}^{ND_j} L_{j,d_j} \tag{P2.10}$$

The constraints of this problem are similar to the constraints listed in Problem P2.9, but the difference is that L_j is replaced with $L_{j,dj}$, which symbolizes the flowrate of the MSA at a certain composition and is ultimately used to determine the optimal outlet concentration of the MSA streams (El-Halwagi, 1997).

Another way to solve the problem after the initial optimization solution is to use optimization for stream matching and synthesizing the process network. As mentioned previously, the mass exchange network may be divided into two subproblems SN_m where m is 1 or 2. The index m represents the areas above and below the pinch respectively. The variable $E_{i,j,m}$ is binary and represents the feasibility of a match between waste stream R_i with lean MSA stream S_j in subregion m. If a match is thermodynamically feasible in a subregion, then $E_{i,j,m}$ will be assigned the value of 1; else, it is assigned 0. The objective function seeks to minimize the total number of exchangers, but as an alternative, weight factors could be applied to each exchanger in order to determine minimum operating cost. El-Halwagi and Manousiouthakis (1990) formulated a mixed integer linear program to synthesize the mass exchange network:

$$minimize \sum_{m=1,2} \sum_{i \in R_m} \sum_{j \in S_m} E_{i,j,m} \tag{P2.11}$$

This optimization program is subject to constraints on material balances for both rich and lean streams around the composition intervals, matching of loads, and non-negativity of residuals and loads (El-Halwagi and Manousiouthakis, 1989).

The above methods deal with developing mass-exchange networks that remove pollutants from terminal streams, but another method known as waste interception involves intercepting in-process streams and removing pollutants at the source of their generation. Waste interception networks (WIN's) are developed in which MSA's intercept process streams to remove pollutants at a potentially lower cost than the solution of recycle and reuse of terminal streams posed by MEN's. While pollution targets are set a priori in traditional MEN's, terminal stream concentration targets in WIN's are optimization variables that are subject to regulatory environmental constraints, which may further decrease fixed and operating costs (El-Halwagi, Hamad et al., 1996).

Source-sink mapping and path diagrams are two graphical tools used in waste interception. Source-sink mapping is used to depict process areas in which a pollutant is generated (sources) and where a pollutant may be consumed by the process (sinks). The lever-arm rule is then used to evaluate the possibility of direct recycle, which is feasible if a sink may be used to consume pollutants generated by a source without violating process

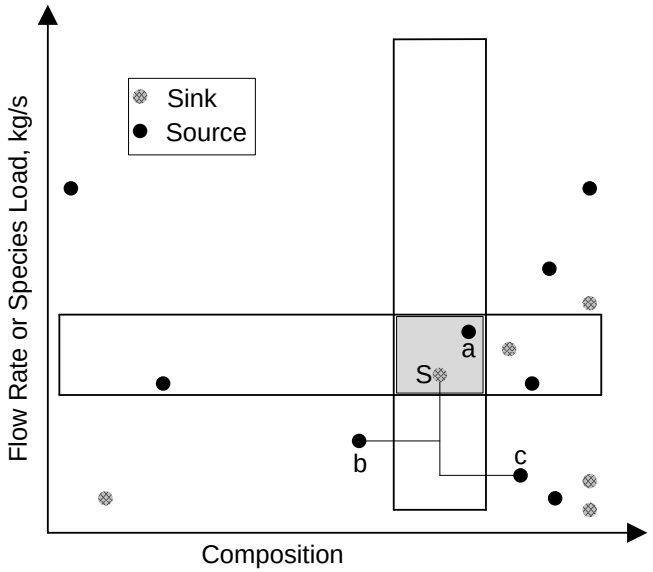

Figure 2.12 – The source/sink diagram (El-Halwagi and Spriggs, 1998).

constraints (El-Halwagi, 1997; Parthasarathy and Krishnagopalan, 2001). Figure 2.12 illustrates an example of the source-sink diagram as well as an application of the lever arm rule. If process constraints are violated by a source-sink solution that appears to be economically advantageous, interception is then used, which involves utilizing an MSA to lower the pollutant concentration of a source so that the recycle solution under consideration may be implemented (El-Halwagi, 1997; Parthasarathy and Krishnagopalan, 2001).

An alternative to the source-sink diagram is a path diagram, illustrated in the top portion of Figure 2.13. The path diagram illustrates the overall flow of a pollutant throughout the plant for a specific carrier phase (i.e. gas, liquid, solid). A hybrid of path and pinch diagrams, in which the MSA concentration scales are included below the path diagram in Figure 2.13, may be used to screen MSA's for intercepting sources (El-Halwagi, 1997; El-Halwagi and Spriggs, 1998).

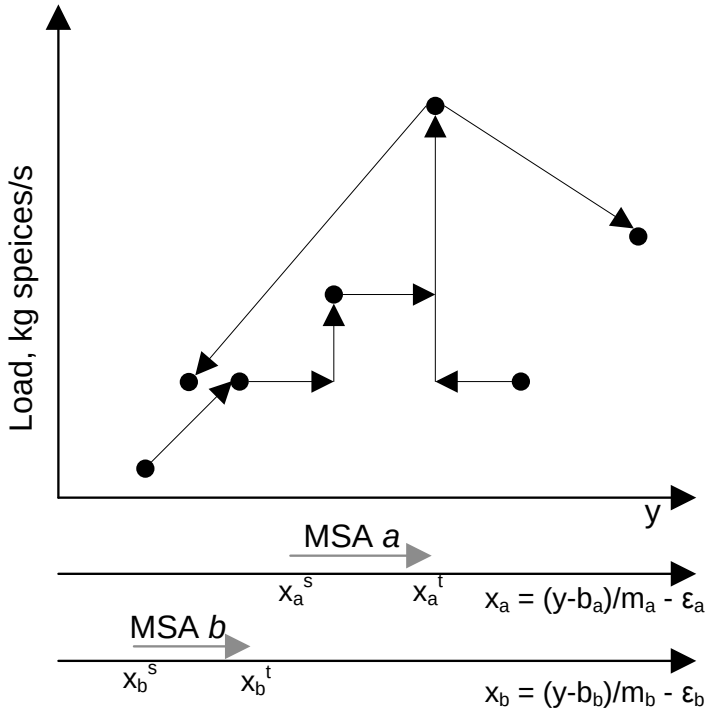

Figure 2.13 – The hybrid pinch/path diagram (El-Halwagi and Spriggs, 1998).

Comparable to the use of optimization in synthesizing and designing mass-exchange networks, optimization may also be used in combination with the hybrid path-pinch diagram to synthesize WIN's as well as evaluate and compare strategies involving interception, segregation, mixing, and recycle (El-Halwagi, Hamad et al., 1996). In the case of interception, an MINLP must be developed in which the objective function of MSA regeneration cost is minimized subject to component mass balance constraints around relevant separation units. Options involving segregation, mixing, and recycle may be evaluated by developing a similar optimization program aimed to minimize terminal pollutant load in wastewater streams with the same mass balance constraints, and these solutions may be compared or integrated with interception solutions in order to improve performance (El-Halwagi, 1997; El-Halwagi and Spriggs, 1998).

There are several alternatives to designing mass exchange networks and waste interception networks through MSA's. Energy separating agents (ESA's) may also be used in which energy is used to induce a phase change that results in the capture and transfer of undesirable species from product and effluent streams, and these ESA's are commonly used to synthesize energy-induced separation networks (EISEN's). The use of ESA's may also be combined with waste interception networks to develop energy-induced waste minimization networks, in which the optimal location is determined to intercept process streams with heat-induced separations to perform mass and heat integration simultaneously (Dunn and El-Halwagi, 2003). Finally, concepts such as material substitution, molecular design, and reaction synthesis of environmentally friendly species are utilized to eliminate the use or generation of potentially undesirable species (Dunn and El-Halwagi, 2003).

2.6 Economic Decision Making

Economic decision making is often used in capital budgeting decisions, which refer to decisions that must take expenditures and receipts into account over a significant time horizon. Process engineers often must deal with capital budgeting decisions, and examples of these decisions include facility expansion, new or revised product lines, replacement, lease or buy, make or buy, and safety or environmental improvements (Keat and Young, 2003). In order to make decisions beneficial to the firm, one must be able to measure the value of possible capital projects and communicate this value to management in universally accepted terms.

As stated previously, receipts and expenditures occur at different points throughout time. Money invested in various investment vehicles today will bear interest over time, and as a result, a set amount of cash in the present is worth more than this same amount in the future due to the power of interest. Therefore, money has a time value that must be taken into account, and cash flows that occur in the past and future should be normalized to a pre-defined time. This interest rate is known as the discount rate, or the cost of capital, and this information is crucial for most valuation techniques. The discount rate may be the cost of debt, the cost of equity, or a combination of the two (Keat and Young, 2003). The cost of debt is merely the interest rate of the debt multiplied by one minus the marginal tax rate, but the cost of equity may be calculated in multiple ways. The dividend growth model assumes that dividends will grow forever at a constant rate g, and with this assumption, the present cost of capital k_0 is (Keat and Young, 2003):

$$k_0 = \frac{D_1}{P_0(1-f)} + g \tag{2.2}$$

where D_1 is the assumed dividend one year from present time, P_0 is the present stock price, and f refers to the percentage of costs associated with underwriting the issue that new stock will be valued at less than the current market price, or flotation costs. While the dividend growth model applies to a company-specific scenario, the capital asset pricing model also takes into account general market performance. The cost of capital based on this pricing model is calculated as follows (Keat and Young, 2003):

$$k_0 = R_f + \beta(k_m - R_f) \tag{2.3}$$

where R_f is the risk-free rate of return on a guaranteed investment, β is the volatility of the firm's stock in relation to the volatility of the overall market, and k_m is the rate of return on the market portfolio.

Valuation techniques such as payback method, which calculates the time necessary to recoup the original investment, and accounting rate of return, which is the percentage of average annual profits divided by average annual investment, do not take into account the time value of money (Keat and Young, 2003). However, there are effective, universal valuation techniques which discount future cash flows to a present value. For example, net present value is defined as the net sum of all cash flows discounted to the present time, and this equation is as follows (Keat and Young, 2003):

$$NPV = \sum_{t=1}^{n} \frac{R_t}{(1+k)^t} - \sum_{t=0}^{n} \frac{O_t}{(1+k)^t} \tag{2.4}$$

where t is the time period, R_t represents cash inflow at time t, O_t is cash outflow at time t, and k represents the discount rate. Another determinant of financial valuation is the internal rate of return, or *IRR*, in which Equation 2.4 is still used, but the *NPV* term is set to zero and the equation is solved for k. The internal rate of return is the discount rate that equates the

present value of the sum of cash inflows to cash outflows (Keat and Young, 2003). It should be noted that if the initial costs of two proposals are different, or if the shape of subsequent cash inflow streams are different, then there may be scenarios in which net present value and the internal rate of return give conflicting advice on capital budgeting decisions (Keat and Young, 2003).

2.7 Environmental Impact Assessment

Traditionally, economic analysis metrics such as net present value, payback period, and internal rate of return have been the predominant tools used in making decisions to build or modify chemical processes. However, with increasing environmental concerns and regulations, decision makers in process design must now take environmental impact into account in addition to economic metrics. As a result, it has become necessary to develop or utilize methodologies that measure and quantify the environmental impact of process synthesis options, and these quantifications may then be used to determine which waste streams impart the highest level of impact and should be targeted for reduction (US-EPA, 2008). Upon assessing environmental impact, one may also see that there may lie a trade-off between economic and environmental performance, and as a result, both economic analysis and environmental impact assessment are critical tools in the decision making process (Smith, Mata et al., 2004).

2.7.1 Waste Reduction Algorithm

One widely used approach to measuring environmental impact and comparing those quantified values among differing process synthesis options is the Waste Reduction (WAR)

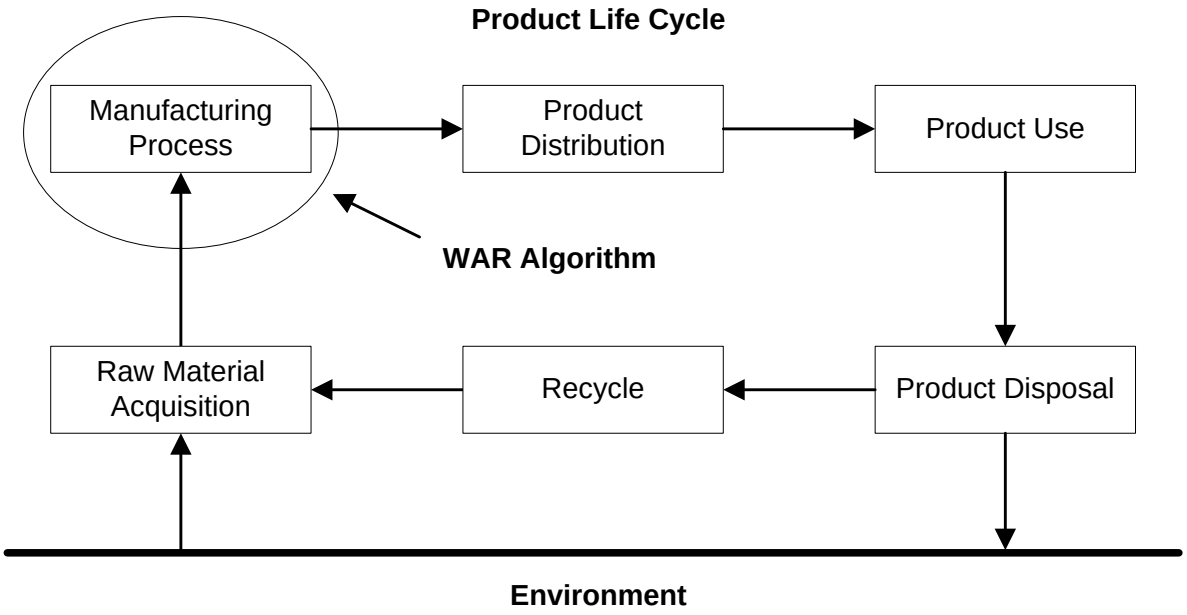

Figure 2.14 – EPA WAR Algorithm in relation to overall life cycle analysis (Young and Cabezas, 1999).

algorithm (US-EPA, 2008). The WAR algorithm can be considered a subset to overall life cycle analysis (LCA), and Figure 2.14 illustrates the system boundary of the WAR algorithm with respect to the product life cycle (Young and Cabezas, 1999).

The developers of the WAR algorithm define potential environmental impact (PEI) as the average possible effect that emissions of mass and energy from a chemical process would have on the environment. Because this impact was initially measured in terms of mass, a conserved quantity, it is believed that PEI can also be considered to be a conserved quantity (Cabezas, Bare et al., 1999). The impact conservation equation is listed as follows and bears resemblance to a mass balance equation:

$$\frac{\mathrm{d}I_{syst}}{\mathrm{d}t} = \dot{I}_{in} - \dot{I}_{out} + \dot{I}_{gen} \tag{2.5}$$

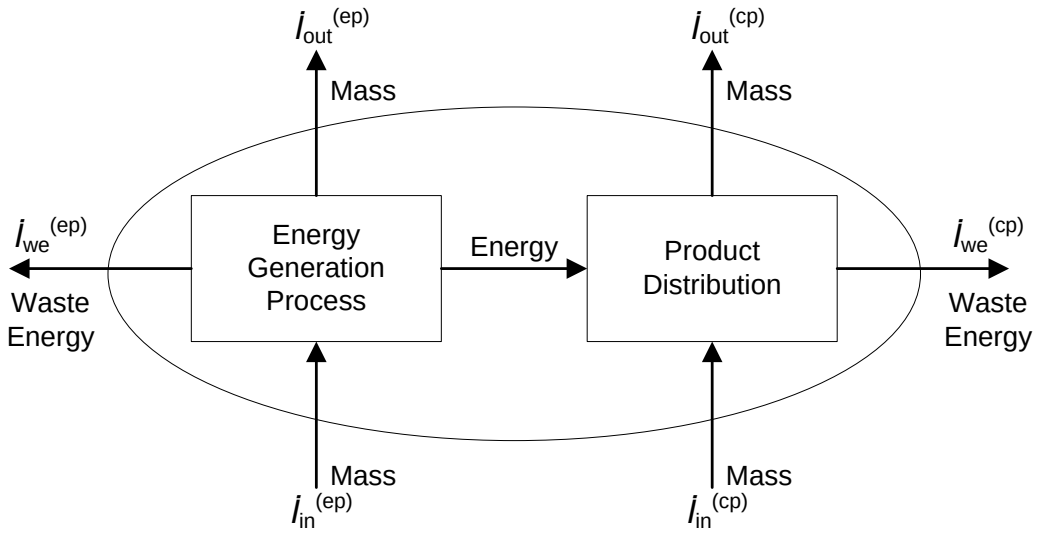

Figure 2.15 – Impact streams for the chemical and energy generation processes (Young and Cabezas, 1999).

where dI_{syst}/dt is the change in system environmental impact over time, $\dot{I}_{in}$ and $\dot{I}_{out}$ are the input and output rates of impact entering and leaving the process, and $\dot{I}_{gen}$ is the environmental impact generated within the system (Cabezas, Bare et al., 1999).

This formulation was later modified to include impacts from the energy generation process necessary to supply energy to the chemical process, as well as waste energy terms from both the chemical and energy generation processes. An illustration of the impact streams for the energy and chemical processes is shown in Figure 2.15 (Young and Cabezas, 1999). The reformulated equation is now defined as:

$$\frac{\partial I_t}{\partial t} = \dot{I}_{in}^{(cp)} + \dot{I}_{in}^{(ep)} - \dot{I}_{out}^{(cp)} - \dot{I}_{out}^{(ep)} - \dot{I}_{we}^{(cp)} - \dot{I}_{we}^{(ep)} + \dot{I}_{gen}^{(t)} \qquad (2.6)$$

where $\partial I_t/\partial t$ is the accumulation (or depletion) of environmental impact in the given system over time, $\dot{I}_{in}^{(cp)}$ and $\dot{I}_{out}^{(cp)}$ are the input and output rates of impact in the chemical process, $\dot{I}_{in}^{(ep)}$ and $\dot{I}_{out}^{(ep)}$ are the input and output rates of impact in the energy generation process,

$\dot{I}_{we}^{(cp)}$ and $\dot{I}_{we}^{(ep)}$ are the impact generated from releasing waste energy to the environment, and $\dot{I}_{gen}^{(t)}$ is the impact generated by chemical reactions within the system (Young, Scharp et al., 2000). Many terms of this equation can be considered zero or negligible for the following reasons:

- With a steady state process, the accumulation of environmental impact over time is equivalent to zero.
- $\dot{I}_{in}^{(ep)}$ is considered to be very small in comparison to the rest of the non-zero terms in the PEI conservation equation. This is because of the assumption that electricity is provided by coal-fired power plants, whose inputs are merely coal, water, and air. Water and air have no adverse environmental impact when being evaluated on potential pollutant capability, but it should be noted that at this time, there is no portion of the WAR algorithm that accounts for global water usage. The remaining input for these power plants is coal, and although coal contains many organic and inorganic molecules and compounds, these potentially harmful chemicals are trapped in a solid matrix (Young, Scharp et al., 2000).
- The waste energy impact terms ($\dot{I}_{we}^{(cp)}$ and $\dot{I}_{we}^{(ep)}$) of both the chemical and energy processes are considered to be very small in comparison to the impact resulting from the consumption and production of energy and chemicals in non-fugitive streams (Young and Cabezas, 1999; Young, Scharp et al., 2000).

After taking these simplifying assumptions into account and rearranging terms, the overall PEI equation reduces to:

$$\dot{I}_{gen}^{(t)} = \dot{I}_{out}^{(cp)} - \dot{I}_{in}^{(cp)} + \dot{I}_{out}^{(ep)} \tag{2.7}$$

The terms on the right-hand side of the equation can be determined with the following equations (Cabezas, Bare et al., 1999):

$$\dot{I}_{out}^{(cp)} = \sum_{j}^{cp} M_j^{out} \sum_{k} x_{kj} \Psi_k \tag{2.8}$$

$$\dot{I}_{in}^{(cp)} = \sum_{j}^{cp} M_j^{in} \sum_{k} x_{kj} \Psi_k \tag{2.9}$$

$$\dot{I}_{out}^{(ep)} = \sum_{j}^{ep-g} M_j^{out} \sum_{k} x_{kj} \Psi_k \tag{2.10}$$

In Equations 2.8-10, M_j^{out} and M_j^{in} represent the mass flowrate of stream *j* leaving or entering the process, x_{kj} represents the mass fraction of a given chemical *k* in stream *j*, and Ψ_k represents the environmental impact score of chemical *k* (Cabezas, Bare et al., 1999). In regards to the $\dot{I}_{out}^{(ep)}$ equation, the summation superscript *ep-g* represents gaseous emissions since modern coal-fired power plants are adept at capturing solid particles in the form of ash, and therefore no solid emissions are released to the environment (Cabezas, Bare et al., 1999). The environmental impact score Ψ_k is determined by Equations 2.10-11:

$$\Psi_k = \sum_{l} a_l \psi_{kl} \tag{2.11}$$

$$\psi_{kl} = \frac{(score)_{kl}}{< (score)_k >_l} \tag{2.12}$$

where a_l is the weighting factor of the impact category *l*, ψ_{kl} is the weighted average environmental impact score of chemical *k* in category *l*, and the bottom term of Equation 2.12 represents the average impact score of all chemicals in category *l* (Young and Cabezas, 1999). The WAR algorithm software contains these average scores, as well as scores for over 1700 individual chemical species (US-EPA, 2008). One limitation of the EPA WAR

algorithm is that the database does not contain information on environmental impact scores for every chemical, but this can be overcome by utilizing a methodology in which molecular modeling software is used for the calculation of impact data for unlisted chemicals (Fermeglia, Longo et al., 2007).

The eight environmental impact categories are as follows (Young, Scharp et al., 2000):

- Human toxicity potential by ingestion (HTPI)
- Human toxicity potential by exposure, both dermal and inhalation (HTPE)
- Terrestrial toxicity potential (TTP)
- Aquatic toxicity potential (ATP)
- Global warming potential (GWP)
- Ozone depletion potential (ODP)
- Photochemical oxidation potential (PCOP)
- Acidification potential (AP)

There are two types of environmental impact indices, and these are further split into four total ways to measure the environmental impact of the process. PEI output indices represent the environmental impact leaving the manufacturing process and entering the environment, while PEI generation indices quantify the amount of environmental impact generated by the process. PEI output indices and PEI generation indices can be considered to be indicators of the external and internal environmental efficiency, respectively (Young and Cabezas, 1999). Both types of indices are mainly evaluated on a rate basis, in terms of PEI/time, or on a production basis, in terms of PEI/mass of product (Young, Scharp et al., 2000).

Regardless of whether one is using PEI output indices or PEI generation indices to evaluate environmental impact, it is necessary to determine $\dot{I}_{out}^{(cp)}$ in either case. The initial formulation of the WAR algorithm states that main products should be left out of the $\dot{I}_{out}^{(cp)}$ evaluation, and that this term should only measure the environmental impact of non-product streams (Cabezas, Bare et al., 1999). However, later formulations state that as a rule of thumb, products should be left out of this evaluation since a product may very well serve a societal need even though the product itself may impart a high level of impact (Young, Scharp et al., 2000). It must be noted that if the main product of a process is included in the evaluation of environmental impact, a process modification that results in higher production of the chemical may have a misleading adverse effect on overall PEI, and because this may negate reductions in impact of non-product streams and energy usage, one must be careful in including products with high societal need and PEI scores (Young and Cabezas, 1999).

2.7.2 Other Environmental Assessment Tools

In addition to the EPA WAR algorithm, several methods exist for assessing and quantifying environmental impact. For example, life cycle analysis (LCA) is commonly used to determine the level of environmental impact that a chemical process may have on its surroundings. Life cycle analysis measures and sums standardized individual net burdens, which are the products of emission coefficients and mass flowrates of individual chemical species. These burdens then compose individual impacts that are similar to the environmental impact categories in the EPA WAR algorithm. LCA is also a useful tool in evaluating process options that may reduce adverse environmental impact. But while the EPA WAR algorithm only covers the manufacturing process, as seen previously in Figure 2.14, LCA

performs a similar analysis around a larger system, which includes raw material acquisition, product distribution, use, disposal, and recycle. In other words, life cycle analysis deals with the entire chemical and energy supply chains in determining environmental impact on a process or species from cradle to grave (Azapagic and Clift, 1999).

The minimum environmental impact methodology (MEIM) incorporates a number of principles from life cycle analysis (Pistikopoulos, Stefanis et al., 1995). Similar to LCA, MEIM requires the definition of a consistent system boundary, and MEIM also focuses on the impact of the system as a whole, including inputs and raw material extraction in addition to waste emissions. However, MEIM differs from LCA in the aspect that the system boundary is typically drawn from the natural raw materials procurement level of the life cycle to the manufacture of products and the production of the aggregate waste streams. MEIM quantifies each category of impact by adding impact quantities that are standardized by either dividing the mass of emission by a standard limit value or multiplying by an environmental impact potential factor. This methodology is incorporated into a multi-objective optimization program, in which operating cost is minimized while adjusting the maximum level of the overall environmental impact vector. The mass of emission of each individual pollutant, and consequently the environmental impact vector, is an implicit function of the decision variables in this optimization program (Pistikopoulos, Stefanis et al., 1995). This methodology can be used to minimize overall environmental impact as well as compare the results of minimizing particular categories of impact on the environmental impact of the entire system (Pistikopoulos, Stefanis et al., 1995; Stefanis, Livingston et al., 1997).

The environmental fate and risk assessment tool (EFRAT) measures environmental impact in a similar fashion to the EPA WAR algorithm, and EFRAT curves plotted against continuous decision variables often share a qualitatively similar shape but different scale to their WAR counterparts (Shonnard and Hiew, 2000). Like WAR, EFRAT involves defining the process boundary around the manufacturing process only. However, the measurement of environmental impact is drastically different in EFRAT, which has three components in relative risk assessment, environmental fate and transport, and air emissions calculations. In the relative risk assessment portion, the risk score of each individual chemical is normalized through dividing by the score of a predetermined benchmark score. The environmental fate and transport section focuses on the amount of pollutants that will ultimately end up in the four media of air, water, soil, and sediment. Finally, the air emissions calculations describe how different processes and different waste products are evaluated to determine the amount of emissions released through the air (Shonnard and Hiew, 2000).

Sustainable development indicators (SDI) assess economic and social indicators in addition to environmental indicators, which are split into environmental impact, environmental efficiency, and voluntary actions (Azapagic and Perdan, 2000). SDI tends to look at the entire life cycle in a similar fashion to LCA, and the individual environmental impacts tend to mimic those measured in LCA. In addition to these environmental impacts, the SDI method also measures environmental efficiency in terms of material and energy intensity, material recyclability, product durability, and service intensity. Furthermore, SDI also takes into account voluntary actions by observing any environmental management systems in place, noting assessment of suppliers, and taking notice of environmental improvements above and beyond legal compliance levels (Azapagic and Perdan, 2000).

2.8 Supply Chain Management

The supply chain is defined as the cradle-to-grave process dealing with the procurement of necessary materials, manufacture into a salable product, and distribution of this product to a customer base. In this sense, the supply chain involves extraction of raw materials, conversion of these raw materials into intermediates and/or components by multiple firms, manufacture of products destined for consumer use, distribution to wholesalers and retailers, and finally sale to the end consumer (Wisner, Leong et al., 2005). Supply chain management is a holistic approach to ensuring optimal performance by each member of the supply chain for the purpose of maximizing value. Management of the supply chain is important because decision makers often take a shortsighted view and ensure local optimization of their particular firm by shifting costs, waiting time, and other inefficiencies to upstream suppliers and downstream customers. Through cooperation, communication, and visibility throughout the supply chain, inefficiencies such as lead times, safety stocks, and quality deficiencies are vastly reduced, resulting in greater profits and higher levels of customer satisfaction (Wisner, Leong et al., 2005).

2.8.1 Purchasing and Procurement

In the context of chemical engineering, industrial procurement is the act of purchasing raw materials for the purposes of conversion into value-added chemicals and/or energy. This function is indeed important, as 50% of all incoming sales revenue is spent on the costs of raw materials (Wisner, Leong et al., 2005). The increasing intensity of global competition has brought scrutiny to the purchasing process, which has resulted in the active pursuit of supply chain strategies that will bolster profit margins. Firm management must

decide whether to pursue backwards integration, in which an operating facility acquires its suppliers and effectively gains more control on raw material supply. Advantages may lie in having a wide supply base in order to make sure that operational capacity is not underutilized, supply interruption risks are minimized, and competitive pressure keeps prices down amongst suppliers (Wisner, Leong et al., 2005).

Advances in computing technology have resulted in widespread time-saving automation of procurement. Electronic data interchange ignited the shift from manual purchasing towards more automated methods, resulting in vast savings in costs and redirection of purchasing staff to the core competencies of the business. Supplier relationship management software completed the transition by extending procurement services to include analytical tools, sourcing and procurement execution, payment and settlement, and supplier performance feedback (Wisner, Leong et al., 2005). Electronic procurement also allows the implementation of reverse auctions, in which suppliers underbid one another in order to secure the business of the customer, which further reduces costs of the procurement function. As a result of automated purchasing, firms may also be able to use third-party logistics and vendor-managed inventories in order to utilize effective supply chain strategies developed by companies whose core competency is the effective transportation of supply materials (Wisner, Leong et al., 2005).

Process systems engineering has been extensively used to develop decision support systems concerning biomass-based supply chains and the determination of plant location and/or remote collection points. One approach in particular uses a two-step method first to determine the facility locations with respect to feedstock density distribution and second to evaluate the internal rate of return of such a supply chain network for comparison with other

feasible supply chain congifurations. Optimization is used in this first step to minimize the transportation cost incurred through feedstock collection by selecting centroids of counties as potential polygeneration facility sites, and this problem is formulated as follows (Sukumaran, 2008):

$$\sum_{j=1}^{n}\left[\beta_f a_j + \beta_m b_j\right] y_{ij} \geq R x_i \qquad \forall\, i \qquad \text{(P2.12)}$$

$$\sum_{i=1}^{n} x_i = p$$

$$\sum_{i=1}^{n} y_{ij} \leq 1 \qquad \forall\, j$$

$$0 \leq y_{ij} \leq 1 \qquad \forall\, j$$

$$x_i \in \{0,1\} \qquad \forall\, i$$

In Problem P2.12, index *i* is the refinery location, index *j* is the county location for available feedstock, β_f and β_m represent fractional availability of forest and mill residues respectively, a_j and b_j represent total available forest and mill residues in a given county respectively, *R* is the total feedstock requirement for a constructed biorefinery, and *p* is the pre-defined total number of polygeneration facilities. The decision variables in Problem P2.12 are y_{ij}, which represents the fraction of feedstock available in county *j* for the refinery in county *i*, and x_i, which is a binary variable representing the existence (x_i=1) or absence (x_i=0) of a biorefinery in county *i*. The solution of this MINLP may be performed in Excel handily for *p* values of 5 or less; however, conventional solvers struggle with determining the solution to this particular formulation for 6 or more biorefineries (Sukumaran, 2008). Once the optimization portion determines where to locate the biorefineries in order to minimize transportation cost,

the internal rate of return for the supply chain network is calculated with the use of financial data for the biorefineries available in literature or practice (Sukumaran, 2008).

A more sophisticated variation of this decision support system involves the integration of mapping software with raw material density data in order to illustrate the availability of feedstocks. Information from this software is combined with road accessibility data to evaluate the cost and feasibility of attaining raw materials from different sources, which can then be quantified to determine the amount of feasible feedstocks to be used in a biorefining process (Ayoub, Martins et al., 2007; Aksoy, Cullinan et al., 2008).

2.8.2 Production Allocation

The scarcity principle, which states that all valuable resources are finite and scarce, leads people to decide the best ways to use their available resources. This translates into production allocation decisions in chemical engineering, in which management must decide how to maximize resources on hand in order to reach goals in short-term scheduling, long-term planning, production, and distribution. Decision makers must also decide whether or not to invest in incremental capacity for existing product lines and/or additions of capacity for new products (Anupindi, Chopra et al., 2006).

Mathematical programming is commonly used to allocate resources effectively in order to optimize product mix in a plant where multiple chemical products may be manufactured. The objective function may be a measure of profit, revenue, or cost. In the case of a profit-based objective function, this function is maximized in respect to the contribution margin of each item i (m_i) multiplied by the number of units i manufactured (x_i) over time (Anupindi, Chopra et al., 2006):

$$Maximize \quad \sum_{i}^{n} m_i x_{i,} \qquad i = 1,2, \dots, n \qquad \text{(P2.13a)}$$

This objective function is subject to constraints on resource availability for all resources *j*, where a_{ji} is the unit load of product *i* on resource pool *j* and b_j is the total scheduled availability. These constraints take on the following form (Anupindi, Chopra et al., 2006):

$$\sum_{i}^{n} a_{ij} x_i \leq b_{j,} \qquad \forall j \qquad \text{(P2.13b)}$$

The production of differing products is also contingent on available market demand, which calls for market constraints where D_i is the demand of product *i* in the marketplace, across all products *i* (Anupindi, Chopra et al., 2006):

$$x_i \leq D_i \qquad \forall i \qquad \text{(P2.13c)}$$

This optimization problem is more commonly known as the production allocation problem, but this formulation is highly simplified. This version assumes that contribution margins are not affected by economies of scale from adding or subtracting capacity, as well as a demand that is known and quantifiable. In addition to these simplifications, setup and changeover are not taken into account in this version of the problem, unlike different supply chain operations models such as the Economic Order Quantity model (Nahmias, 2005). While this initial formulation may be solved as an MILP using readily available solution tools, the implementation of nonlinearities greatly increases the complexity and size of production allocation problems, resulting in an MINLP formulation with greatly increased computational time needed for solutions that may not be globally optimal.

As stated previously, in a hypothetical chemical processing facility in which the manufacture of multiple product lines may take place either simultaneously or in sequence, there may be common process resources that are used in more than one product line. The

effective capacity of a particular product line is essentially the effective capacity of the resource with the smallest throughput, which is known as the effective bottleneck (Anupindi, Chopra et al., 2006). To avoid a failure at the bottleneck, the entire process must be adjusted so that the capacity at the bottleneck is not exceeded. Additionally, this bottleneck resource could be analyzed to determine what process improvements, if any, will result in higher throughput and increased capacity. If no improvements will relieve the bottleneck, one may have to consider replacing the bottleneck equipment in order to handle higher throughput, which will cause movement of the effective bottleneck to another resource.

The impact of a bottleneck impediment on a global process is illustrated in a study conducted on a chemical plant in which two chemicals in two formulations each are manufactured and shipped through various channels to supply chain partners domestically and abroad. In this study, two similar yet distinct active ingredients are produced for the purpose of formulation into a low-cost, mature herbicide. The active ingredient is produced in the United States, at which point it is shipped in bulk to global customer sites for reformulation and local delivery, or it is distributed domestically either as a final reformulated product or as an active ingredient to be reformulated by the customer. Because of these options, the firm must determine how much of the manufacturing process should be performed by the company and the level of manufacturing to be assigned to the customer (Sousa, Shah et al., 2008).

Upstream resources such as raw material procurement and downstream resources in the form of distribution and demand cause delays at the bottleneck resources, and thus the effective capacity of the process is then reduced. Effective scheduling and supply chain management must allow these bottleneck resources to work at their maximum capacity so

that the overall process will indeed realize its effective maximum capacity. Therefore, these delays must be eliminated or rearranged within the supply chain so as not to impede the work of bottleneck resources (Sousa, Shah et al., 2008). The study develops an optimization framework to tackle this problem in which the objective function is net present value and is subject to constraints on taxation, raw material availability, mass balances, customer demand, production capacity, storage capability, and site selection. It is crucial to note that even with only two chemicals and two formulations, the number of variables illustrates the daunting complexity of the problem, resulting in a need for a better framework to solve this type of problem.

Supply chain management dictates that a holistic view is imperative for economic supply chain efficiency, which means that supply and demand considerations should be taken into account in addition to the production allocation problem (Wisner, Leong et al., 2005). Many supply chain studies analyze production allocation simultaneously with the purchasing and distribution aspects of supply chain management. For example, one study seeks to minimize total production and distribution costs with respect to constraints on satisfying customer transportation preferences and capacity availability both in production and transportation. In scenarios in which production costs greatly exceed transportation costs, production should be allocated to the most efficient resources instead of those resources that may incur lower transportation costs due to proximity to suppliers and/or customers (Ayindel, Sowlati et al., 2008).

Heuristics alone may not determine the best solution, which results in a need for optimization to determine the supply chain configuration with minimal systematic cost. When performing supply chain optimization, one should make sure to include all costs

associated with the decision variables, and not just the costs for production alone. Sensitivity analysis should be used in addition to optimization to determine the most important determining factor on supply chain cost. For example, optimization and sensitivity analysis have shown in a particular multiproduct example that the most effective way to reduce production allocation costs is to minimize the amount of changeover necessary to satisfy customer demand (Tsiakis and Papageorgiou, 2008).

2.8.3 Distribution and Demand

The converse of purchasing and procurement is distribution of product to the customer, and similar to the issue of procurement, transportation plays a key role in ensuring that the customer receives the right products, at the right place, and in the right time. Transportation modes can be classified, in decreasing regulatory stringency, as common carriers, contract carriers, exempt carriers, and private carriers. Transportation may be pursued via multiple modes such as motor, rail, air, water, pipeline, and every combination thereof. These modes carry specific advantages and disadvantages depending on the speed required, cargo value, reliability, cargo physical properties, and weight limitations. Firms may also decide to outsource the transportation function to third party logistics providers such as freight forwarders, brokers, and shippers' associations. All of the above factors need to be taken into account when developing a distribution strategy that will result in optimal added value for the global supply chain (Wisner, Leong et al., 2005).

The function of warehouses is to provide storage for incoming materials, work-in-progress goods, and/or finished goods, and the location of warehouses plays an important role in developing a supply chain strategy for both incoming and outgoing logistics. In a

product-positioned strategy, warehouses serve as consolidating collection points for inbound raw materials, whereas a market-positioned strategy dictates that warehouses are located close to customers in order to maximize distribution service. Hybrid strategies also exist in which a warehouse may be placed in a location which is a compromise between proximity to supply sources and downstream customers and used both as collection points and distribution centers (Wisner, Leong et al., 2005).

Warehousing allows for the storage of safety stocks in case of a disruption in inbound or outbound logistics. A safety stock of raw materials will ensure that production will not be stopped due to unforeseen supply interruptions, while excess product inventory potentially serves as a buffer against demand fluctuations and emergency orders. However, this protection against supply or demand abnormalities bears the extra expense of inventory carrying cost, and one must perform risk analysis to determine the impact of this extra carrying cost on the profitability of the firm and its supply chain partners (Wisner, Leong et al., 2005). Just-in-time production and lean manufacturing both dictate that safety stocks should be minimized, or even eliminated altogether, but this hinges on increased reliability in both inbound and outbound logistics in order to be successful. Furthermore, if the order lead time to produce a given product at a multiproduct facility is shorter than the lead time to manufacture the product, then just-in-time production will be infeasible since there is not enough available time to manufacture made-to-order goods, which will cause a need for warehousing to ensure that demand is fulfilled (Wisner, Leong et al., 2005).

Optimization may also be used to determine the location of warehouses and distribution centers, but it must be noted that a reduction in one cost dimension may result in increases in other cost dimensions. For example, a reduction in distribution costs may result

in increased production costs, outsourcing expenses, duties and tariffs, infrastructure costs, and material handling costs (Tsiakis and Papageorgiou, 2008).

Optimization programs used for determining the most effective distribution network for meeting customer demand must also make sure to follow practical constraints with respect to production as well as distribution. For example, one established method for minimizing global supply chain network cost involves an objective function which considers production and distribution simultaneously (Tsiakis and Papageorgiou, 2008):

$$Minimize \sum Infrastructure\ Cost + \sum Production\ Cost \qquad (P2.14)$$
$$+ \sum Material\ Handling\ Cost\ at\ Dist.Centers$$
$$+ \sum Transportation\ Cost + \sum Duties\ Cost$$

In this formulation, infrastructure costs refer to fixed costs related to the establishment or closure of a production facility or distribution center, while production costs are the sum of production rates multiplied by unit production cost, cost of changeovers in terms of lost production, outsourcing costs to third parties to meet excess customer demand. Material handling costs at distribution centers are generally linear functions of throughput of the center. Transportation costs account for transportation between the production facility and distribution center, and between centers and end customers, while duty costs represent the cost incurred by the company when shipping finished product across regional or international borders (Tsiakis and Papageorgiou, 2008). This objective function is subject to practical constraints on production capacity, transportation capacity, customer preferences, material balances, utilization factors, material handling throughput, and transportation cost (Ayindel, Sowlati et al., 2008; Tsiakis and Papageorgiou, 2008). Furthermore, within these

optimization problems utilized in supply chain management, optimal distribution networks must allow process bottleneck resources to operate at maximum capacity in order to realize the maximum effective throughput (Sousa, Shah et al., 2008).

2.9 Product Platform Design

The systematic approach commonly used for the purpose of supply chain optimization may be taken one step further in polygeneration decision making. While it is indeed critical to develop, optimize, and evaluate biorefining polygeneration options, there may be situations where the value of the final product and necessary processes extend beyond the scope of manufacturing the specific targeted product. The ability of selected chemicals to serve as chemical platforms for other value-added products also needs to be taken into consideration.

Figure 2.16 illustrates a hypothetical chemical platform process flow diagram in order to clarify the definitions of terms commonly used in product platform design. While most modern research into product platform design is utilized in a mechanical engineering context, many of the fundamental principles transfer into the knowledge area of chemical engineering. A mechanical product platform is originally defined as a common subsystem that is leveraged across a series of downstream products by means of shared product and process architecture (Meyer and Dalal, 2002). In the context of chemical engineering, a chemical product platform is a salable feedstock that may be converted into multiple derivative chemical products by means of a fixed, finite number of processing steps. In reference to Figure 2.16, Chemical A serves as the chemical platform that can be sold or used on its own, or further converted into other valuable derivative products B, C, and D. In both

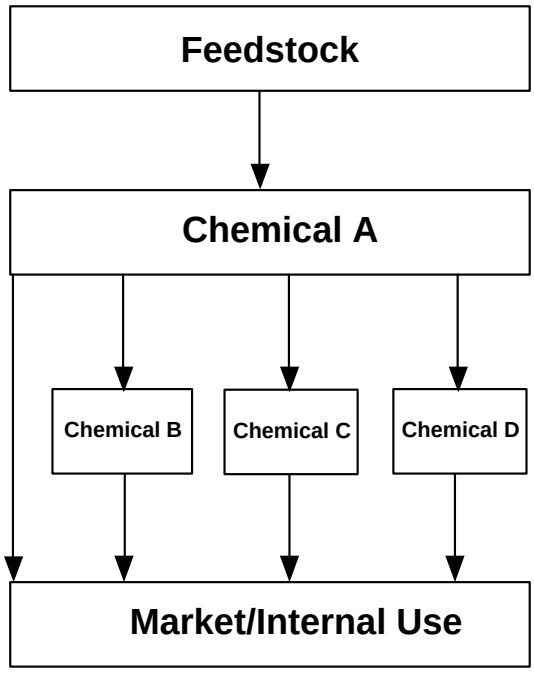

Figure 2.16 – Generic chemical product platform flow diagram.

fields of engineering, the product family refers to the original product platform and all of its derivative products, and the product family in Figure 2.16 includes the platform chemical A as well as its derivatives B, C, and D (Meyer and Dalal, 2002). A collection of multiple product families compose the overall product portfolio, which ideally represents all of the value propositions that the firm has to offer to the general market.

As stated previously, extensive research has been conducted in the area of product platform design with respect to mechanical engineering (Robertson and Ulrich, 1998; Meyer and Dalal, 2002; D'Souza and Simpson, 2003; Simpson, 2004), and a methodology for decision analysis with respect to mechanical product platform design has been developed (Simpson, Maier et al., 2001). However, there is little scholastic research that focuses on chemical product platform design and the decision analysis necessary to evaluate and pursue platform concepts. Polygeneration facilities easily produce chemical platforms such as

syngas, Fischer-Tropsch liquids, dimethyl ether, ethanol, and other bio-based products, and a glaring need exists for a systematic methodology capable of evaluating the production of these chemical platforms and subsequent product families and portfolios.

2.10 Summary

Because of the ever-increasing need for technology that is sustainable while meeting societal needs of a growing population, a framework is needed to measure, optimize, and study the sensitivity of economic and environmental sustainability of both mature and novel polygeneration technologies. Based on the theoretical background presented in this chapter, it should be clear that there is indeed an opportunity to apply core principles from process systems engineering, supply chain management, and economics in order to develop a powerful tool to evaluate biorefining polygeneration processes. Fundamentals from process design and synthesis, mathematical optimization, process integration, economic decision making, environmental impact assessment, supply chain management, and product platform design are combined to develop this framework. This tool will utilize theory and information from a diverse array of academic fields in order to assist leaders in industry, academia, and political systems to make the most optimal decisions about biorefining polygeneration technology in order to provide maximum profitability to economic stakeholders while being able to measure and observe possible changes in local and global environmental impact.

Chapter 3

Methodology

3.1 Introduction

Biomass-based polygeneration facilities, including but not limited to integrated biorefineries, have the potential to provide a strong, self-reliant, sustainable alternative to the use of non-renewable resources for the production of bulk and fine chemicals, such as polymers, fiber-derived products, and pharmaceuticals as well as energy, liquid fuels and hydrogen. Although most of the fundamental biorefining processing steps are well-known, there is a need for a framework capable of integrating these processes and then evaluating the integrated processes in order to identify the optimal set of products and production pathways. The diverse range of possible polygeneration products results in a highly complex product allocation problem which cannot be solved by heuristics alone. Such processing facilities demand a process systems engineering approach utilizing process synthesis, process integration, and mathematical optimization techniques. This targeted systematic approach will then serve as an interface between simulation work and experimental efforts. The objective of this work is to assist decision makers in polygeneration industries such as biorefining in evaluating the profitability of different possible production routes and product portfolios while measuring environmental impact and the effects of decisions on this impact. Ultimately, the developed framework could be used to maximize stakeholder value through global optimization of the supply chain. To meet these ends, a mathematical optimization

based framework has been developed, which enables the inclusion of profitability measures and other techno-economic metrics along with process insights obtained from experimental as well as modelling and simulation studies.

3.2 Background and Possibilities

Current chemical and energy industries are heavily reliant upon fossil fuels as feedstocks, solvents, and sources of heat and power. However, because fossil fuels are not renewable, they are unsustainable as evidenced by estimates from the U.S. Department of Energy which state that proven and accessible fossil fuel reserves may only cover estimated production and consumption through the year 2030 (Doman, Staub et al., 2008). Furthermore, the use of imported fossil fuels may lead to economic and political vulnerability in having to deal with unstable regions and nations or companies whose interests are contrary to those of national security or the economy as a whole. Biomass, a renewable resource, has incredible potential to complement the use of fossil fuels in order to fulfill the energy and chemical needs of society while reducing environmental impact and increasing sustainability (Bridgwater, 2003). The process of separating biomass constituents for the purpose of conversion to value-added products and/or energy is known as biorefining, and the integrated polygeneration biorefinery has the potential to revitalize numerous industries through the development of new sustainable product lines (Bridgwater, 2003).

Sustainability on both economic and environmental fronts is achieved through the optimal use of renewable biomass feedstocks. A need exists for a process systems engineering (PSE) approach to ensure maximum economic return to a prospective firm and optimal societal benefit through minimizing the usage of raw material and energy resources. Furthermore, a holistic supply chain approach is needed in order to reduce and minimize

unnecessary costs involved in supply chain operations intrinsic to polygeneration. The bioprocessing industries have become increasingly aware of the benefits of incorporating PSE methods to this emerging field.

To maximize the applicability of such systematic methods and to integrate experimental and modeling work, a unique partnership has been established here as part of this project. This alliance consists of researchers in academia and industry along with government entities, equipment vendors and industry stakeholders to procure the wide range of information necessary such as data needed for process simulation models, information on capacity constraints, financial data, and nonlinear optimization techniques. The breadth of collaborative efforts infused into this framework ensures that the data used in the decision making process is realistic and that the research addresses problems of both industrial and regulatory interest. The primary goal of this work is to develop a system that will enable decision makers to evaluate different production pathways in biorefining in order to maximize net present value while measuring and minimizing environmental impact. This system is able to assist in evaluating the economic and environmental performance of polygeneration technologies, which may be constructed as a greenfield project, or retrofitted onto an existing facility. Ultimately this work could be incorporated into the foundation of a holistic methodology involving logistics and distribution that will provide assistance in all decision making along the supply chain from cradle to grave.

The motivation for this work lies in the ever-growing complexity of polygeneration pathways and processes emerging as a result of rapid technological advancement. In the forest-based products industry, new biomass-based polygeneration technologies are developed and pursued in order to bolster profit margins that are decreasing due to growing

competitive pressures. One predominant example within this industry is in the specific case of gasification of black liquor. Black liquor is a byproduct of the Kraft pulping process and is a mixture of spent liquor and a vast array of hydrocarbons extracted from the pulp. These hydrocarbons are separated from the black liquor when it is regenerated into white liquor to be reused in the pulping process. The hydrocarbons are combined with residual wood products that are unsuitable for pulp and paper production, and are traditionally burned to generate steam in Tomlinson boilers. However, at the end of the useful life of these boilers, they may be replaced with technology which would gasify these hydrocarbons to produce synthesis gas, which is a mixture of primarily hydrogen and carbon monoxide. This synthesis gas, or syngas for short, may then be used to make a wide variety of liquid fuels, chemicals, and power. In addition to the recovery of hydrocarbons from black liquor and conversion into salable products, hemicelluloses may also be extracted from wood feedstock before conversion into pulp and paper, and these hemicelluloses may be converted into a variety of chemicals and polymers including ethanol and acetic acid. Furthermore, trees absorb carbon dioxide from the atmosphere as they grow, while releasing oxygen, which causes an overall reduction in environmental impact compared to traditional pulp and paper mills.

While the retrofit of a biorefinery onto an existing pulp and paper mill demonstrated many possibilities to develop new product streams and reduce environmental impact, this example demonstrates only a small fraction of the options that may be taken into consideration when evaluating biorefining technologies. Figure 3.1 illustrates a more thorough flowchart of different classes of products that are made through biorefining technology, as well as the different chemical processes that are involved in order to manufacture these products (Sammons, Eden et al., 2006). Biorefining feedstocks include

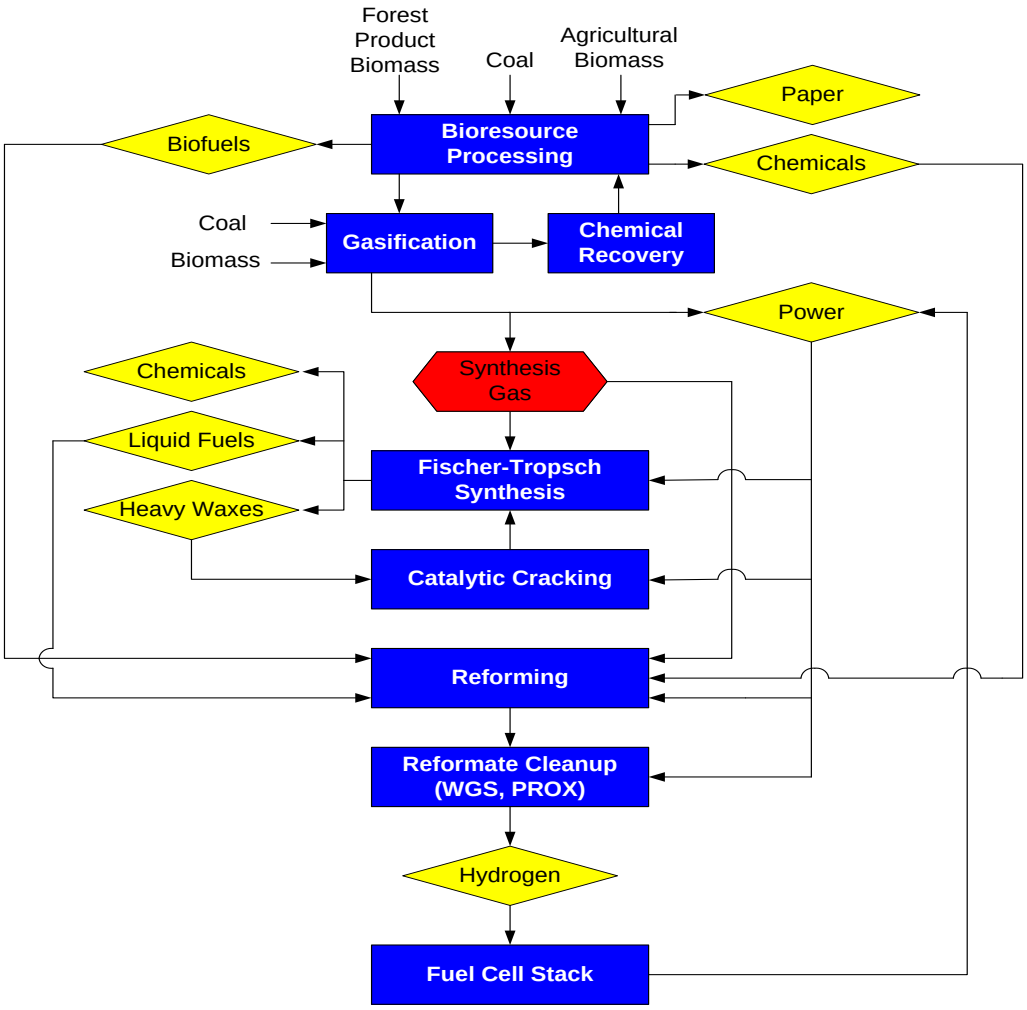

Figure 3.1 – Flowchart of biorefining technologies and corresponding product classes (Sammons, Eden et al., 2006).

forest products, agricultural products which include primary crops and crop residues, and coal in the case of clean coal technologies. These feedstocks may be directly processed into paper, chemicals, and biofuels. Residuals from direct biomass processing, such as the hydrocarbons extracted from black liquor in the previous example, and unprocessed feedstocks themselves may also be gasified to produce syngas and/or facilitate chemical recovery into the original biomass processing step. This syngas may be used to generate

power to be used internally by the facility or sold externally onto the public electricity grid. Syngas may also be used in Fischer-Tropsch synthesis to produce a wide variety of chemicals, liquid fuels, and heavy waxes, which may be broken down into lighter chemicals through catalytic cracking. Syngas, as well as other fuels and chemicals could be reformed to produce clean hydrogen for use in fuel cells, which will also produce power for internal or external use. It should be noted that this expanded example is not all-inclusive, and the growing technological prowess of biorefining means that more technologies and product classes will become feasible over time.

3.3 Presentation of Framework

As seen in the aforementioned examples, it is apparent that such a large number of possible process configurations and products results in a highly complex problem that cannot be solved using simple heuristics or rules of thumb. Business decision as well as policy makers must be able to strategically plan for and react to changes in market prices and environmental regulations by identifying the optimal product distribution as well as process configuration. Thus, it is necessary to develop a framework which includes environmental impact metrics, profitability measures, and other techno-economic metrics. Such a framework should enable policy and business decision makers to answer a number of important questions like:

- For a given set of product prices, what should the process configuration be, i.e. what products should be produced in what amounts?
- For a given product portfolio, how can process integration methods be utilized to optimize the production routes leading to the lowest environmental impact?

- What are the discrete product prices that result in switching between different production schemes, i.e. what market developments or legislative strategies are required to make a certain product attractive?
- What are the ramifications of changes in supply chain conditions on the optimal process configuration?

3.3.1 Methodology for Integrating Modeling and Experiments

The introduction of PSE methods into polygeneration research provides a systematic framework capable of seamlessly interfacing results generated in simulation studies as well as experimental work. Such a framework is imperative when attempting to combine knowledge and information from a variety of research areas and disciplines. The objective of this portion of the approach is to create a library of rigorous simulation models for the processing routes along with a database of corresponding performance metrics. Wherever possible, experimental data are used to validate the performance of simulation models, and for processes that commercial software packages are incapable of describing adequately, the performance metrics are initially based on experimental results until a satisfactory model has been developed.

Figure 3.2 shows a schematic representation of the strategy employed for identification of characteristic performance metrics of the individual subprocesses. First, it is necessary to develop a preliminary superstructure using the knowledge base available to the prospective design team. This superstructure may be product-focused, in which the feedstocks may be fully fixed or partially specified, and possible products are determined dependent on existing equipment and available technology as well as other considerations

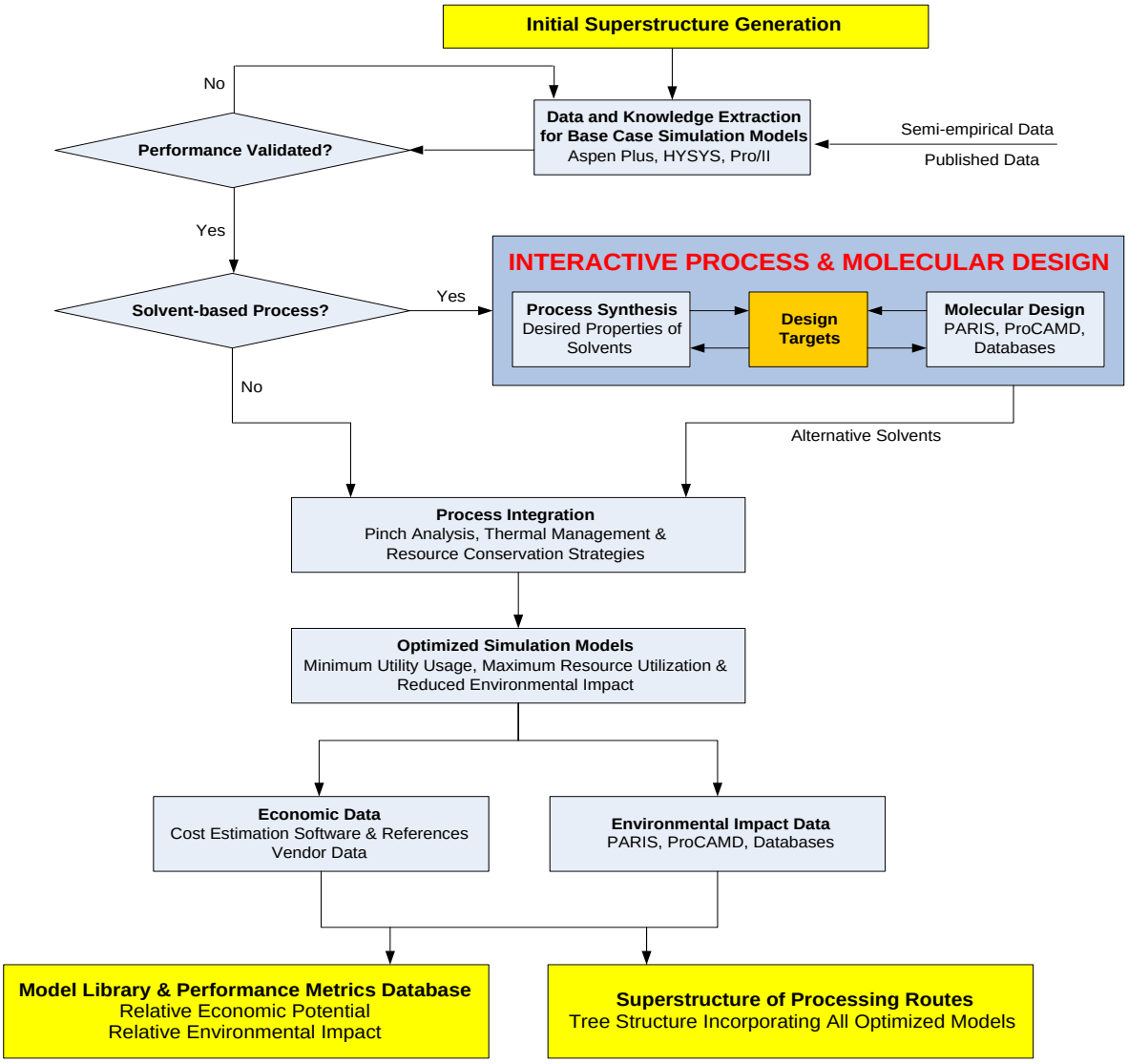

Figure 3.2 – Approach designed to generate library of models and performance metrics (Sammons, Eden et al., 2007).

such as existing customer networks, legal issues, and core competencies. Conversely, the initial superstructure may be feedstock-focused, in which the product streams are fixed or partially specified, and possible feedstocks are then discovered in order to achieve the specified product streams.

Information is then extracted from experimentation and literature in order to construct base case simulation models of the processes and pathways in the initial superstructure. The detail of these models may vary from complete to black-box models, and the number of process configurations should be limited since process options may be modified at a later stage in the framework. The simulation models for each process will be developed by extracting knowledge on yield, conversion, and energy usage from literature as well as experimental data. The following information should be extracted and recorded from these simulation models for their subsequent use in economic and environmental analysis:

- Approximate total capital cost based on accepted engineering methods
- Conversion rate from input to output for each separable process step
- Heating and cooling requirements
- Variable cost of unit outputs
- Outlet composition of product and effluent streams

If a given process requires the use of a solvent, computer-aided molecular design techniques and property clustering techniques should be employed to identify alternative solvents that minimize environmental and safety concerns. The solvent design problem can be solved utilizing either reverse problem formulation or mixed-integer nonlinear programming, but the combination of reverse problem formulation with property clustering have been shown to provide a robust solution (Eden, Jørgensen et al., 2000; Harper and Gani, 2000; Eljack, Eden et al., 2006).

Process integration techniques will then be used to optimize the simulation models. This is an integral step in the model development as it ensures optimal utilization of biomass and energy resources. Process integration refers to any method that will result in reducing the

energy and mass required for a chemical process, and as a result, process efficiency increases while reducing cost. Heat integration methods are used to minimize the amount of energy needed for a process in the forms of external heating and cooling utilities, while mass integration focuses on recapturing mass that may be harmful for the environment, which serves the twofold goal of waste minimization and pollution prevention.

Finally, the optimized models will be used to generate data for the economic as well as environmental performance metrics. The end result is a superstructure of all the possible processing routes, a library of simulation models for those routes, and a database of economic and environmental metrics for the simulation models.

3.3.2 Methodology for Biorefinery Allocation Optimization

The optimization framework is given in Figure 3.3, and it combines the library of processing routes and corresponding economic performance metrics with a numerical solver in order to obtain candidates that achieve optimal economic performance (Sammons, Eden et al., 2008). The relative environmental impact of these candidate solutions is also measured, and the candidates are ranked based on their relative impact scores.

It should be noted here that the environmental performance is not included in the objective function measuring profitability. Environmental impact is difficult to quantify in terms of profit or net present value unless there were monetary penalty functions applied to the categories of impact, thus making it impractical to include environmental impact in the objective function of gross profit. Multi-objective optimization in which Pareto solution curves are defined will result in environmental impact indicators being minimized (Pistikopoulos, Stefanis et al., 1995). But because maximum shareholder value is attained

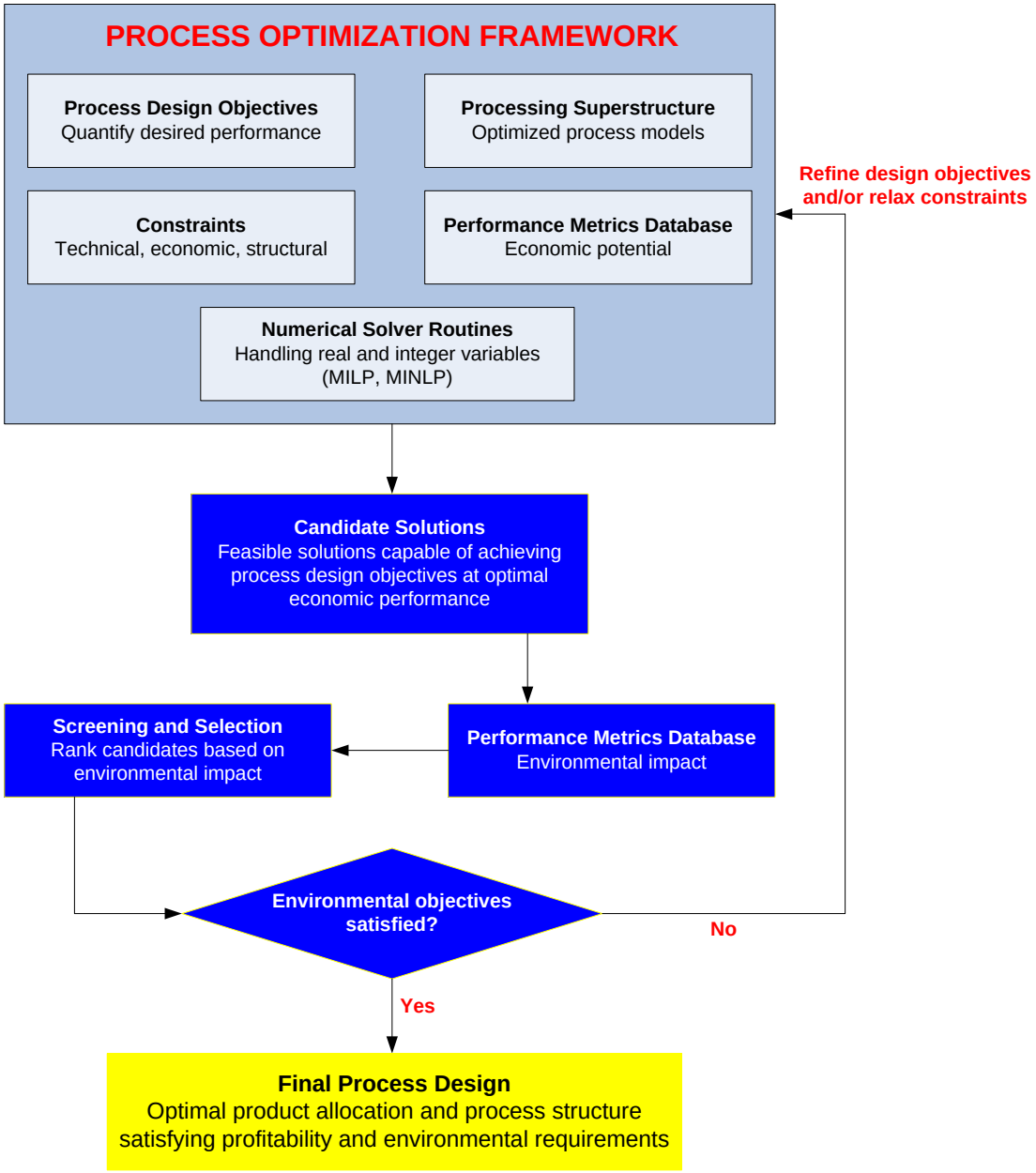

Figure 3.3 – Framework for determining optimal biorefinery allocation options (Sammons, Eden et al., 2008).

only with optimal economic performance, these solutions with minimized environmental impact would not be pursued since the solutions could have an adverse effect on shareholder value in comparison to the economic optimum. One example of this is if optimization were to

focus on purely minimizing environmental impact, in which the framework would consequently identify the trivial zero impact facility as a solution, corresponding to no biomass being processed at all and no value being added to the firm or industry in question.

Since multi-objective optimization is impractical without monetizing environmental impact, the objective of the optimization step is to use pre-existing, robust optimization programs to identify candidate solutions that maximize economic performance. The candidates are then ranked according to environmental performance, and thus, environmental performance is used as a screening tool. If a candidate satisfies the environmental objectives, then the optimal production scheme has been identified. If none of the candidates satisfy the environmental impact constraints, then the desired economic performance requirements are relaxed until a solution with acceptable environmental performance has been identified. It should be emphasized that by decoupling the complex models from the optimization and decision making framework, the methodology is more robust and also provides added flexibility by only having to update the performance metrics for a given process as new information, e.g. a new catalyst with higher conversion, is identified. This approach is analogous to the reverse problem formulation framework used for decoupling the complex constitutive equations from the balance and constraint equations of an individual process model (Eden, Jørgensen et al., 2004). The design targets linking the two reverse problems are constitutive or property variables, which in this framework are represented by performance metrics.

3.4 Optimization Problem Formulation

Optimization is used to maximize economic performance while measuring and minimizing environmental impact, but before optimization can be utilized, some form of superstructure must be constructed. From this superstructure, data on fixed and variable cost can be extracted for use as scalars in the optimization problem. The decision variables are the products to be manufactured and the pathways utilized to attain the optimal product portfolio.

3.4.1 Superstructure Example

Many references to process superstructures have been made up to this point, and Figure 3.4 depicts a generic example of such a superstructure (Sammons, Eden et al., 2008). In this superstructure, a given bioresource *m* has many options for conversion into a range of products that can be sold to market and/or processed further into other salable products. It should be noted that for problems in which the products are fixed and the bioresources are the decision variables, this superstructure would essentially have the same form except with different biomass feedstocks replacing the possible products.

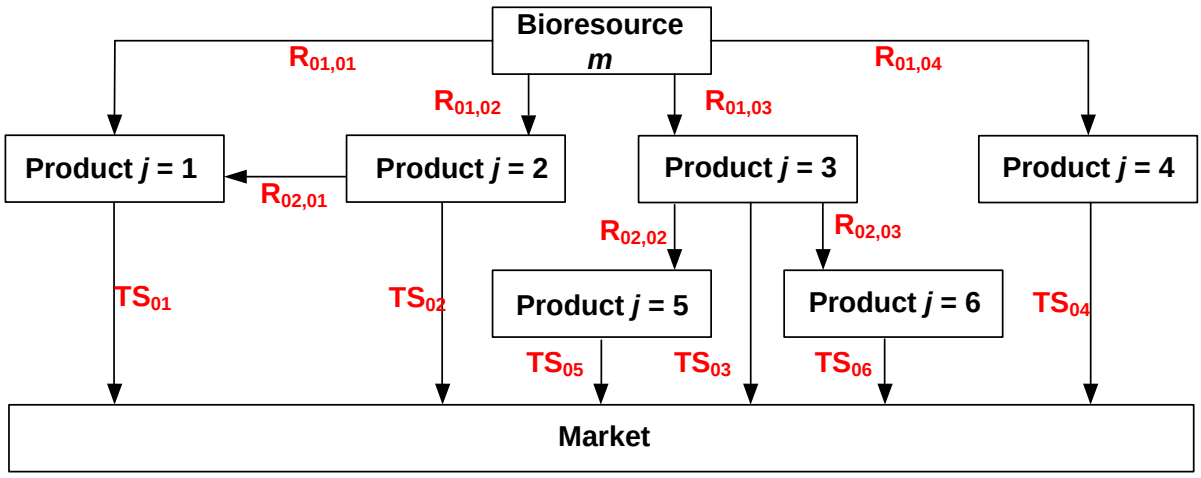

Figure 3.4 – General example of process superstructure (Sammons, Eden et al., 2008).

In Figure 3.4, internal production routes take on the form of R_{ij}, in which i is the number of processing steps away from the raw material (i.e. 1 for direct raw material processing, 2 for subsequent processing step, etc.) and j represents the product or intermediate being made at that particular processing level. External market pathways are denoted by TS_k, where k represents the particular salable product.

3.4.2 Optimization of Economic Metrics

There are many methods through which the economic performance of these chemical processes may be evaluated, but two of these methods are studied in-depth in this work. The Gross Profit method measures revenues minus costs over a pre-determined time basis, and is simple, less computationally expensive, and does not have the need for predicting future economic conditions. On the other hand, the Net Present Value method is better for longer time horizons, is more robust, and takes into consideration issues such as policy changes, tax incentives (or penalties), hedging, and different depreciation schedules.

Fixed cost and variable cost are the two main components needed for the Gross Profit method, and the optimized processes present in the superstructure provide adequate economic data in order to calculate both cost components. The fixed cost component is determined by looking at the list of equipment necessary for the given simulation model, adding up the cost for this given capacity, and determining the cost for a host of different capacities, which is converted into an equation that shows fixed capital investment as a function of capacity. In the very limited case of straight line amortization and not any other depreciation schedule, the amortized function is divided by the amount of product made over a given time period to determine fixed cost per product flow per time. Variable costs are

determined using established methodologies and again divided by product throughput over time to determine variable cost per output basis (Peters, Timmerhaus et al., 2003). The fixed cost and variable cost per output are then entered into an objective function in the form of Problem P3.1:

$$\max Profit = \sum_{m}\left(\sum_{k} TS_{mk}\, C_{k}^{S} - \sum_{i}\sum_{j} R_{mij}\, C_{mij}^{P} - C_{m}^{BM}\sum_{j} R_{m1j}\right) \qquad \text{(P3.1)}$$

Using this nomenclature, the first set of terms in Problem P3.1 represents the sales revenue from the products made from each bioresource *m*. TS_{mk} is a variable that denotes the production rate of product *k* from bioresource *m* that is sold to the market. C_k^S is the sales price of product *k* which is a scalar and is determined through a survey of published prices and vendor quotes. The second set of terms represents the total processing cost incurred by the pathways pursued in production. R_{mij} is a variable that represents the processing rate of route *ij* while C_{mij}^P is a scalar that represents the cost of processing bioresource *m* through route *ij* and is the sum of the fixed and variable costs per unit output discussed previously. The third set of terms represents the total cost of the biomass resource *m*, and this is broken down into the scalar purchase price of bioresource *m* in C_m^{BM} and the combined rate of biomass processed by the plant in R_{m1j}. Although both TS_{mk} and R_{mij} are variables in the optimization program, they are not independent since the variables are related to each other via mass balance constraints around the product points.

Because of the robustness of the NPV method, much more information is needed in addition to the fixed cost and variable cost data needed for the Gross Profit method, which is depicted as an objective function in Problem P3.2:

$$\max NPV = \sum_t \left[\frac{GP_t(1 - Tax_t) + Dep_t Tax_t - Hedge_t + Gov_t}{(1+R)^t} \right] \quad \text{(P3.2)}$$

$$\mathrm{GP_t} = \sum_m \left(\sum_k TS_{mkt}\, C_{kt}^S - \sum_i \sum_j R_{mijt}\, C_{mijt}^P - C_{mt}^{BM} \sum_j R_{m1jt} \right)$$

The gross profit for a given time period *t* is calculated in a similar fashion to the gross profit method and then inserted into the objective function. One must also specify the window of time over which to apply the methodology and a marginal tax rate Tax_t at which decisions are made. The term Dep_t represents tax credits due to depreciation, and this allows for the flexibility of differing depreciation schedules for different equipment as well as pursuing advantageous depreciation strategies. $Hedge_t$ represents expenses associated with hedging against unforeseen market changes and risk. Gov_t represents possible government rebates or penalties associated with current or probable future policy issues that favor or penalize the production pathways or products in the models. The sum of gross profit and these auxiliary factors are all divided by $(1+R)^t$ so that all revenue streams are adjusted based on the expected rate of return, *R*, in order to take into consideration the time value of money.

While the objective function is designed to maximize the performance metrics of either gross profit or net present value, both forms are subject to the same classes of constraints. Conversion factors dictate how much output will result from processing a certain amount of input, and these factors are then implemented into mass balances around the chemical processes. Figure 3.5 presents a visualization of the variables and parameters to be used in the mass balances, and this class of constraints takes on the following form:

$$\sum_l CF_l * R_{mijl} = \sum_n R_{m(i+1)j'n} \quad (3.1)$$

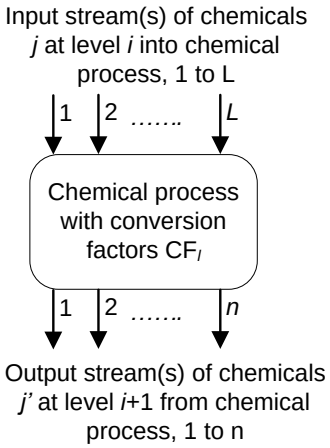

Figure 3.5 – Variables and parameters necessary for mass balance constraints.

In Equation 3.1, CF_l represents the conversion factor of each incoming stream l to be used to convert it into outgoing stream n, R_{mijl} is the amount of input into the chemical process, and $R_{m(i+1)j'n}$ is the output of the specified process.

There may be specific examples in which a maximum process capacity or customer demand for a product may result in the framework suggesting that multiple processes are built in order to maximize gross profit or net present value. To avoid reaching this solution, it is indeed possible to introduce mixed integer constraints that will restrict the framework into exploring only solutions in which a single primary product is manufactured in a polygeneration facility that will still produce secondary chemical products or services such as heat and power. Equations 3.2-4 specify the general forms of these constraints:

$$\sum_j y_{ij} = 1 \qquad i = 1 \tag{3.2}$$

$$\sum_j y_{ij} = \sum_j y_{(i-1)j} \qquad i = 2,3,\dots I \tag{3.3}$$

$$R_{mij} < M * y_{ij} \tag{3.4}$$

In these constraints, the variable y_{ij} represents a binary variable that may only have values of either 0 or 1. The first constraint ensures that in the first level of processing, which is direct processing of the raw material, only one pathway is activated. The second set of constraints holds for all subsequent levels of processing and enforces that a downstream pathway is only activated if an upstream pathway is activated and leads into a relevant process that will result in usage of the downstream pathway. The third constraint is known as a Big-M constraint, in which M is sufficiently large enough so that if the particular y_{ij} value is 1, then there would be no additional restriction on R_{mij}, but if the value is 0, then R_{mij} is forced to be zero as well (Biegler, Grossmann et al., 1997). In addition to constraints on mass balances and single process configurations, constraints on maximum feedstock amounts and maximum processing capacities, examples of which are reserved for the case study examples, also play vital roles in the optimization problem.

3.4.3 Measurement of Relative Environmental Impact

The measurement and minimization of environmental performance is decoupled from economic performance, and relative environmental impact is quantified through the use of the US-EPA Waste Reduction (WAR) algorithm (Young and Cabezas, 1999). As discussed previously, the WAR algorithm measures the environmental impact of mass flows that are entering and leaving both the chemical process and the corresponding process that provides energy to the chemical process, and combines the potential environmental impact of these streams based on a weighting factor and normalized score.

Profitability metrics are very intuitive in that most of the metrics are in terms of monetary currency or a percentage return on investment, but environmental impact is not as

simple to understand. First, potential environmental impact (PEI) must be determined on either an output basis or a generation basis, and this impact must also be accounted either in terms of PEI/time or PEI/mass of product (Cabezas, Bare et al., 1999). Once both decisions have been made for the chosen accounting basis, the appropriate equations are then used to calculate PEI on a per time or per mass of product basis. Equations 2.7-10 have been reproduced here to illustrate how the generated environmental impact may be calculated, while Equation 3.5 should be used in conjunction with Equations 2.8 and 2.10 if the output PEI is chosen as the basis. It should be noted that the following equations result in the evaluation of PEI on a per time basis, but in order to use a PEI per mass of product basis, mass balances are used to determine the mass flowrates for all input and output streams based on a given production output.

$$\dot{I}_{gen}^{(t)} = \dot{I}_{out}^{(cp)} - \dot{I}_{in}^{(cp)} + \dot{I}_{out}^{(ep)} \tag{2.7}$$

$$\dot{I}_{out}^{(t)} = \dot{I}_{out}^{(cp)} + \dot{I}_{out}^{(ep)} \tag{3.5}$$

$$\dot{I}_{out}^{(cp)} = \sum_{j}^{cp} M_j^{out} \sum_{k} x_{kj} \Psi_k \tag{2.8}$$

$$\dot{I}_{in}^{(cp)} = \sum_{j}^{cp} M_j^{in} \sum_{k} x_{kj} \Psi_k \tag{2.9}$$

$$\dot{I}_{out}^{(ep)} = \sum_{j}^{ep-g} M_j^{out} \sum_{k} x_{kj} \Psi_k \tag{2.10}$$

To review, M_j^{out} and M_j^{in} represent the mass flowrate of stream *j* leaving or entering the process, x_{kj} represents the mass fraction of a given chemical *k* in stream *j*, Ψ_k represents the environmental impact score of chemical *k*, and the summation superscript *ep-g* represents gaseous emissions from the energy generation process (Cabezas, Bare et al., 1999). By

decoupling the economic and environmental criteria, potential environmental impact can then be used as a screening tool for the most economically appealing process decisions. It is also possible to construct pareto-optimal curves which can be used to qualitatively visualize profitability against adverse environmental impact and determine the trade-offs, if any, between the two.

3.5 Preliminary Results

The generalized model, in which the objective function and constraints are linear, is easily solved using commercially available optimization software. It should be noted here that while earlier works incorporate process models into the optimization problem, the proposed framework separates the wide range of polygeneration models from the optimization portion, thus reducing the complexity of the problem for the solver while maintaining the robustness achieved with proven optimization techniques (Sahinidis, Grossmann et al., 1989).

Many adjustments were made to the parameters such as sales price, processing cost, processing rate conversions, and capital investment functions, and constraints were added on capacity as well as minimum and maximum sales quantities. These modifications were made to determine if the algorithm would give the product distributions that were intuitively determined to maximize profit. In every case, the code returned the solutions including predictable results on the product distribution as well as the pathways necessary to manufacture the product while maximizing value.

Without including any constraints on capacity of the processing steps, the solution is a single-product configuration in which all available biomass is converted into the most

profitable product. The most profitable product is defined as the one with the highest contribution margin, which is calculated as unit revenue minus unit variable cost. However, if constraints are imposed on the most profitable route, the framework identifies the additional products and processing routes required to maximize the overall profit. The framework seeks products with the next highest contribution margin, thus leading to a polygeneration facility (Sahinidis, Grossmann et al., 1989).

In order to effectively address the strategic planning objectives of business decision makers, it is necessary to incorporate the total capital investment as a constraint in the formulation. The capital investment for a given unit or process can be approximated as a function of its capacity or processing rate, and approximate capacity constraints are based on a variety of sources, e.g. existing equipment, vendor data and qualitative process information provided by academic and industrial collaborators. Both linear and nonlinear expressions for capital investment in terms of capacity have been successfully implemented in the framework. Inclusion of capital cost constraints is crucial for practical application of the results, i.e. enabling evaluation of the potential benefits to be obtained for a given maximum investment by retrofitting an existing facility or constructing new plants.

While environmental impact and economic profitability are indeed decoupled in this methodology, both factors are critical in determining which polygeneration pathways should be pursued in order to add value while maintaining a minimal level of environmental impact. The framework is capable of calculating the level of environmental impact through the use of the EPA WAR algorithm, and this data may be plotted against economic performance to construct a pareto-optimal curve that depicts the ideal environmental impact at each level of profitability, or vice versa. Pareto-optimal curves of this nature have been successfully

constructed and have been utilized to illustrate the trade-off between economic and environmental performance.

3.6 Summary

A systematic framework has been presented in order to assist decision makers in evaluating the economic potential and environmental impact of the implementation of polygeneration technology, and Figure 3.6 reviews the necessary steps of the methodology. Process system engineering methods are widely used in order to simplify the problem into one which can be solved while still taking into account important economic and environmental factors. The framework allows decision makers to allocate polygeneration

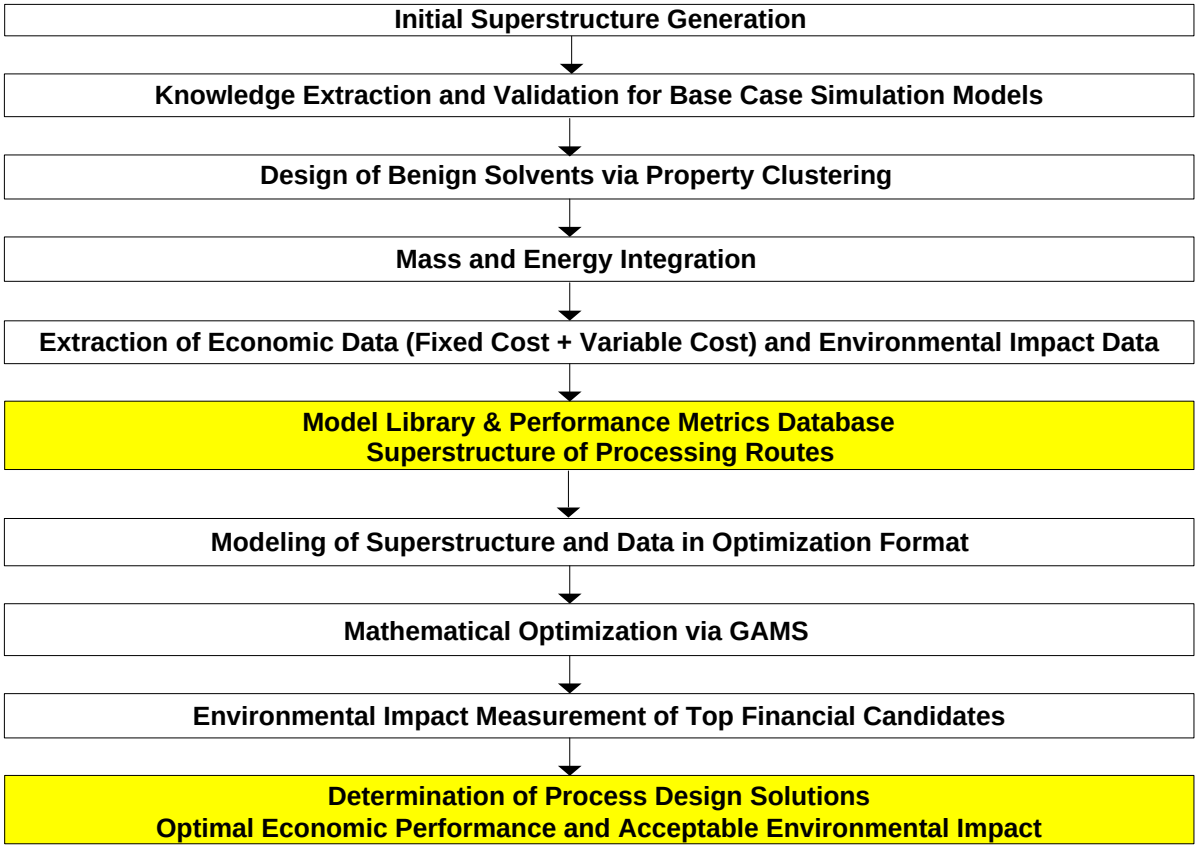

Figure 3.6 – Summary of polygeneration production allocation methodology.

resources to specific pathways in order to maximize economic performance given fixed market prices. Conversely, the allocation solution may be held constant while market prices become variable, which allows the framework to determine the price points at which the allocation solution may change from one pathway to another. Because of the novelty of biorefining technology, process integration plays a vital role in reducing the process costs inherent with chemical processes, and this is done by pursuing mass and energy integration simultaneously. Finally, supply chain conditions such as supply and demand location, supply density, transportation issues, and customer agreements are also critical in evaluating the long-term profitability of various polygeneration pathways.

Chapter 4

Case Studies

4.1 Introduction

The objective of the framework presented in this work is to provide a systematic methodology that can be ultimately utilized by decision makers in industry, government, and academia to evaluate the economic and environmental merits of novel biorefining polygeneration technology. The flexibility of this methodology allows for an expedient incorporation of changing technological or market conditions into the existing decision analysis network. As a result, managerial entities will realize increased responsiveness to these changing conditions, be able to measure the economic and environmental impact of those changes, and quantify and convey those impacts to concerned stakeholders.

To demonstrate how this methodology may be applied to decision analysis in realistic polygeneration scenarios, it is imperative to develop case study examples that clearly illustrate the formulation and solution of product allocation problems within the framework. In these examples, an initial superstructure is constructed in order to visualize the number of potential polygeneration routes, and in the event that this number is considered to be too large for adequate analysis, pre-screening may be used to reduce the possibilities to a finite number of pathways. Simulation models are then constructed for these process-product combinations, and these models are optimized through solvent replacement and process integration. From these models, the necessary economic and environmental data may be

extracted for use in optimization and screening, and as a result, pareto-optimal solutions may be determined resulting in high levels of profitability and minimal levels of environmental impact. Furthermore, the presented methodology may be modified to study different metrics of economic profitability, and as a result, both short-term and long-term decisions may be pursued.

4.2 Case Study: Chicken Litter Biorefinery

To illustrate the application of the framework, a simple case study was performed on a potential biorefinery involving the conversion of chicken litter to syngas. Chicken litter is not considered to be an environmental hazard when it is traditionally used as a fertilizer for farmland. However, when chicken litter is over-applied, contaminants accumulate in soil and surrounding water sources due to its high concentration of phosphorus and nitrogen. This waste product can be gasified into syngas, which could be either sold on the market via a pipeline to a local customer, or converted on site into hydrogen or electricity. Conversion into hydrogen takes place through a water gas shift reaction, while electricity is produced through the usage of a combined cycle power island. Base case simulation models were constructed, and data on conversion rates for yields on the gasification, electricity generation, and water gas shift reaction were obtained from literature (Larson, Consomi et al., 2006; Gadhe and Gupta, 2007). In this example, there are no solvents involved in any of the aforementioned processes, so the step of using property clustering to find safer, more environmentally sound solvents is bypassed. Figure 4.1 shows the simplified superstructure of possible pathways for production and sale of these chemicals on the commodity market, and Figs. 4.2-4 illustrate the simulation models used in the case study (Sammons, Eden et al.,

2007). Due to the complexity of the combined cycle power island, a black box power generation model is presented for simplicity. Because the purpose of this case study is merely to demonstrate the formulation of the optimization part of this problem, issues such as environmental impact, solvent selection, and process integration are omitted. Furthermore, for the sake of simplicity and due to the lack of data available to employ the Net Present Value method for economic valuation, the Gross Profit method is utilized.

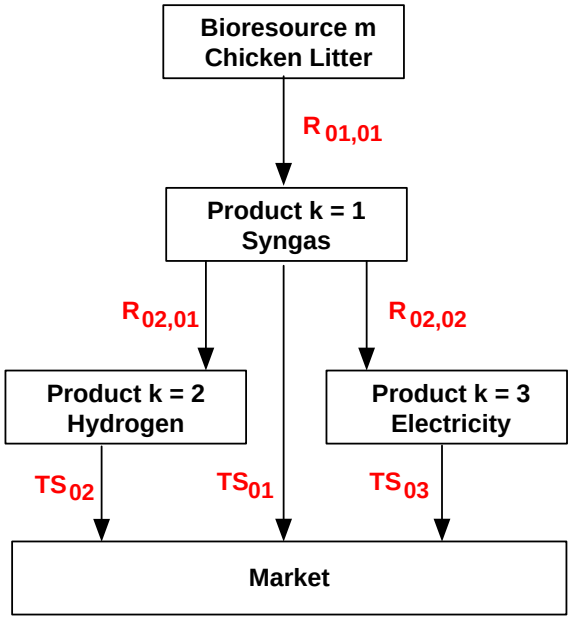

Figure 4.1 – Chicken litter biorefinery: Unsolved decision tree with variable designations (Sammons, Eden et al., 2007).

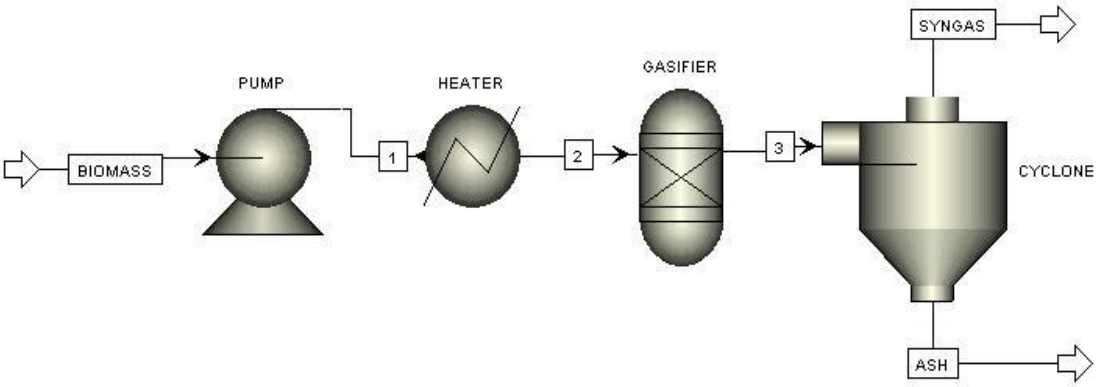

Figure 4.2 – Biomass to syngas simulation model.

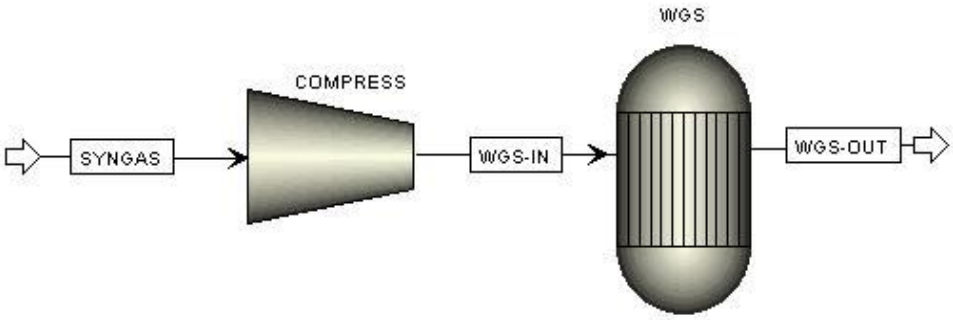

Figure 4.3 – Syngas to hydrogen simulation model.

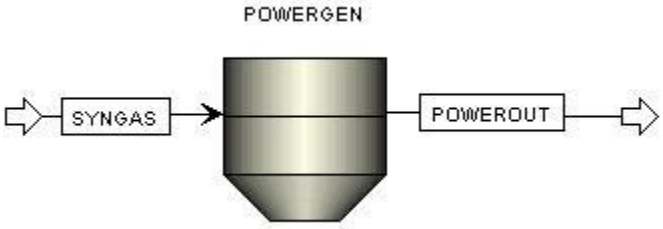

Figure 4.4 –Syngas to power black-box model. Details of equipment used in combined-cycle power island can be found in (Larson, Consomi et al., 2006).

In order to evaluate the economic performance of the three processes, it was necessary to procure information on the scalars C_{mk}^{s}, or market sales price of product k; C_{m}^{BM}, or biomass feedstock price; and C_{mij}, or the combined fixed cost and variable cost per unit output. The market prices of products and biomass were determined through a survey of suppliers, and these prices are listed in Table 4.1. However, the calculation involved to determine the combined fixed cost and variable cost is much more detailed since it is necessary to procure detailed economic data on fixed and variable cost.

The equipment needed for the simulation models was used to determine the fixed cost components of all three processes, and the prices of the individual components are detailed in

	Market Price
Chicken litter feedstock	$0.010/kg
Syngas	$0.214/kg
Electricity	$53.370/MW
Hydrogen	$0.220/$m^3$

Table 4.1 – Market prices for feedstock and final products for chicken litter biorefinery.

Appendix A. Similarly, variable cost was determined using pre-defined design heuristics, and the variable cost is a sum of utilities, operating labor, operating supervision, maintenance, operating supplies, laboratory charges, overhead, and administrative cost as defined by those heuristics, and detailed variable cost information is also listed in Appendix A (Peters, Timmerhaus et al., 2003). Annualized fixed costs at cost of capital R over the defined time window are determined, and then added to annual variable costs and divided by total output in order to determine C_{mij} in terms of fixed and variable cost per unit output, and this information is detailed in Table 4.2.

In this example, the objective function to be maximized is as shown in Problem P4.1:

$$\max Profit = Revenue_{syngas} + Revenue_{hydrogen} + Revenue_{electricity} - Cost_{syngas} - Cost_{hydroge\ n} - Cost_{electricity} - Cost_{feedstock} \quad \text{(P4.1)}$$

	Biomass to Syngas	Syngas to Electicity	Syngas to Hydrogen
Total Fixed Cost	$112,302,000	$100,091,000	$461,527,000
Annualized Fixed Cost @ 8% interest over 25 years	$10,401,000	$9,270,000	$42,745,000
Total Variable Costs	$13,618,000	$15,301,000	$202,114,000
Total Annual Product Costs	$24,019,000	$24,571,000	$244,859,000
Annual Output	$4.018*10^8$ kg	$1.065*10^6$ MW	$8957*10^8$ m^3
Cost per Output	$0.0598/kg	$23.07/MW	$0.273/$m^3$

Table 4.2 – Calculated cost per output of each model in chicken litter biorefinery.

This objective function is subject to constraints based on mass balances of the individual processes in which a multiplicative conversion rate has been determined based on the simulation models so that the conversion of feedstock to output of a given process is linear. The optimization program also contains constraints on the amount of feedstock available, so that a pre-determined feed basis will determine how much is produced, which in turn will be related to gross profit through market prices, processing cost, and feedstock cost.

Due to the simplicity of the problem, the optimization was executed in one iteration through the use of CPLEX in GAMS in 0.035 seconds and determined the optimal objective value of $1.922/s profit (GAMS, 2009). The execution of the optimization code verified the results obtained from manual calculation; producing syngas from chicken litter and selling it on the market would maximize profit due to the high costs involved in converting the syngas to hydrogen or electricity. Figure 4.5 illustrates the active pathway chosen by the optimization program (Sammons, Eden et al., 2007).

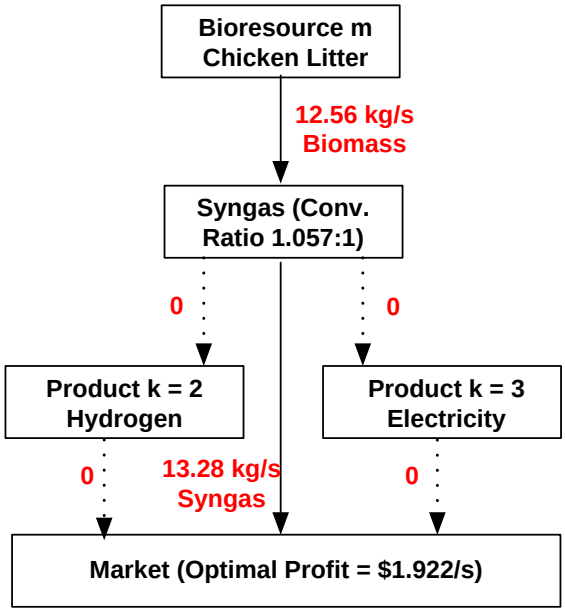

Figure 4.5 – Chicken litter biorefinery: Solved decision tree with flowrate and objective values (Sammons, Eden et al., 2007).

4.3 Case Study: Product Portfolio Design

Systematic design and analysis methods are crucial in determining the overall economic value, environmental impact, and supply chain conditions for pursuing chemical polygeneration process pathways in order to produce a variety of chemicals. Platform chemicals are used as the starting point for subsequent process and product decisions, and chemicals that can be manufactured from the same starting platform compose what is known as the product family. Product platforms and product families combine to form product portfolios, and product portfolio design refers to the systematic approach to solving the overall polygeneration decision-making problem not just in terms of what chemical products should be made and in what quantities, but how this list of products is enumerated, developed, and evaluated.

The polygeneration product allocation framework may be used as a single tool within the greater methodology concerning chemical product portfolio design. This larger methodology is presented in external literature (Solvason, Sammons et al., 2010), but will be summarized here to provide clarity as to the importance of the product allocation framework in the overall portfolio design methodology. Given a feedstock of relevance that can be utilized in a polygeneration facility, first systematic computational methods in combination with a thorough literature search must be utilized to determine the feasible products that can be made from the given feedstock as well as the necessary reaction networks for those products (Broadbelt, Stark et al., 1994; Broadbelt, Stark et al., 1995; Solvason, Sammons et al., 2010). While the superstructure enumeration is proficient at accounting for the majority of possible chemical products, it is necessary to utilize a pre-screening method which will pare the superstructure down to a finite number of processes for further evaluation.

Once the potential superstructure has been narrowed down from a large number of possibilities to a finite list of potential chemical product platforms, a superstructure is then created to enumerate the candidate platform chemicals. The process options listed in the superstructure are then synthesized using traditional process synthesis methods based on the information available in either in literature or in practice. The synthesized processes are then designed in detail in order to procure the necessary information needed for economic and environmental analysis, as well as analysis of other factors necessary in a multi-criteria decision making matrix, or MCDM (Wang, Jing et al., 2009). This methodology is then repeated for the most promising chemical platform(s) in order to determine possible chemical products based on these platforms and evaluate potential product possibilities on economic, environmental, and other aspects of technical performance.

In this specific case study, the feedstock of interest is assumed to be pure cellulose as an initial simplification of the pulping process in a theoretical pulp and paper facility. A base case is selected in which cellulose is converted to ethanol through an existing and mature commercial process (Wooley, Ruth et al., 1999). Utilizing a combination of superstructure enumeration, literature review, and existing expertise, a list of twelve potential chemical platforms derived from cellulose was developed (Solvason, Sammons et al., 2010). Figure 4.6 demonstrates the initial superstructure of cellulose-based chemical product platforms.

From this list of twelve potential platforms, it was then necessary to perform pre-screening in order to determine which possibilities would hold the most promise in terms of economic profitability. To do this, a quick, efficient calculation may be used to determine the Profitability Upper Bound (PUB), which is an estimate of the theoretical amount of value added to the supply chain from a certain product/process combination (Solvason, Sammons

et al., 2010). This approximated PUB is calculated by multiplying a given feedstock mass m_j by its market price per mass P_j, multiplying the calculated output mass of the products m_i by their market prices, P_i and subtracting the input from the output. Equation 4.1 illustrates the necessary equation, and Table B.3 in Appendix B lists the twelve chemical platforms and their PUB calculation values.

$$PUB = \sum_{i=1}^{products} m_i P_i - \sum_{j=1}^{inputs} m_j P_j \tag{4.1}$$

To determine the mass flowrates in and out of each process, one must first set an input basis to be used for each PUB calculation, and in the instance of this case study, that input basis was pre-determined to be 100 kg of cellulose. In order to determine the mass out of each

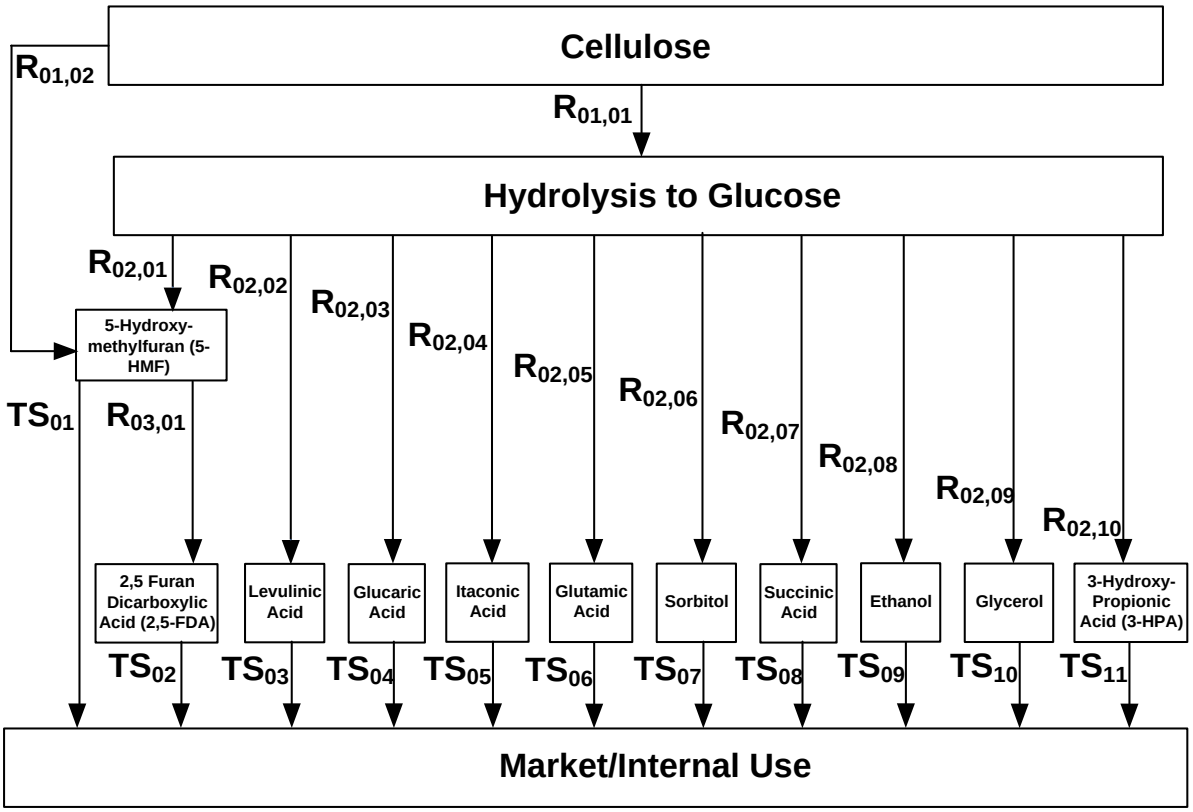

Figure 4.6 – Validated superstructure of chemical platforms based on cellulosic feedstock (Solvason, Sammons et al., 2010).

salable product, yields and conversions were extracted from literature in order to construct quasi-chemical reactions used to calculate the mass output of each product within an order of magnitude of error. Table B.1 in Appendix B lists the calculated output of each possible process within the initial superstructure with a basis of 100 kg of cellulose as starting material.

While the market price of cellulose and some of the chemical platforms are readily available from market data or vendor inquiries, it should be noted that price data for novel biorefinery products may not be available due to a lack of a bulk market at the time of evaluation. To approximate the bulk price based on lab prices of smaller quantities, a widely used correlation is invoked, in which P represents price, Q denotes quantity, and the subscripts B and L represent values at the bulk and lab scale respectively (Solvason, Sammons et al., 2010):

$$P_B = P_L \left(\frac{Q_B}{Q_L}\right)^{-0.75} \tag{4.2}$$

Table B.2 contains a list of the prices of all chemicals for which PUB calculations were performed, as well as whether or not this lab to bulk scale-up correlation was used in estimating the price. Table B.3 contains the PUB calculations performed for all validated processes present in the initial superstructure.

Due to the nonexistence of a bulk market for the chemicals 2,5-FDA, glucaric acid, and 5-HMF, the pricing correlation listed in Equation 4.2 was used to estimate the bulk price of these specialty/pharmaceutical chemicals to be an incredibly high number on a mass basis. As a result, the PUB calculations were unrealistically high (e.g. 100 kg of cellulose yields greater than $US 18,000 of glucaric acid and $US 300,000 of 2,5-FDA and 5-HMF!), and had to be temporarily discarded until evidence of a bulk market and realistic bulk prices

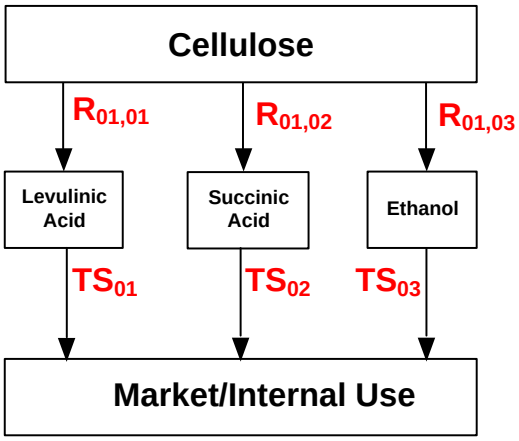

Figure 4.7 – Modified superstructure for cellulose to first level of platform products (Solvason, Sammons et al., 2010).

become available. However, succinic acid, levulinic acid, and ethanol showed approximated PUB values in the range of $200-$300 per 100 kg of cellulose, which were realistic yet profitable values. These three chemical platforms were then chosen to be further analyzed ultimately using the polygeneration product allocation framework, and Figure 4.7 illustrates the modified superstructure for analysis of the conversion of cellulose into these three most promising platforms (Solvason, Sammons et al., 2010).

In order to utilize the framework to determine the value of these chemical platforms, it was then imperative to synthesize and design the processes for the chemical conversion of cellulose to succinic acid, levulinic acid, and ethanol. Because the process conditions for fermentation of cellulose into ethanol and succinic acid are very similar, Figure 4.8 depicts the process flow diagram of both chemical processes (Wooley, Ruth et al., 1999).

However, the conversion of cellulose into levulinic acid occurs through a more complex sulfuric acid catalysis known as the Biofine process (Bozell, Moens et al., 2000). In this particular process, formic acid is formed as a byproduct, and since formic acid forms an

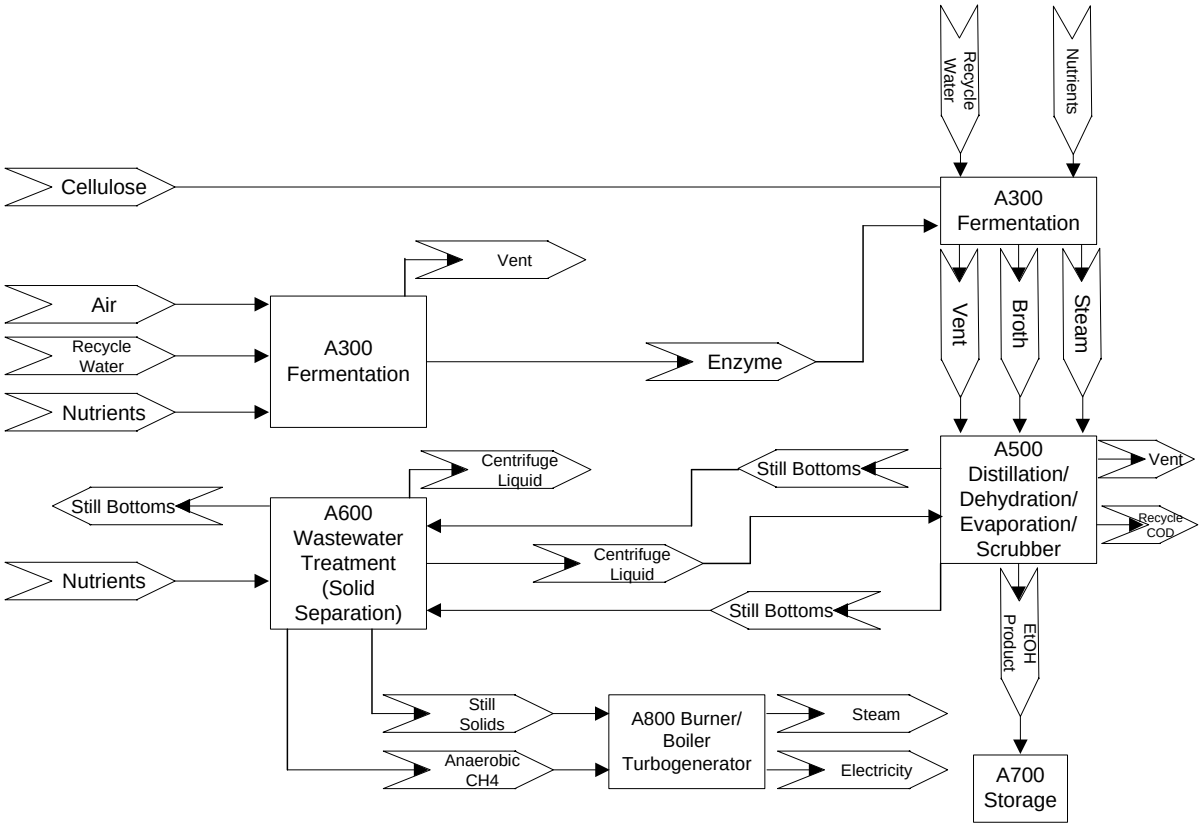

Figure 4.8 – Flow diagram representing both cellulose to ethanol and succinic acid processes (Wooley, Ruth et al., 1999; Solvason, Sammons et al., 2010).

azeotrope with water, the distillation/evaporation combination in the ethanol and succinic acid processes may not be used to purify the product stream. Instead, an amine separation unit, consisting of a flashing unit and amine regernation column, is implemented in which chemical absorption is used to break the water-formic acid azeotrope, and this modified process flow diagram is shown in Figure 4.9.

For the base case of cellulose to ethanol, all material balances, energy balances, equipment sizing, and capital cost derivations are completed and used as the basis for the other chemical processes (Wooley, Ruth et al., 1999). In the designed and synthesized processes, the cellulose feed rate specified in the original cellulose-to-ethanol base case is

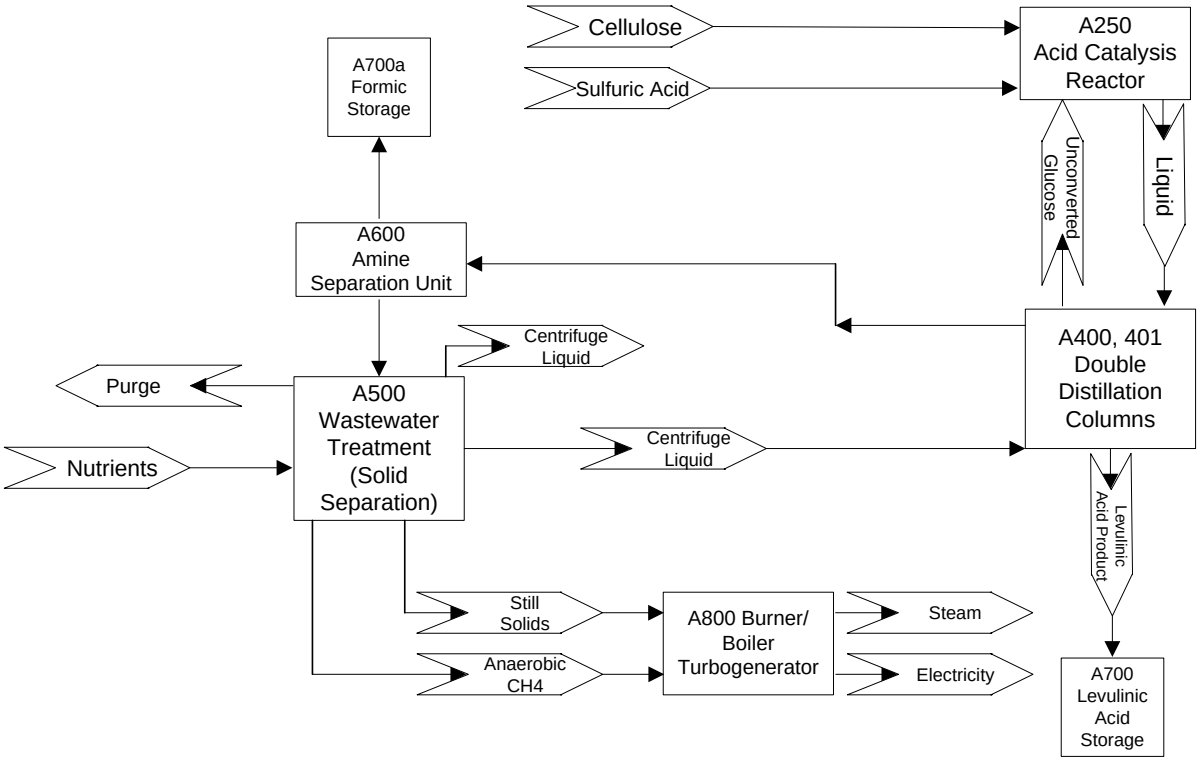

Figure 4.9 – Flow diagram of cellulose to levulinic acid process (Wooley, Ruth et al., 1999; Bozell, Moens et al., 2000; Solvason, Sammons et al., 2010).

utilized for the levulinic acid and succinic acid. The algorithms, scaling factors, and cost factors from the base case are used in similar process blocks in the newly developed processes, and when the developed process blocks have no parallel to the highly specified base case, traditional chemical engineering approaches are used for the estimates of fixed and variable cost (Peters, Timmerhaus et al., 2003). Tables B.4-6 detail the calculations used to estimate the fixed capital cost of the base case cellulose to ethanol process, cellulose to levulinic acid process, and cellulose to succinic acid process successively. The fixed capital cost was then annualized on a basis of 8% interest and 25 year payment schedule. The variable cost, minus the cost of energy and materials, was assumed to be 4% of the total

capital investment, and this assumption is often used in process modeling (Larson, Consomi et al., 2003). The annualized fixed cost and annual variable cost were summed together, resulting in total annual product costs.

Material balances were also calculated for each of the process flow diagrams for the purpose of determining cost factors per unit output. It should be noted that energy balances should be performed in addition to material balances for the ultimate purpose of mass and energy integration; however, due to the novelty and level of patent protection for these polygeneration processes, many of the process specifics are not available in literature, which would make process integration much less effective. By dividing the total annual product cost by the total annual output of each process, a cost factor per unit output could be determined, and this information is listed in Table 4.3.

	Cellulose to Ethanol	Cellulose to Levulinic Acid	Cellulose to Succinic Acid
Total Overnight Capital Cost in Jan. 2009$	138,692,192	104,441,861	131,996,531
Annualized Fixed Cost @ 8% interest over 25 years	12,992,515	9,783,986	12,365,274
Total Variable Costs	5,547,688	4,177,674	5,279,861
Total Annual Product Costs	18,540,203	13,961,660	17,645,135
Annual Output, Primary Product	153,880,090 kg ethanol	114,354,240 kg levulinic acid	129,989,650 kg Succinic Acid
Cost per Primary Output	$0.106/kg ethanol	$0.104/kg levulinic acid	$0.121/kg succinic acid

Table 4.3 – Calculated cost per primary output for cellulose-based product platforms. Fixed cost calculations available in Tables B.4-6. For cellulose to ethanol product, from Wooley, Ruth et al., page 124, stream 515, denatured ethanol is being produced by overall process at 18473 kg/hr, multiplied by 8330 annual operating hours. For all other processes, product output flow is taken from simulation files and multiplied by 8330 opearting hours per year.

At this point, all of the scalars needed for the mathematical optimization are known for the analysis of converting cellulose to platform chemicals, and the necessary information is entered into the GAMS optimization software. The optimization program recommends that all of the cellulose be processed into levulinic acid, and this answer emerges for a number of reasons. First, the processing cost scalar of levulinic acid is calculated to be $0.104/kg levulinic acid, compared to $0.106/kg ethanol and $0.121/kg succinic acid. Second, the estimated bulk market price of levulinic acid ($11.02/kg) is an order of magnitude higher than those of ethanol ($5.83/kg) and succinic acid ($4.4l/kg). This incredibly high market price for levulinic acid results in the highest contribution margin of the three possibilities, and therefore all cellulose should be converted to levulinic acid via dilute acid catalysis. The solved superstructure for this first round of analysis is illustrated in Figure 4.10.

Now that levulinic acid has been determined to be the most profitable platform chemical to produce from a cellulosic feedstock, a similar analysis is performed among second-tier chemicals, which may be platforms for other downstream chemical products or could be end-user chemicals products. A literature search similar to the one conducted at the beginning of the first tier analysis is performed once more, and the resulting second tier

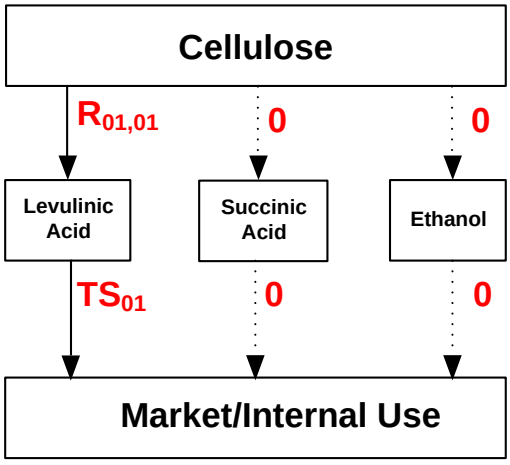

Figure 4.10 – Solved superstructure for cellulose to first level of platform products.

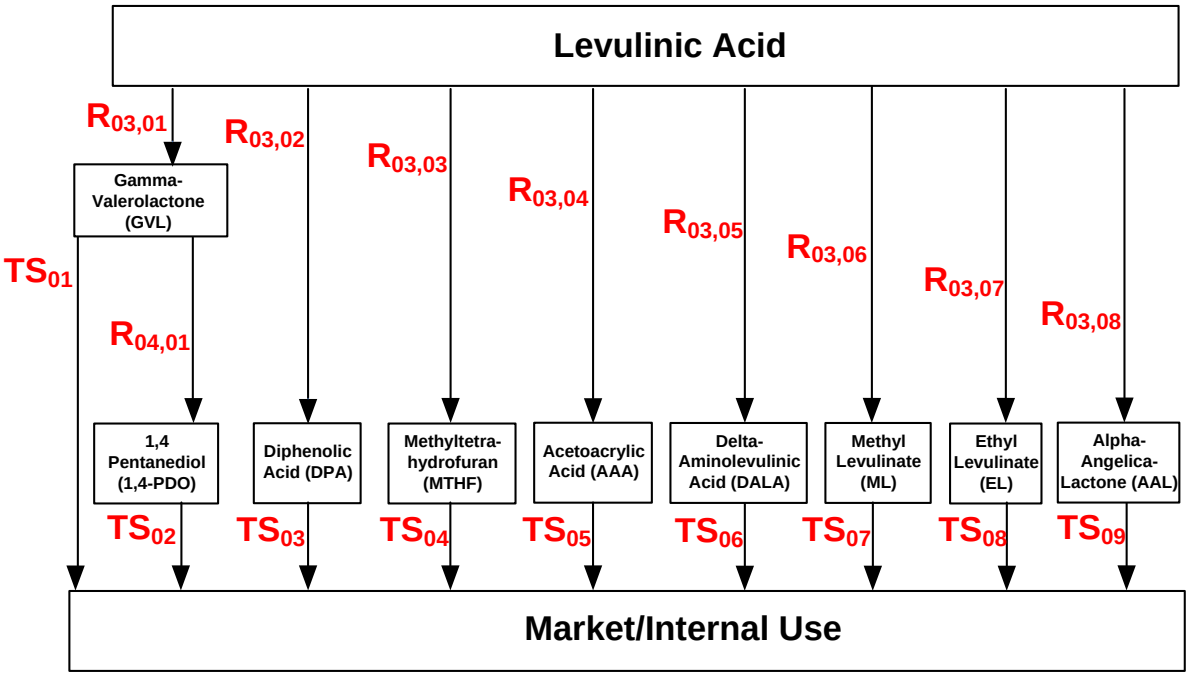

Figure 4.11 – Validated superstructure of products based on levulinic acid feedstock (Solvason, Sammons et al., 2010).

superstructure is available in Figure 4.11.

Again, the PUB calculations are repeated for the second level of processing cellulose. This time, the basis 100 kg of levulinic acid plus stoichiometric amounts of reactants needed for the reactor(s). Because none of the products in the superstructure have a bulk market and may all be considered to be specialty chemicals in small batches, none of the processes were discarded due to an artificially high PUB value. Instead, while the absolute PUB values hold very little meaning when the bulk market is nonexistent, the relative PUB values are quite useful in determining the qualitative ranking of the potential added value of these chemical products. The products with the highest PUB values were determined to be 1,4-pentanediol (PDO), acetoacrylic acid (AAA), and δ-aminolevulinate (DALA), and as a result, these three chemicals were selected for process synthesis and subsequent utilization of the

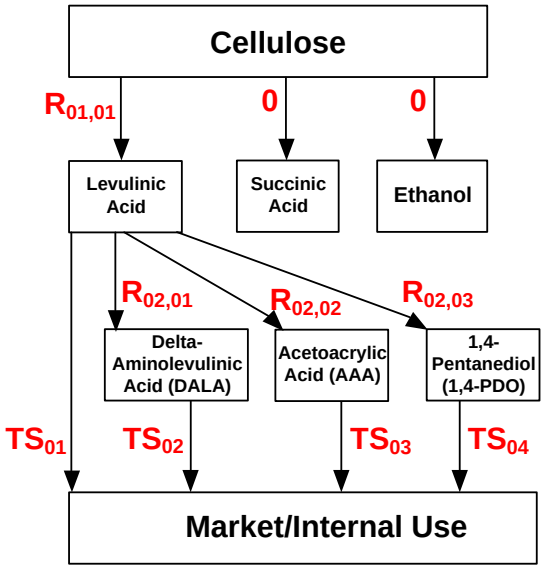

Figure 4.12 – Modified superstructure for cellulose-based platform design, second stage (Solvason, Sammons et al., 2010).

polygeneration methodology to determine the most promising chemical process. The PUB calculations for the second tier are available in Table B.3, and the narrowed superstructure is represented in Figure 4.12.

Large block diagrams were then constructed for the three most promising chemical processes. Figure 4.13 illustrates the large block diagram for the overall process of converting cellulose to DALA through the levulinic acid platform. Because formic acid is a byproduct of the reaction to create DALA, the formic acid and water stream leaving the DALA distillation columns is combined with the water and formic acid stream leaving the levulinic acid reaction in the amine separation unit. This is important to keep in mind, as a larger amine separation unit will be needed to handle the increased flowrate, and this will incur an incremental cost over the original amine separation unit in the cellulose to levulinic acid large block diagram in Figure 4.9. In addition, larger equipment will also be needed in

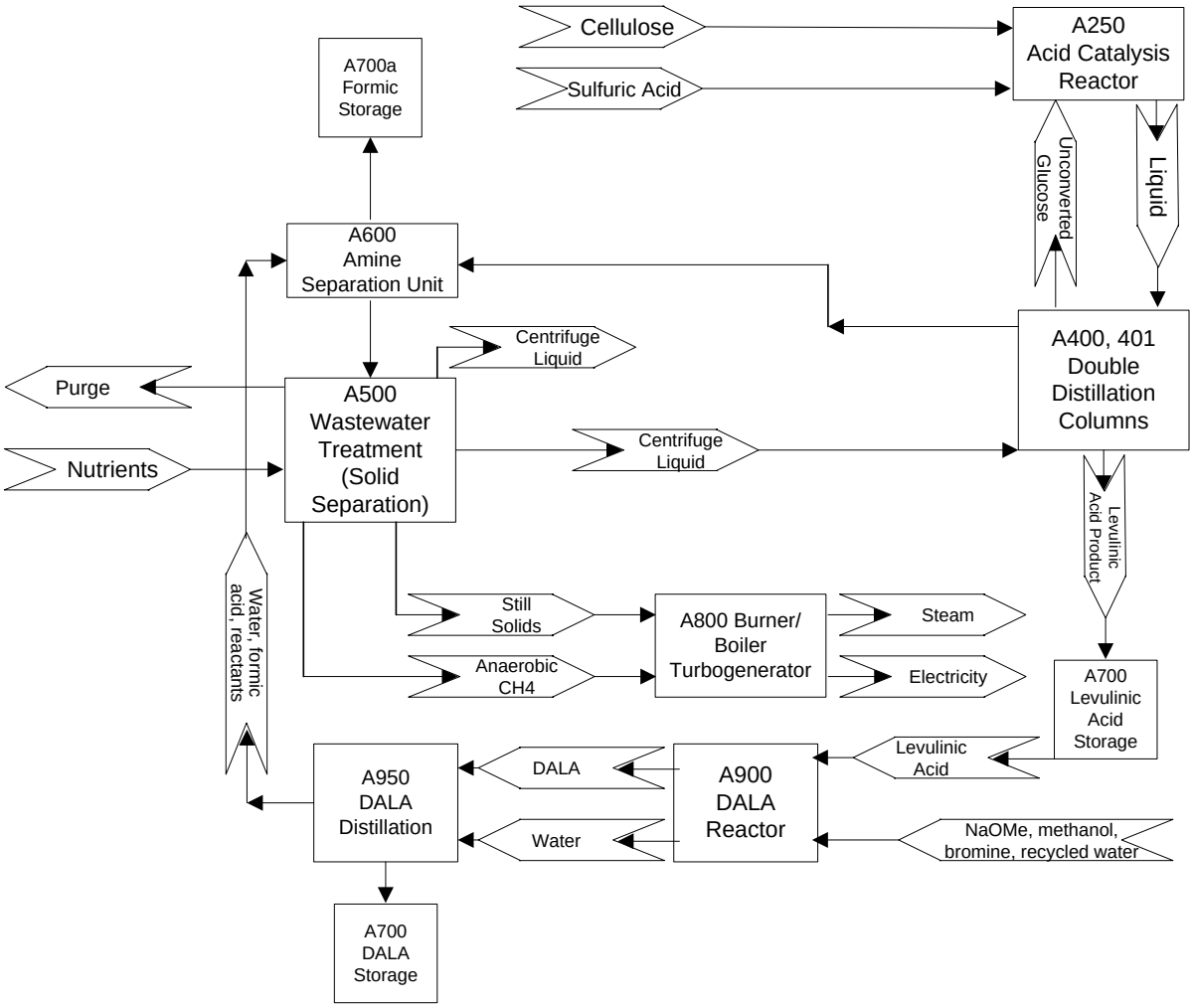

Figure 4.13 – Large block diagram for conversion of cellulose to DALA via levulinic acid (Solvason, Sammons et al., 2010).

the wastewater treatment and product/feed storage modules, which will incur additional incremental costs. Furthermore, there are entirely new unit operations in the forms of the DALA reactor and subsequent separation train. It should be noted that since the levulinic acid flowrate is much less than the flowrates involved in the cellulose to levulinic acid process that these combined incremental costs will pale in comparison, and these incremental capital cost calculations are included in Table B.7.

For the cellulose-to-PDO and cellulose-to-AAA processes, there is no formic acid byproduct being formed, so the amine separation unit from the levulinic acid process will remain unchanged. However, there are still larger loads involved in wastewater treatment and product/feed storage, so these incremental costs must still be taken into consideration when calculating the incremental capital investment. These capital cost calculations for the AAA and PDO processes are available in Tables B.8 and B.9 respectively, and Figure 4.14 illustrates the large block diagram that may be used to visualize the major aspects of both

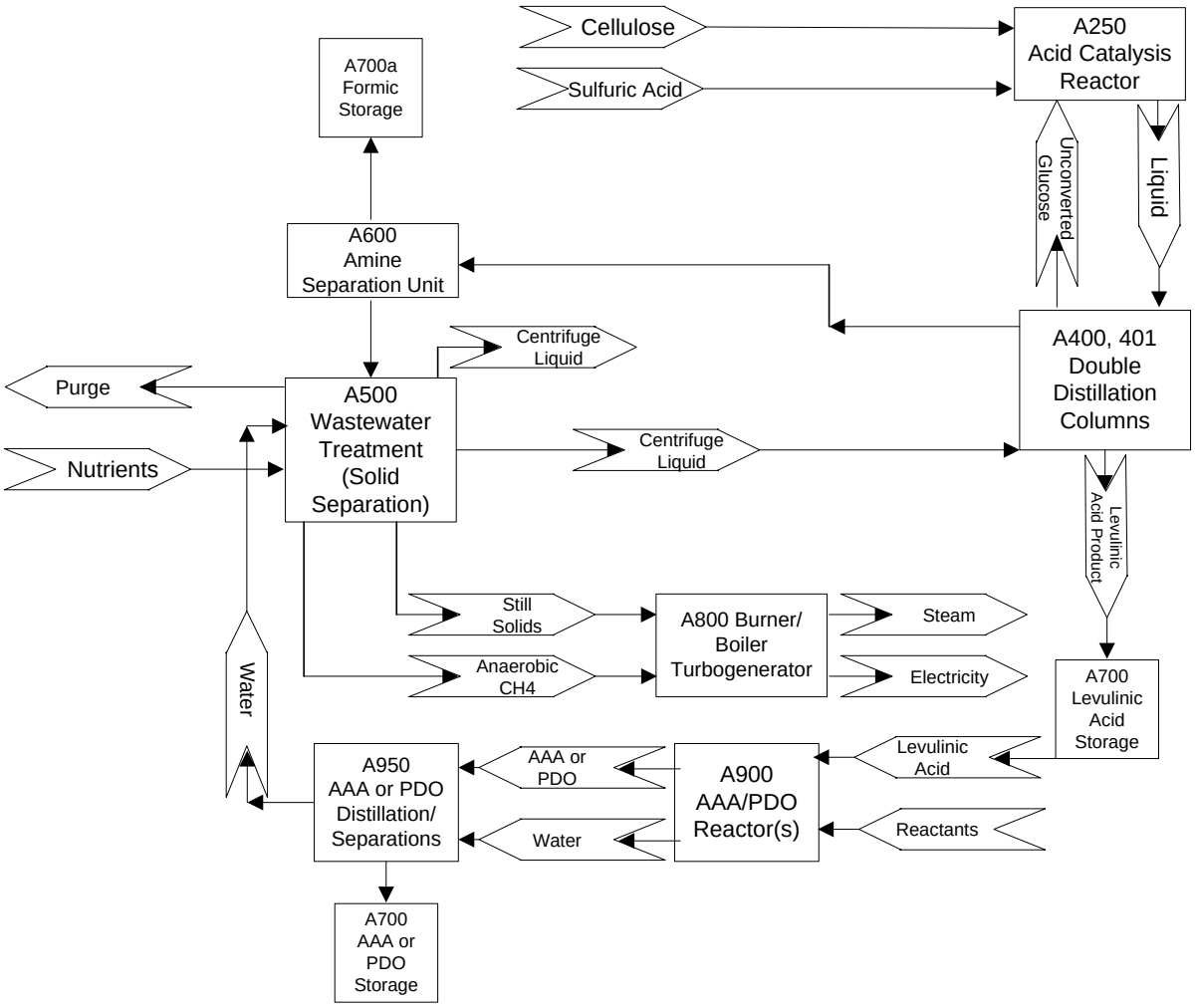

Figure 4.14 – Large block process flow diagram for cellulose-to-AAA and PDO processes (Solvason, Sammons et al., 2010).

processes. The major difference between the two processes is that the AAA process requires only one reaction step, and therefore only one reactor, while the PDO process requires two reaction steps in two separate reactors, and this difference is taken into account in the capital cost calculation tables.

By following a similar strategy to what was executed in analyzing the conversion of cellulose to platform chemicals, the incremental fixed cost, annualized over 25 years at 8% interest, was summed with the variable cost to determine total annual product cost for each process. These costs were then divided by the total annual output to determine the total cost per output, and Table 4.4 illustrates all of the information necessary to determine these cost factors.

With all of the scalars and parameters available to execute the optimization program, the product allocation problem may now be solved for the conversion of cellulose to various products via the levulinic acid platform. The optimization-based framework dictates that all of the levulinic acid should be converted into DALA in order to maximize the value added to the cellulose-based supply chain, and this solved problem is illustrated in Figure 4.15. The

	Levulinic to DALA	Levulinic to AAA	Levulinic to 1,4-PDO
Total Overnight Capital Cost in Jan. 2009$	4,301,079	2,073,048	3,089,007
Annualized Fixed Cost @ 8% interest over 25 years	402,920	194,201	289,374
Total Variable Costs	172,043	82,922	123,560
Total Annual Product Costs	574,963	277,123	412,935
Annual Output, Primary Product	74,908,191 kg DALA	89,386,648 kg AAA	65,031,310 kg PDO
Cost per Primary Output	$7.676E-3/kg DALA	$3.100E-3 /kg AAA	$6.350E-3 /kg PDO

Table 4.4 – Calculated cost per primary output for levulinic acid-based products. Fixed cost calculations available in Tables B.7-9. For all processes, product output flow is taken from simulation files and multiplied by 8330 opearting hours per year.

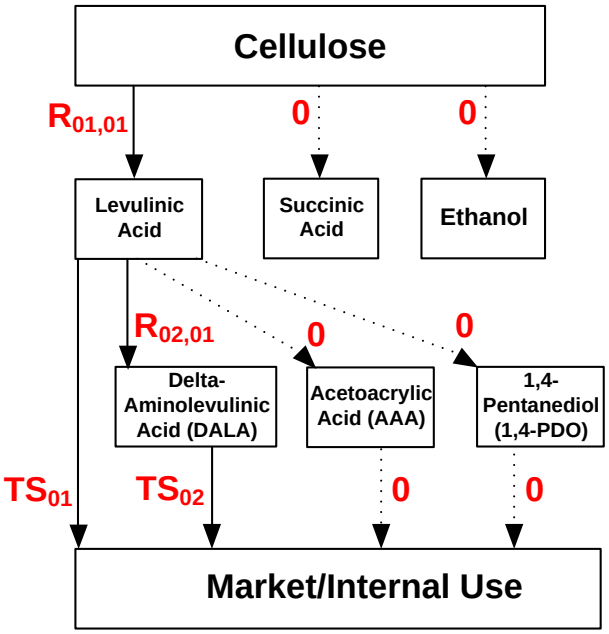

Figure 4.15 – Solved superstructure for cellulose to products based on levulinic acid platform.

overriding reason for this solution is that the estimated bulk market price of DALA ($3250/kg) is much higher than those of AAA or PDO ($1968 and $1325/kg respectively). However, it should be noted once again that no bulk markets currently exist for these products, and these bulk prices are merely estimates based on current lab-scale quantities. As a result, the uncertainty inherent in this particular market scenario greatly decreases the predictive power of the given problem solution.

This uncertainty can be abated, however, by utilizing a Monte Carlo simulation in which the bulk market price varies according to a pre-defined distribution, and the optimization program is then executed for a large number of market price scenarios. Instead of a single product solution, this strategy will result in a distribution of solutions in which the decision-maker may evaluate the market risk involved with pursuing any of the single

product solutions. In this particular example, the market prices for DALA, AAA, and PDO follow a normal distribution with the mean at the calculated bulk market prices and a standard deviation of one-half of the mean. The average values were kept at the estimated bulk market prices of the specialty chemicals in order to maintain their qualitative order of ranking based on current values of lab scale quantitites, and the standard deviations were chosen so that more than 98% of the simulation runs would have market prices between zero and double the estimated bulk price. For the market price of levulinic acid, it was kept constant at $11.02/kg as a failsafe in the event that the market prices of all three specialty chemicals were to be negative in order to avoid a scenario in which negative value is added to the supply chain. Figure 4.16 illustrates the distribution of framework solutions based on the above variation in price. While the predominant solution dictates that levulinic acid should be converted into DALA, the Monte Carlo simulation highlights the market risk inherent in this group of chemical products such that certain movement in the market may shift the optimal solution to a different member of the chemical platform family.

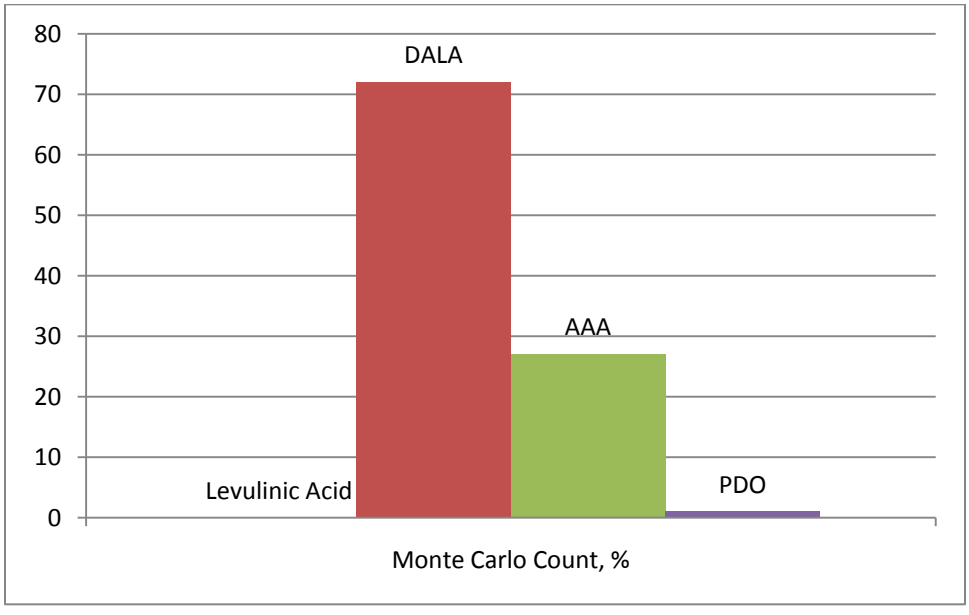

Figure 4.16 – Histogram of Monte Carlo price movement simulation from optimization.

The framework that has been developed to solve the product allocation problem using mathematical optimization is an integral part of a larger methodology concerning product platform design. Prior to utilization of the optimization-based framework, superstructure generation must be utilized in order to determine the possible chemical products, and preliminary screening via Profitability Upper Bound calculations is crucial in reducing the search space to a smaller number of product solutions. Process synthesis and design must then be used in order to generate the data necessary to utilize the optimization-based framework. After execution of the product allocation framework and possible Monte Carlo simulations for varying market price scenarios, the economic performance must then be incorporated into a larger Multi-Criteria Decision Making matrix, which will take into account the environmental considerations not considered so far in the generation and solution of this particular case study, as well as other significant issues such as process risk, supply chain performance, and other unforeseen metrics. By incorporating the product allocation solution methodology into this global MCDM matrix, buy-in for process and product ideas is assured for stakeholders who place significant weight on metrics including and aside from economic performance considerations (Solvason, Sammons et al., 2010).

4.4 Case Study: Black Liquor Biorefinery

Polygeneration facilities may also play a role in decisions concerning the replacement of Tomlinson boilers in Kraft paper mills. Currently, Tomlinson boilers are used to burn black liquor, which is a byproduct of paper production via the Kraft process. Black liquor is rich in lignin and hemicelluloses, and it may be burned to generate steam for use in the remainder of the paper mill while recovering costly pulping chemicals. Tomlinson boilers

have been used extensively in Kraft mills to the point that the vast majority of them have been rebuilt in the past 10-20 years, and as a result, many of these rebuilt Tomlinson boilers are reaching the end of their useful lives and will need to be removed from the Kraft process or completely replaced (Larson, Consomi et al., 2003). With the emergence of biomass gasification and biorefining, managerial entities within the pulp and paper industry are faced with the decision to replace these Tomlinson boilers with newer ones, or to install a gasifier and other significant equipment necessary for polygeneration. In addition to black liquor, other biomass resources available for polygeneration at pulp and paper facilities include bark and waste wood, which are typically burned in separate boilers also mainly for the production of steam (Larson, Consomi et al., 2003).

While there are abundant biomass resources available on-site at paper manufacturing facilities in the forms of black liquor, waste wood, and wood bark, there are also other untapped sources of biomass such as forest and agricultural residues that may be collected utilizing the existing infrastructure and core competencies of the pulp and paper industry (Larson, Consomi et al., 2003). Thus, there is a vast opportunity for stakeholders in pulp and paper production to embrace polygeneration as a means to improve profit margins by generating heat and electricity efficiently while incorporating value-added liquid fuels into their portfolios. To highlight this availability within the industry to replace Tomlinson boiler systems with polygeneration technology, Larson, Consomi et al. (2003) have conducted an extensive study into the economic and environmental potential of the implementation of black liquor gasification systems and biorefineries onto a hypothetical fully functioning paper production facility. In this technical report, the authors compare the "business as usual" base case of installing a new Tomlinson boiler with the implementation of theoretical

Short Name	Full Name	Product range	Description
TOM	Tomlinson boiler	Electricity, steam	Base case, business as usual
BLGCC	Black liquor gasification, combined cycle	Electricity, steam	Replace Tomlinson boiler with combined cycle turbine fired by syngas
DMEa	Dimethyl ether, process A	Electricity (negligible), steam, dimethyl ether	No gas turbine, no wood gasification, 97% recycle of syngas
DMEb	Dimethyl ether, process B	Electricity, steam, dimethyl ether	Wood gasification sent to gas turbine, 97% recycle of syngas
DMEc	Dimethyl ether, process C	Electricity, steam, dimethyl ether	Wood gasification sent to gas turbine, one pass synthesis
FTa	Fischer-Tropsch synthesis, process A	Electricity, steam, FT liquids*	Wood gasification sent to gas turbine, one pass synthesis
FTb	Fischer-Tropsch synthesis, process B	Electricity, steam, FT liquids*	Wood gasification sent to larger gas turbine, one pass synthesis
FTc	Fischer-Tropsch synthesis, process C	Electricity, steam, FT liquids*	Wood gasification sent to product synthesis, one pass synthesis
MA	Mixed alcohols	Electricity, steam, C1-C3 alcohols	Wood gasification sent to product synthesis, 76% recycle of syngas
*Mixture similar to crude oil consisting of C4-C24 hydrocarbons sent to a petroleum refinery for separation			

Table 4.5 – Potential biorefineries to be added onto an existing pulp and paper facility (Larson, Consomi et al., 2003).

biorefineries based primarily on the gasification of black liquor from the Kraft pulping process. These seven potential biorefineries are described in further detail in Table 4.5.

4.4.1 Economic Analysis

Larson and Consomi performed extensive modeling and rigorous calculations to determine the internal rate of return and fugitive emissions for the base case and proposed biorefineries (2003). However, the methodology presented in this work is capable of enhancing their previous analysis by quantifying the net present value of these proposed

polygeneration facilities, evaluating the environmental impact through the use of the EPA WAR algorithm, and providing the data necessary to construct the pareto-optimal curve for economic and environmental performance. It should be noted that process integration was already accomplished in the original technical paper, which negates the use for redundant work in the framework.

To analyze the different polygeneration pathways proposed by Larson and Consomi, it is first necessary to construct a superstructure, as seen in Figure 4.17, that represents the main processes that may be pursued by a paper production facility interested in polygeneration. Basic simulation models are then constructed for these individual processes based on process flow diagrams, heat and energy balances, and equipment specifications, which are all readily available in Larson and Consomi (2003). Similar to the chicken litter biorefinery in Section 4.2, scalars for market price, feedstock price, and combined fixed and variable processing cost must also be determined.

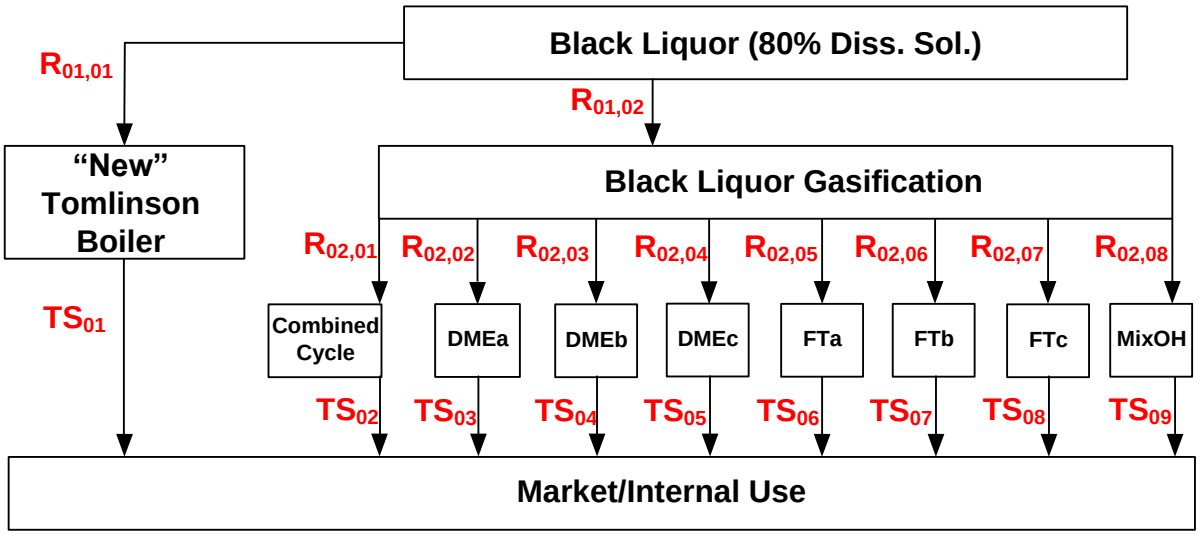

Figure 4.17 – Unsolved superstructure for black liquor biorefinery based on technical report (Larson, Consomi et al., 2003).

The scalars for market price are easily determined from market data, and the scalar for feedstock price is essentially zero since the feedstock is a byproduct of the main pulping process. However, as seen in the simplified chicken litter biorefinery case study, the calculation for the combined processing cost scalar is slightly more complex, and Tables C.1-5 in Appendix C contain the numerical data necessary for these calculations. First, the overnight capital cost must be determined based on necessary equipment as stated in the original technical paper (Larson, Consomi et al., 2003). Assuming straight line amortization over 25 years at 8% cost of capital, this overnight capital cost can be translated into an annualized fixed cost. This annualized fixed cost should then be combined with annual variable costs in the form of water, energy, and operating and maintenance costs (O&M), the latter of which was specified in the Larson and Consomi study as a fixed 4% of overnight capital cost. The combined annualized fixed cost and variable cost is then divided by total annual output assuming 8330 annual operating hours and adhering to the published mass balances, and as a result, the scalar values for total cost per unit output for each process (C_{mij}^{P}) are determined.

From the developed simulation models, it is then imperative to determine conversion factors for process points in terms of product conversion per unit input. Because this is a true polygeneration facility, it is important to account for all salable products in each process pathway, and thus one must develop conversion factors for each distinct output. Tables C.6-8 contain all of the relevant calculations and conversion factors necessary for the process routes studied in this particular case study. It should be noted that because electricity is commonly measured in units of kWh for billing purposes, an atypical convention is sometimes used in the referred spreadsheets as processes generating kilowatt-hours per a

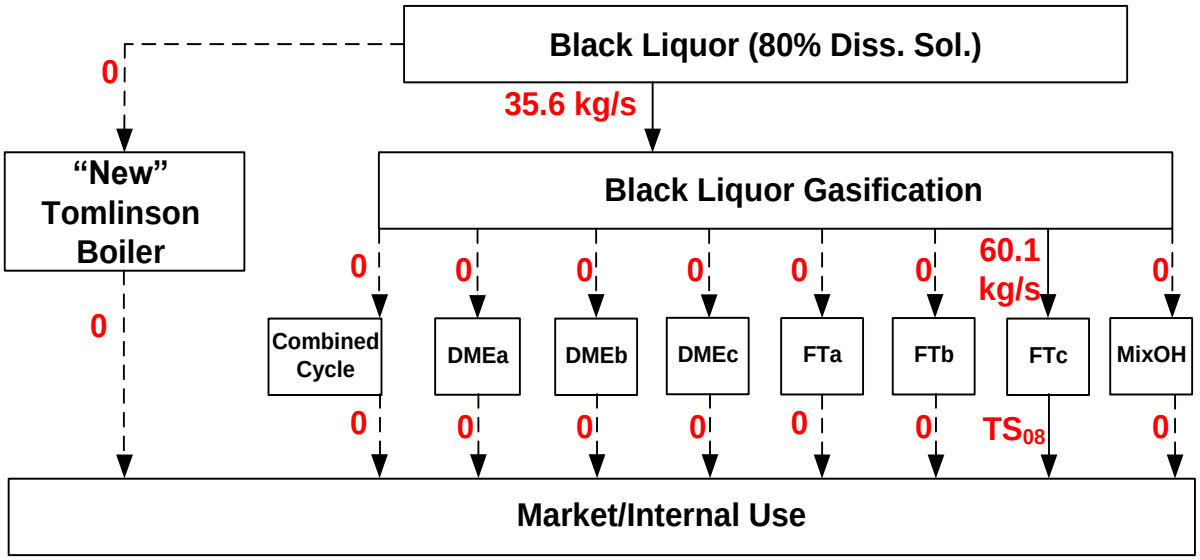

Figure 4.18 – Solved decision tree for black liquor biorefinery with highest profitability.

time window of production, e.g. kWh/s or kWh/yr. While this would typically simplify to a measure of watts, this convention is maintained in order to evaluate the profit potential of the process pathways.

At this juncture, all of the necessary information is available to perform the optimization in GAMS to determine the products sold TS_k and processing pathway amounts R_{mij}. Figure 4.18 illustrates the solved decision making tree and the most optimal solution in terms of economic performance. The framework dictates that the business-as-usual base case should not be pursued, and that all available black liquor should be gasified and then synthesized into Fischer-Tropsch liquids (FT liquids), which is a mixture of C4-C24 hydrocarbons that is then sent to a traditional oil refinery for separation. There are three pathways in the superstructure that will produce FT liquids, but the one chosen by the framework is the FTc pathway, which represents supplementation of the black liquor with gasified biomass in the form of waste wood. As a result of the chosen process pathway, 2.898

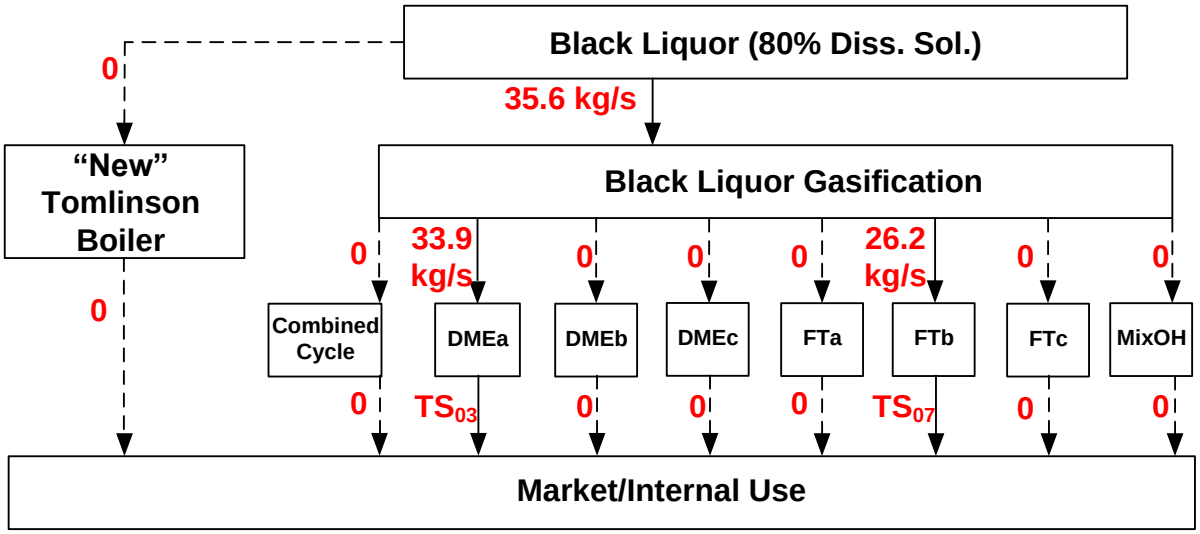

Figure 4.19 – Solved decision tree for black liquor biorefinery with next highest profitability.

gal/s of FT liquids, 214 lb/s process steam, and 21 kWh/s of electricity are generated for an estimated annual gross profit of $39.2M. All steam needs for the pulp and paper facility are satisfied, and approximately 75% of the total electric load is generated by this process.

Because of the increased number of available pathways compared to the chicken litter biorefinery example discussed previously, it is now possible to eliminate the most profitable solution to find the next best answer. This can be done repeatedly in order to ultimately construct a list of candidate solutions for further consideration. In this case, the FTc route is eliminated as a possible solution by constraining the process pathway between gasification and the FTc process to zero, which will force the framework to find a different solution with the next highest level of profitability illustrated in Figure 4.19.

In this particular process solution, again all of the black liquor is gasified into syngas, but it is then split into two separate processes. Slightly more than half of the black liquor is sent to the DMEa process, which produces 1.303 gal/s of dimethyl ether, 121 lb/s of process steam, and near zero electricity. The remainder of the black liquor is then sent to a different

Fischer-Tropsch process, which produces 0.411 gal/s of FT liquids, 93 lb/s of process steam, and 28 kWh/s of electricity. The main reason that the syngas is sent into two different processes is because of the pricing assumptions made for electricity. Larson, Consomi et al. assume that there is a price penalty between avoiding electricity purchases and exporting electricity to the grid due to the power company having control of the transmission system and being able to charge a premium for their own power generation (2003). According to their technical report, the price for avoided electricity is $56.2/MWh, while the price for exported electricity to the grid is $51.8/MWh. This pricing difference alone did not result in the framework selecting multiple process-product combinations to avoid the export of electricity, but a modified price for exported electricity to the grid of $40/MWh caused the framework to avoid this price penalty by generating just enough electricity to meet the needs of the entire pulp and paper mill while exporting zero power to the grid.

Recall that the DMEa process has a backpressure turbine instead of the combined cycle turbine found in all of the other gasification-based solutions, which results in a negligible amount of electricity generation in comparison. Also recall that the FTb process has a larger combined cycle (CC) gas turbine than the rest of the processes outside of DMEa. The framework allocates just enough syngas to satisfy electricity needs from the large CC gas turbine and then seeks to allocate the remainder of the syngas into a process that generates almost zero electricity to avoid the pricing penalty. The price premium for FT liquids ($1.54/gal) over dimethyl ether ($0.99/gal) is not enough to overcome the electricity pricing penalty, and the conversion of syngas into DME on a gallon of fuel per kg of syngas basis is twice that of FT liquids. As a result, the framework suggests the construction and

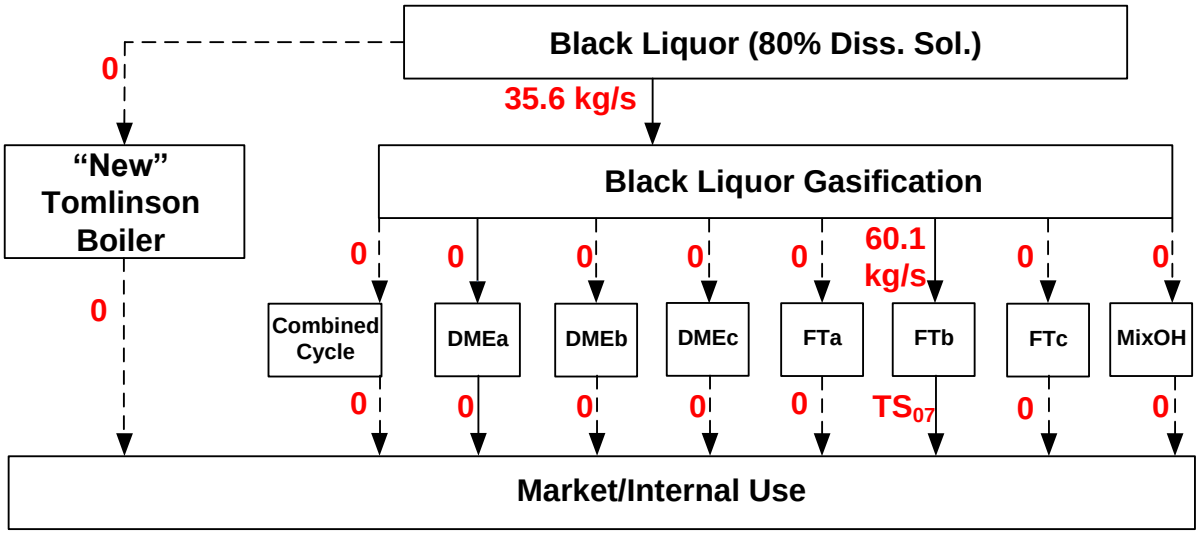

Figure 4.20 – Solved tree, single primary product solution with next highest profitability.

utilization of two processes for the conversion of syngas into energy and salable products while meeting the global steam demands of the facility.

It should be noted, however, that the construction of two separate processes may be infeasible or impractical, but within the optimization portion of the framework, it is possible to specify a set of constraints that will result in the framework choosing only one primary product pathway in order to avoid the multi-process solution. These constraints were discussed previously in Equations 3.2-4, and when they are implemented into the mass balance constraints, the framework presents the next best single primary product configuration in Figure 4.20.

The split primary product solution dictated that the black liquor be sent to the DMEa and FTb processes, but by enforcing a single primary product solution, the framework calculates that increased value is realized by choosing only the FTb process as opposed to DMEa. This particular configuration produces 0.943 gal/s of FT liquids, 214 lb/s of process

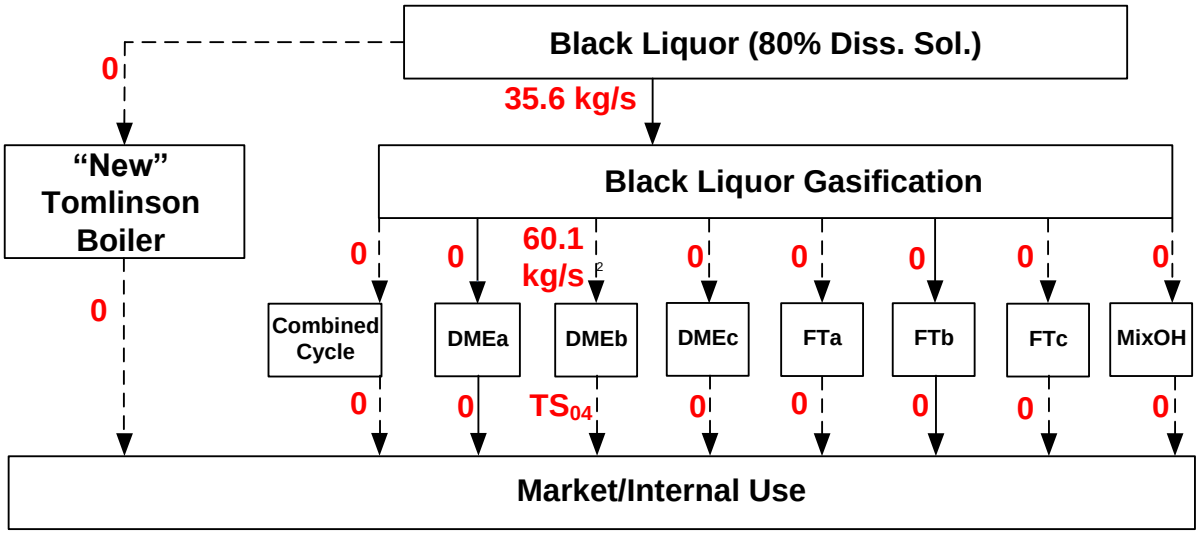

Figure 4.21 – Solved tree, single primary product solution with third highest profitability.

steam for the entire facility, and 64 kWh/s of electricity to be used internally with the remainder being sold on the grid at the aforementioned price penalty.

Intuitively, by eliminating the FTb process as a feasible solution, the framework should then suggest pursuit of the DMEa process pathway. Recall that in the split primary product solution presented in Figure 4.19, the framework suggested first maximizing the amount of syngas that can be processed through the FTb pathway until the electricity needs of the mill are met, and then sending the rest of the gasified black liquor through the DMEa pathway which generates almost zero electricity. In a single primary product solution, however, the electricity price penalty is much less of a factor at the initial decision-making stage as it is when the decision is able to shift once the electricity threshold is realized in the split process solution. As a result, the framework suggests pursuing the DMEb pathway, which represents the production of dimethyl ether and the addition of a gas turbine to be used for combustion of gasified wood. From this process, 2.311 gal/s of dimethyl ether, 214 lb/s of process steam, and 24 kWh/s of electricity are produced. In this case study, it appears that the

production and price of electricity is one of the most important driving factors in determining which process pathway should be pursued.

4.4.2 Environmental Analysis

The larger number of eligible process pathways for selection also allows for the determination of environmental impact for each process solution to be used as a screening tool alongside economic performance. In order to determine the environmental impact accurately, it is necessary to perform mass balances around the entire processes in order to quantify the mass flowrates of products and fugitive emissions. These flowrates are then combined with a graphical user interface that contains a database for environmental impact scores based on the EPA WAR algorithm (Cabezas, Bare et al., 1999).

Appendix D contains all of the relevant WAR score data necessary to calculate the environmental impact of each process pathway, starting with Table D.1, which represents the calculated WAR scores for all specified classes of pollutants process steam and electricity generated, black liquor, syngas, and final products (Larson, Consomi et al., 2003). Table D.2 converts the WAR scores for the products of dimethyl ether, FT liquids, and mixed alcohols from a mass basis to a volumetric basis since these products are commonly purchased per gallon.

Environmental emissions are often categorized into much larger groups instead of single chemical components, and as a result, it is necessary to approximate the chemical composition of these emission groups in order to determine their overall effect on environmental impact scores. Tables D.3 and D.4 contain the approximate chemical composition, individual component scores, and overall category scores based on literature for

volatile organic compounds from wood and gas combustion respectively. Tables D.5 and D.6 perform similar breakdowns for particulate matter of 10 microns or less (PM_{10}) and total reduced sulfur (TRS) (Larson, Consomi et al., 2006).

Some of the products and services provided by these proposed biorefineries require translation into weighted average scores of single chemical components or, in the case of electricity, comparison with coal and/or gas powered utility generation. Table D.7 details the calculations performed to estimate the environmental impact of process steam that is used as a source of process heat as well as electricity via a backpressure turbine. Table D.8 calculates the environmental impact of Fischer-Tropsch oil product, which is based on the weight fraction breakdown available in Table D.9 for an Anderson-Schulz-Flory chain-length value of 0.65 (Schulz, 1999). Table D.10 determines the environmental impact of the mixed alcohol product stream. Finally, Table D.11 calculates the baseline environmental impact of black liquor based on the chemical composition approximation shown in Table D.12.

It should be noted that generally an atomic breakdown is available for the heterogeneous black liquor mixture, instead of one that lists the individual chemical compounds present. As a result, in this case it is necessary to estimate the chemical compounds present based on the atomic composition in order to determine the environmental impact of black liquor. Ideally, one would measure or procure the various atmospheric and toxicological data of black liquor that is used for calculating WAR scores, but because this heterogeneous mixture differs so widely between facilities, it is inherently difficult to determine the impact scores of Kraft black liquor.

To utilize the environmental impact scores for the pollutant categories of PM_{10}, SO_X, NO_X, TRS, VOC, CO, and CO_2, it is necessary to uncover the emission factors for the

stationary sources of the polygeneration facility as listed in a separate volume of work based on the same black liquor biorefinery analysis (Larson, Consomi et al., 2003). These emission factors must then be translated into mass flowrates on the same per product basis as used previously in the first 13 tables in Appendix C for use in the EPA WAR algorithm. Tables E.1-10 in Appendix E include the calculations necessary to convert the emission factors for the major unit operations into environmental impact scores on a per product mass basis.

These PEI scores from the emission factors indicate the amount of environmental impact generated by pursuing a given process pathway, and the impact scores are combined with the scores listed on a per mass basis in Tables D.1-12. The calculated adverse potential environmental impact was then normalized by setting the least environmentally friendly PEI score to zero and subtracting this amount from the absolute WAR scores calculated for all of the other processes.

4.4.3 Pareto-Optimal Performance

Keeping the constraints necessary for the framework to suggest only single process configurations, Figure 4.22 illustrates this normalized adverse impact against gross profit per second. Recall that lower WAR scores represent less adverse impact to the environment. The thick vertical line that intersects the x-axis at the zero point of gross profit represents the edge of the pareto-optimal curve, as any profitability values to the right of this point will result in negative profitability, which should be infeasible solutions for enterprises willing to realize a positive return on investment. While these solutions are indeed infeasible for profitable entities, it is interesting to note the behavior of solutions outside of the pareto-optimal zone.

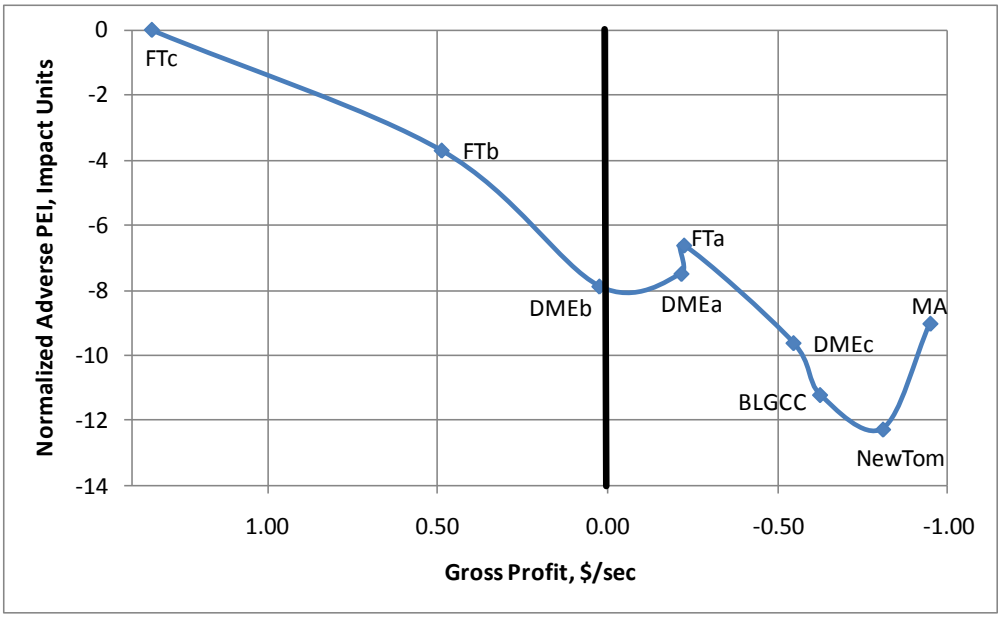

Figure 4.22 – Pareto chart of PEI versus gross profit for single primary product solutions only. Data for chart available in Table E.10.

It is preferable to optimize the economic potential of polygeneration facilities while using environmental impact as a screening tool as opposed to dual optimization of profitability and environmental impact. As can be seen in Figure 4.22, optimization of environmental impact alone would dictate that a new Tomlinson boiler should be installed, but this process solution is highly unprofitable and results in a substantial loss of financial value. Instead, profitable process solutions to the left of the zero profitability line illustrate the pareto-optimal curve of economic and environmental performance, and as a result, the trade-off between economic and environmental performance may now be visualized and quantified.

To the left of the zero profitability line, intuitive behavior is noted that as adverse environmental impact decreases, so does process profitability. This represents the increased cost and decreased gross profit often observed as the result of implementing process and

product changes with the sole aim of decreasing negative environmental impact. However, to the right of the zero profitability line, there are regions in which decreased environmental impact results in decreased profitability, which is counterintuitive to the traditional approach of process engineering. In switching solutions from DMEb to FTa and NewTom to MA, this behavior can be observed.

To understand the specific reasons behind the counterintuitive behavior present in the graph of profitability versus environmental impact, the constraints that confine the framework to single primary product solutions are deactivated. As a result, the framework is now permitted to suggest solutions in which multiple product pathways are pursued. While the multiple primary product solution may not be realistic for polygeneration facilities to pursue, these split process solutions allow the user of the framework to more accurately determine the trade-offs between economic and environmental performance as well as the

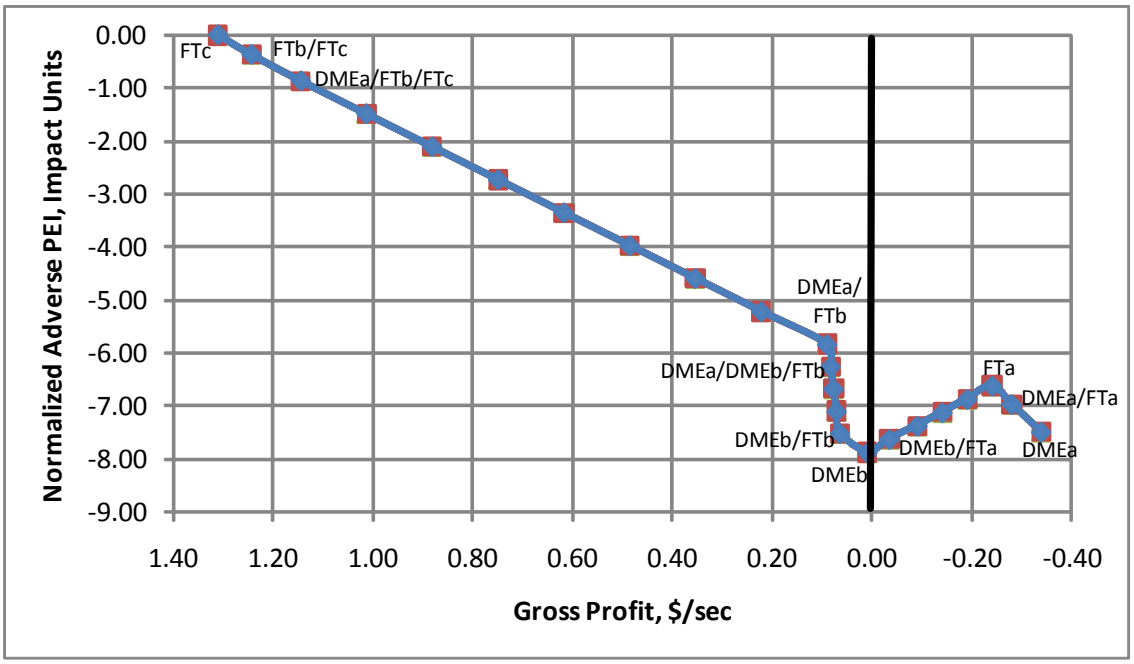

Figure 4.23 – Pareto chart of PEI versus gross profit for split primary product solutions. Data for chart available in Table E.11.

reasons behind counterintuitive graph behavior. Figure 4.23 illustrates the use of the framework without single primary product constraints in which split primary product solutions are often dictated.

The first data point in the graph is the same single primary product solution from the previous figure, in which all of the black liquor is gasified and sent down the FTc pathway. To arrive at split primary product solutions, the maximum output of the FTc pathway is incrementally decreased by 10%, which causes activation of the FTb pathway. Therefore, the second data point represents a split primary product solution in which 90% of the gasified black liquor is sent into the FTc pathway, and the remaining 10% is sent into the FTb pathway. At this point, a further 10% reduction in the FTc pathway results in enough electricity being produced to meet the needs of the plant, which means that excess electricity would be sold to the grid, and the price penalty would decrease overall profitability. This particular solution is suboptimal, so the framework dictates that if 80% of the black liquor is sent to the FTc pathway, the remaining 20% would be sent to the FTb pathway until the electricity needs of the plant are met, at which point the remaning syngas would be sent to the DMEa pathway.

The data points are labeled at only the points where the framework changes which process pathways are activated, and as such, data points 3 through 10 represent the activation of the FTc, FTb, and DMEa pathways as the maximum amount of syngas sent to the FTc pathway is incrementally reduced to zero. Once the FTc pathway is completely excluded as a process solution in data point 11, the framework suggests sending as much syngas into the FTb pathway resulting in the electricity needs of the plant being met, with the remainder sent into the DMEa pathway. At this point, another constraint may be added so that either the FTb

pathway or DMEa pathway is incrementally reduced to zero, and because the single primary product solutions demonstrate that FTb is more profitable than DMEa, the FTb pathway is chosen for reduction to zero by increments of 20%. The percentage reduction is chosen for ease of graphical representation. Because the FTb pathway represents the highest amount of electricity production per mass of syngas, reduction of the capacity of the FTb pathway results in a reduction in electricity generation, which allows for electricity to be generated in other processes without encountering the price penalty for sale of electricity to the grid. As a result, the framework will maximize FTb production up to the maximum allowed by the incremental reduction, then sending syngas into the DMEb pathway until the maximum amount of electricity needed for the entire facility is satisfied, with the remainder being sent into the DMEa pathway. The DMEa pathway realizes a decrease in syngas as the FTb production pathway is decreased enough to allow for the more efficient syngas conversion in DMEb, and this split product pathway solution holds true for data points 12, 13, and 14 until the amount of syngas in the DMEa pathway is reduced to zero at data point 15 due to being far enough away from the electricity threshold that would result in activation of the price penalty.

At data point 16, the maximum capacity of the FTb pathway is reduced to zero, and all of the gasified black liquor should then be sent into the DMEb pathway, which will then be incrementally reduced by 20%. Once the DMEb pathway maximum capacity is reduced, the process solutions are no longer in the pareto-optimal zone as these solutions result in negative profitability. As the DMEb pathway is being reduced, the remaining syngas is then sent into the FTa pathway, resulting in a split primary product solution for data points 17-20. Once the DMEb pathway is completely eliminated as a possible process solution, the

framework suggests sending all of the gasified black liquor into the FTa pathway in data point 21. The maximum output of the FTa pathway is then decreased by 50% in data point 22, which results in the emergence of DMEa as a viable process solution. Once the FTa pathway is completely negated as a possible solution, the framework dictates that the DMEa pathway has the optimal, albeit negative, profitability level.

Many observations could be made by executing the methodology in such a manner. First and foremost, and as stated previously, the production of electricity is an important driving factor in the economic performance of process solutions. The price penalty in exporting excess electricity to the grid causes the framework to determine which process solutions will result in meeting the electricity needs of the polygeneration facility exactly, and then seeking out the DMEa pathway which results in negligible electricity generation while allowing for the production of dimethyl ether and process steam. Conversely, as the amount of electricity is decreased from the threshold at which all mill needs are satisfied, the DMEa pathway becomes less viable as coproduction of electricity and products through more efficient processes have a greater impact on the economic performance of the process solution.

From an environmental impact standpoint, the analysis of split primary product solutions highlights the reasons for the behaviors of economic and environmental performance. For example, the decrease in environmental impact between data points 1 and 2 shows that the FTb process is less environmentally harmful than the FTc process, and this is likely because of the increased power generation of the FTb process, which results in positive environmental impact due to the avoidance of burning coal to generate electricity. Also, the DMEa process further decreases the overall adverse environmental impact due to the fact that

the WAR score of a gallon of dimethyl ether is an order of magnitude less than that of a gallon of FT oil (0.715 vs. 3.69). Furthermore, additional decreases in adverse impact occur during the phase-in of the DMEb pathway in data points 11 through 15, as the coproduction of electricity with dimethyl ether has a synergistic effect on the environmental impact of the process solution due to both avoiding coal combustion and producing the more environmentally friendly dimethyl ether. This is further confirmed by the appearance of a local minimum for environmental impact, which is observed at the process solution that dictates sole pursuit of the DMEb pathway. However, as the DMEb pathway is incrementally phased out, the adverse impact increases as the framework dictates increased production via the FTa pathway, which results in the counterintuitive behavior of decreasing profit and increasing adverse environmental impact. The reverse is then observed as the FTa pathway is phased out and the DMEa pathway is phased in. In conclusion, by forcing incremental phase-outs of subsequently optimal primary product solutions, one can gain a much clearer understanding of the reasons behind the economic and environmental performance of potential polygeneration facilities.

4.4.4 Net present value optimization

As stated previously, the usage of net present value (NPV) for economic evaluation is more robust than using only gross profit due to the fact that many important factors may be taken into consideration in NPV, such as tax breaks from depreciation, incentives or penalties from governing entitites, and hedging expenses. Furthermore, the time value of money may be taken into account, which is important in situations where the timing of sales revenue would have a greater impact on evaluating the profitability of a potential process solution.

The major disadvantage of the NPV approach is the necessity of forecasting future economic conditions, and as such, it should only be used in scenarios where future events and conditions may be predicted with relative certainty.

The optimization program executed to determine the optimal polygeneration facility from the black liquor biorefinery options presented by Larson, Consomi et al. needs to be revised so that an expression for net present value may now be maximized. Recall Problem P3.2 from Chapter 3 for the expression used to measure net present value:

$$\max NPV = \sum_t \left[\frac{GP_t(1 - Tax_t) + Dep_t Tax_t - Hedge_t + Gov_t}{(1+R)^t} \right] \qquad \text{(P3.2)}$$

While previous execution of the optimization code has resulted in the maximization of gross profit, or GP_t, the code must now be modified to allow for maximization of value with respect to the time value of money. The constraints for ensuring a single pathway solution have been kept intact, and Figure 4.24 presents the results of sequential elimination of single

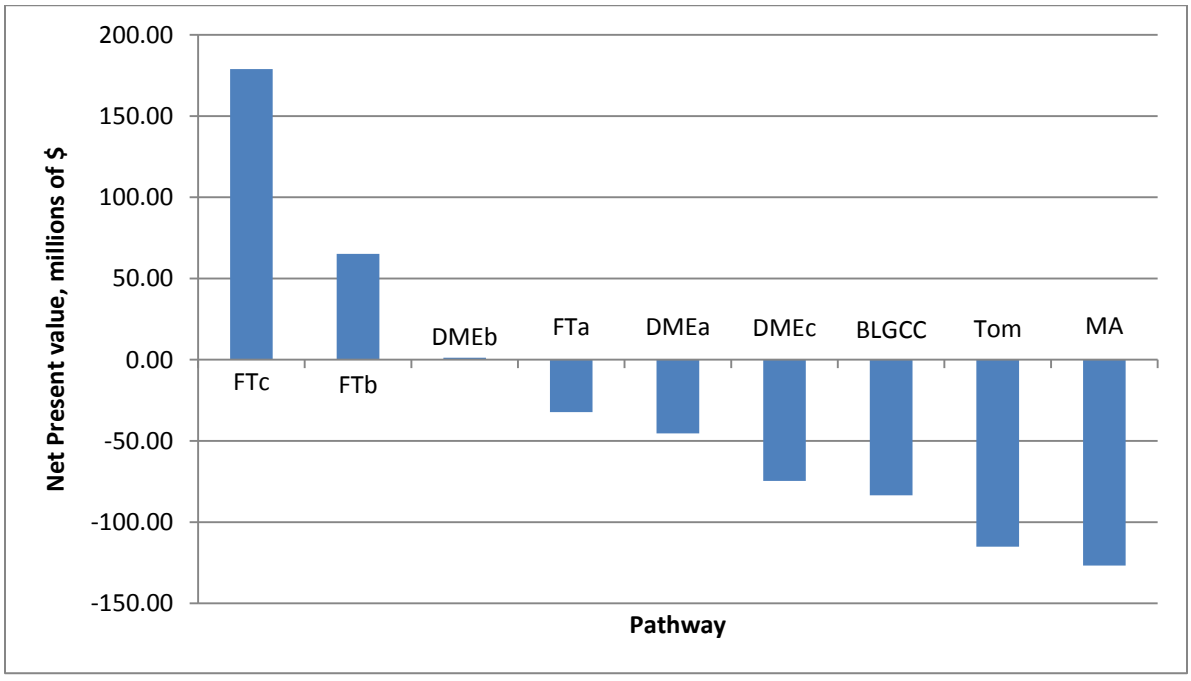

Figure 4.24 – Net present value (NPV) of black liquor gasification polygeneration pathways.

pathway solutions in order to observe the economic value added by all of the possible single pathway configurations. In this particular case study, it is assumed that all polygeneration projects have a useful, depreciable life of 25 years. Furthermore, the cost of capital is assumed to be 15%, and the marginal taxation rate is assumed to be 40%. Because this first optimization run only includes net profit adjusted on the time value of money, the qualitative ranking order of the solutions will match earlier results, with the FTc pathway showing the highest level of profitability, followed by FTb, DMEb, DMEa, FTa, DMEc, BLGCC, NewTom, and MA.

The absolute values for net present value may be obtained manually by taking the gross profit for each year, dividing by the necessary denominator to discount future cash flows, and summing all discounted future cash flows to determine overall value in current dollars. Thus, there should be no difference in the ranking of solutions whether the gross profit method or the net present value method of economic evaluation is used. However, this net present value approach allows for the flexibility of taking depreciation into account, and this will have an apparent effect on the net present value of these different process options.

Straight line amortization does not have a significant effect on the ranking of the process solutions since fixed costs are taken into account in the process cost scalar by using a straight-line method. Therefore, the deduction of tax breaks due to straight line depreciation will always have a congruent impact on the profitability of a process in which there are no financial advantages to be realized in the depreciation of processes of differing capital investments. However, when a modified depreciation schedule such as MACRS is used, the effect of depreciation on net present value of a given polygeneration project is much more pronounced. Modified depreciation schedules such as MACRS allow for a greater amount of

depreciation to be claimed in the early years of the project instead of an equal amount for each year, resulting in greater tax savings and an increased net present value.

A caveat should be mentioned at this point concerning accelerated depreciation and the inclusion of fixed cost within the processing cost scalar. In practice, fixed cost is tracked separately from variable cost as variable costs may be deducted from sales revenue in the form of cost of goods sold, while fixed cost must be depreciated along either an accelerated schedule or straight-line schedule depending on classification of equipment, current practices, and tax regulations. As such, fixed cost should only be included within the processing cost scalar in the very limited case of internal economic evaluation with the assumption of straight-line amortization. Furthermore, depreciation results in a reduced tax liability and typically does not represent the actual expenditure for the equipment in a given tax period. At this point, due to the use of accelerated depreciation and the anticipation of modifying fixed capital investment values, it is prudent to decouple the fixed and variable cost components from the processing cost scalar, which will result in the following modified equations for gross profit and net present value:

$$\mathrm{GP_t} = \sum_m \left(\sum_k TS_{mkt}\, C_{kt}^{S} - \sum_i \sum_j R_{mijt}\, VC_{mijt}^{P} - C_{mt}^{BM} \sum_j R_{m1jt} \right) \tag{4.3}$$

$$\max NPV = \sum_t \left[\frac{GP_t(1 - Tax_t) - FCI_t + Dep_t Tax_t - Hedge_t + Gov_t}{(1+R)^t} \right] \tag{4.4}$$

In these modified equations, fixed cost and variable cost may now be accounted separately, and the taxation component is also calculated separately in order to handle depreciation properly. In Equation 4.3, the second term in the summation VC^{P}_{mijt} is now variable cost only, which is unaffected by changes in fixed capital investment. The fixed capital investment is

taken into account in Equation 4.4 in the second term, where FCI_t represents the payment for the fixed capital investment at time period t adjusted on the basis of the time value of money.

As a result of this change in objective function and optimization formulation, the net present values of all the processes are lower since only a portion of fixed cost is counted for depreciation purposes. Within the gross profit method, the entirety of the fixed cost plus 25 years of interest is included within the processing cost scalar against sales revenue. This difference is visible in Figure 4.25, which illustrates the net present value of polygeneration projects that take depreciation into account via the MACRS accelerated schedule.

While the dominant process solution is still the pursuit of the FTc pathway, there are many interesting points that arise from the incorporation of net present value into the economic valuation. Before depreciation was incorporated into the net present value function, only three single-process solutions could be considered to operate in the pareto-

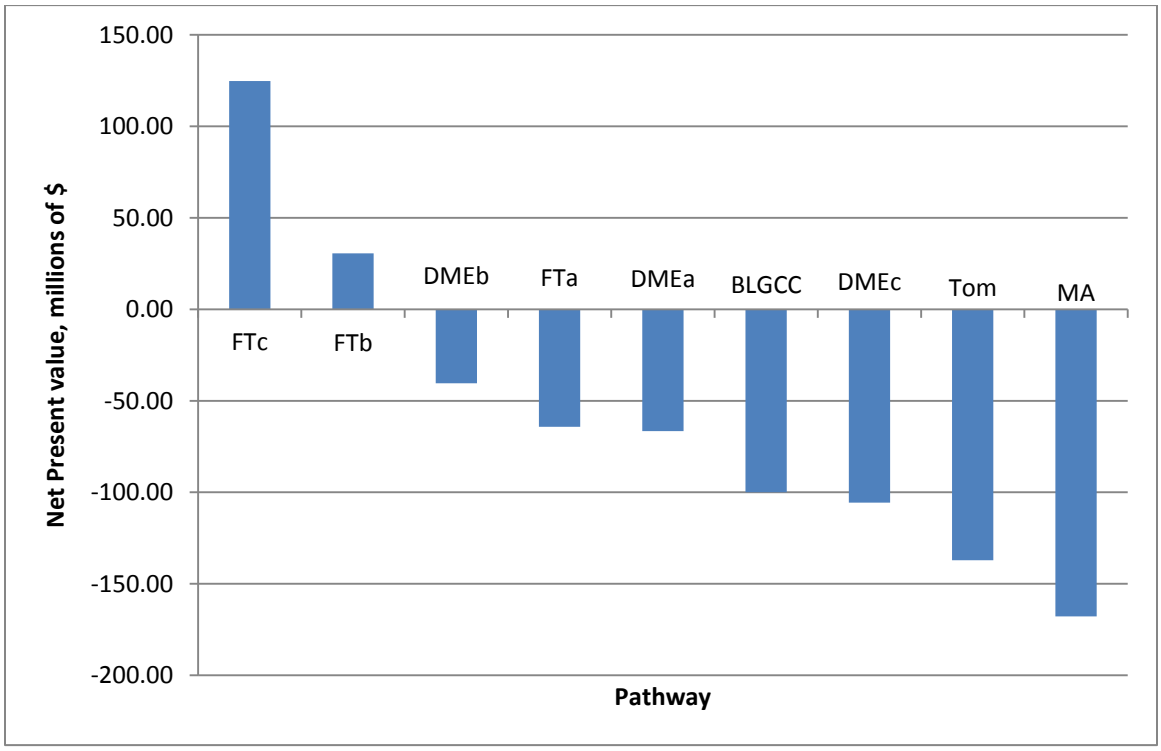

Figure 4.25 – NPV of black liquor polygeneration pathways, with depreciation.

optimal frontier of positive profitability and positive environmental impact (FTc, FTb, and DMEb). However, after the inclusion of depreciation, only FTc and FTb offer positive profitability, with the DMEb process solution migrating into the negative profitability region. In addition to the larger number of process solutions that offer positive economic value, the ranking of the process solutions has changed.

While the first five most profitable process solutions still offer the greatest present value, the BLGCC and DMEc processes switch places within the rankings due to the fact that the difference in capital investment between the two process solutions (>$95 MM) is great enough to have an even larger effect on net present value when it is decoupled from variable cost. Because the ranking of solutions may easily change due to the implementation of additional rules and constraints, it is important to follow sound, widely accepted accounting practices even in an informal setting where the main goal may be internal economic evaluation.

4.4.5 Capital investment as function of capacity

In order to incorporate depreciation into the net present value function, it is necessary to include an equation within the optimization program in which the total fixed capital investment could be calculated as a function of the activated flowrates of the processing routes. In this initial formulation, an "all or nothing" approach was taken in which it is assumed that either one full-scale facility is built for a given process solution, or no facility for that route was built at all. As a result, it could be surmised that the capital investment of these "all or nothing" plants could be considered linear based on the input or output of the process streams entering or leaving the facility respectively, and as a result, capital

investment factors in terms of money per product output have been calculated and are available in Table C.9. However, in process engineering, the scaling of installed chemical facilities is rarely considered to be linear, and is often considered to be nonlinear in the aspect that multiple scaling exponents may be used to estimate the overall cost of a chemical production facility (Peters, Timmerhaus et al., 2003). Such a formula is given in Equation 4.5:

$$FCI_b = FCI_a \left(\frac{Capacity_b}{Capacity_a}\right)^{exp} \tag{4.5}$$

where *FCI* represents the fixed capital investment and *exp* reprsents the scaling exponent used in the calculation based on literature and process knowledge (Peters, Timmerhaus et al., 2003). As stated previously, there is a need to decouple fixed cost and variable cost, and to this extent, variable cost will remain the same within a process regardless of the fixed capital investment.

In order to illustrate the ability of the framework to handle capital investment as nonlinear functions based on capacity, a hypothetical scenario has been constructed that eliminates the bound on black liquor feedstock. Instead of having bounds on incoming black liquor which dictate capacity for the rest of the facility, an upper bound will be placed on fixed capital investment, which was previously unbounded due to the feedstock limitation. In order to reach a balance between simplicity and practicality, scale-up factors will remain constant within a process but different among processes. A more rigorous study would include determining the exponential factors for each individual piece of equipment and then determining a process-wide equation for investment as a function of capacity, but the above simplifying assumption should have the same effect within the methodology. Table 4.6

Process	Scale-up Factors	Original FCI, MM$	Original Primary Output
NewTom	0.81	148.09	.214 Klb/s steam
Gasifier	0.85	69.31	60.1 kg/s syngas
BLGCC	0.66	167.87	.0317 MWh/s electricity
FTa	0.61	289.88	.944 gal/s FT fuel
FTb	0.72	438.41	.944 gal/s FT fuel
FTc	0.79	436.2	2.899 gal/s FT fuel
DMEa	0.68	204.65	2.311 gal/s DME fuel
DMEb	0.73	382.84	2.311 gal/s DME fuel
DMEc	0.74	282.85	1.021 gal/s DME fuel
MA	0.65	361.65	0.559 gal/s MA

Table 4.6 – Capital cost and flowrate data for black liquor polygeneration processes.

highlights the exponential factors of scale for the polygeneration processes which are randomly generated to be between 0.5 and 0.9, as well as the original cost and process outputs on which the scale-up calculation will occur within the optimization program.

Figure 4.26 illustrates the resulting net present value that occurs when maximum capital investment is varied from $100 million to $8 billion. Due to the vastly superior economic performance of the FTc process, it is selected by the optimization program for every run regardless of fixed capital investment. The high profitability counteracts the price penalty for electricity sold to the grid once all internal power needs are satisfied. Because this is essentially an unbounded problem in terms of feedstock supply and product demand, there is no cap on net present value as fixed capital investment increases. However, constraints on supply and demand, as well as price penalties that are activated once a certain threshold is exceeded, will allow the user of the framework to observe if and when the framework switches between optimal process solutions while being able to quantify net present value and environmental impact.

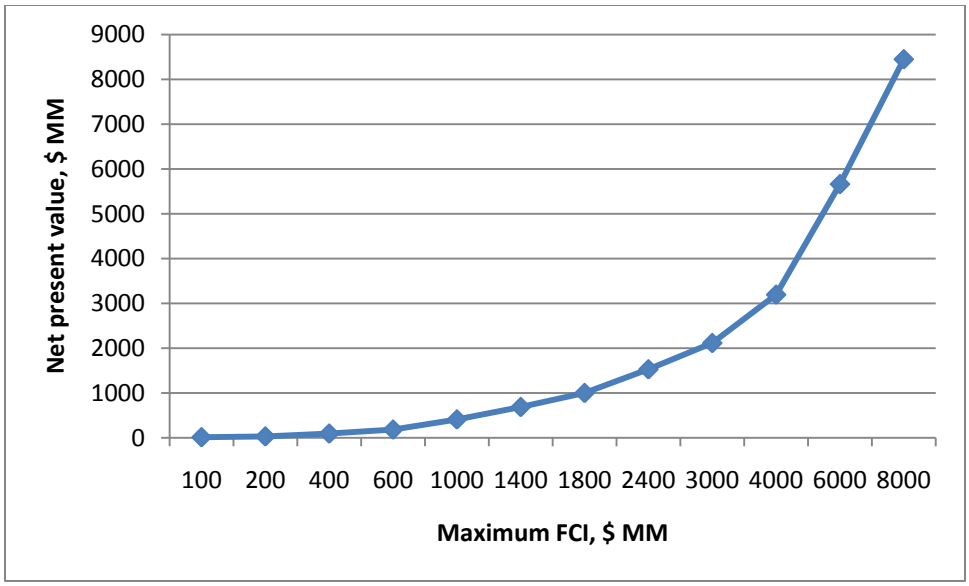

Figure 4.26 – Net present value of FTc process for maximum fixed capital investment.

4.5 Summary

The presented and demonstrated optimization-based methodology for polygeneration facility evaluation has been utilized in a number of case studies to highlight its adaptability to changing financial and environmental conditions as well as to determine, both quantitatively and qualitatively, the pareto-optimal front in which both positive economic and beneficial environmental impact may be observed in process solutions. Through the application of the framework to the analysis of a theoretical chicken litter biorefinery, a cellulose-based chemical product platform, and a detailed design study of black liquor gasification into electricity and fuels, the flexibility and ability of the framework to quantify the economic and environmental performance of different process solutions is made apparent.

Chapter 5

Accomplishments and Future Directions

5.1 Accomplishments

In this work, a methodology has been presented to solve the polygeneration product allocation problem for the emerging field of biorefining, in which optimal product portfolios and processing pathways may be determined in order to maximize economic return while being able to quantify environmental impact and identify process inefficiencies that can be improved in order to reduce further relative environmental impact. An initial superstructure is first generated in order to visualize the polygeneration pathways in biorefining that are possible for either given feedstock or given products or classes of products. The chemical processes in this superstructure are then simulated in order to determine the necessary equipment as well as conversion factors for subsequent use in the optimization program. Computer-aided molecular design may be used to modify solvent-based processes, and process integration seeks to further optimize these production pathways through the efficient use of mass and energy. Environmental and economic metrics are then measured for each optimized simulation model for use in an optimization-based program that will determine maximum economic performance while measuring relative environmental impact.

From the initial use of this methodology, it is seen that products with the highest contribution margin are selected for production. Constraints on the most profitable product cause the framework to subsequently select the remaining product pathways with high

contribution margins, resulting in a multi-product portfolio. Capital budgeting constraints have also been tested successfully, which is useful for industrial applications since capital constraints are often a limiting factor in pursuing new projects. Various cost factors and market prices have been used in the framework, and the solutions returned by the framework match those determined by hand calculations.

The presented framework has also been demonstrated in a number of case studies, and the lessons learned have served to enhance the robustness of the framework further. In the case of pre-design analysis of implementation of a chicken litter biorefinery, gross profit was used as the sole metric to determine which general process route and chemical product or service holds the most economic promise. This process-product combination is recommended for exploration in further detail using traditional process systems engineering approaches for design including rigorous process modeling as well as process integration.

The polygeneration allocation framework is also available for the purpose of evaluating chemical product platforms and families. The feasible process and product options are also determined via process systems engineering in which computational methods are utilized to enumerate the initial product superstructure. Preliminary profitability upper bound analysis is necessary to reduce the vast search space of the particular cellulose-based platform inquiry. After this screening, process synthesis and design may be performed on the most promising options in order to extract the data necessary to utilize optimization to determine which platforms and/or families add maximum value to the supply chain.

Lastly, this methodology has shown a great deal of potential in the evaluation of black liquor gasification-based polygeneration facilities and their economic and environmental evaluation with respect to a “business-as-usual” replacement of Tomlinson

boilers in the pulp and paper industry. The qualitative ranking of both economic and environmental performance presented by the original authors of the black liquor design study have been confirmed and quantified by the polygeneration framework. The transition from gross profit to net present value as the key economic metric has been executed, and from this transition, one may see the effects of changing maximum capital investment on the value added by the chosen process. The decoupling of fixed cost from variable cost has been shown to have a significant effect on the net present value of the process solutions returned by the optimization portion of the framework.

5.2 Future Directions

Although this methodology is a very powerful tool in the evaluation of new biorefining technology, progress may still be made on many fronts. The next phase of this work involves development of additional process models for the generation of performance metrics, specifically information on conversion, yield, and production cost for economic metrics and data to be used to generate a measure of environmental impact. Although the case study illustrated previously demonstrates real world usage of this methodology, many simplifications have been made, and over time the simplifying assumptions will be further reduced in order to increase the realism and rigor of the framework as an evaluation tool. From there, process integration will be systematically utilized to optimize the process models by reducing energy usage, material consumption, and waste streams.

An alternative formulation of the product allocation problem will be developed using a combination of general disjunctive programming (GDP) with the use of genetic algorithms (GA) (Odjo, Sammons et al., 2008). The current formulation of the problem is a mixed-

integer nonlinear problem (MINLP), and even state of the art MINLP solvers have difficulty in solving problems with a large number of mixed integer variables, which may very well be the case within the polygeneration allocation framework. However, the use of GA and GDP has been shown to solve nonconvex, discontinuous optimization problems more efficiently than the iterative MILP-NLP approach used in many solver programs. The alternative formulation would involve constructing logical disjunctions to map out the decision making tree and decoupling the system of disjunctions from the optimization portion of the framework. The disjunctions will then be converted into chromosomes of decision variables, and genetic algorithms will then be used to determine which combination of mixed integers would result in the optimal solution. At this point, the computation time and objective values of optimal solutions between the two solution methods will be compared to determine which formulation is more effective in solving this general problem, and the reformulation will also be utilized to solve problems with many more mixed integer variables, which will also increase the robustness of the framework (Odjo, Sammons et al., 2008).

The framework will also become a stronger financial tool through the incorporation of various economic ideas and analyses. The development of qualitative predictive models for capital investment as a function of capacity could determine the right process and product configuration for given maximum levels of capital investment. As stated previously, the usage of net present value as a metric for economic valuation depends on the prediction of future conditions. Since the future by definition is uncertain, optimization under uncertainty could then be utilized in conjunction with this framework to determine a multitude of economic outcomes and optimal process pathway solutions necessary to maximize added value for each set of economic conditions (Chakraborty, Colberg et al., 2003; Chakraborty,

Malcolm et al., 2004). Furthermore, options theory, which is the usage of advanced financial tools in order to hedge against risk, may be incorporated into the framework during Monte Carlo runs to determine the buffered effects of adverse market activity on optimal primary product solutions.

References

Aksoy, B., H. Cullinan, N. E. Sammons Jr and M. R. Eden (2008). "Identification of Optimal Poultry Litter Biorefinery Location in Alabama through Minimization of Feedstock Transportation Cost." Journal of Environmental Progress **27**(4): 515-523.

Androulakis, I. P. and V. Venkatasubramanian (1991). "A Generic Algorithm Framework for Process Design and Optimization." Computers & Chemical Engineering **15**(4): 217-228.

Anupindi, R., S. Chopra, S. D. Deshmukh, J. A. V. Mieghem and E. Zemel (2006). Managing Business Process Flows: Principles of Operations Management. Upper Saddle River, NJ, Pearson Prentice Hall.

Asante, N. D. K. and X. X. Zhu (1996). "An Automated Approach for Heat Exchanger Network Retrofit Featuring Minimal Topology Modifications." Computers & Chemical Engineering **20**(Suppl.): S7-S12.

Aspen Technology (2006). HX-Net. Cambridge, MA.

Ayindel, M., T. Sowlati, X. Cerda, E. Cope and M. Gerschman (2008). "Optimization of production allocation and transportation of customer orders for a leading forest products company." Mathematical and Computer Modeling **48**: 1158-1169.

Ayoub, N., R. Martins, K. Wang, H. Seki and Y. Naka (2007). "Two levels decision system for efficient planning and implementation of bioenergy production." Energy Conversion and Management **48**(3): 709-723.

Azapagic, A. and R. Clift (1999). "The application of life cycle assessment to process optimisation." Computers & Chemical Engineering **23**(10): 1509-1526.

Azapagic, A. and S. Perdan (2000). "Indicators of Sustainable Development for Industry." Institution of Chemical Engineers **78**(B): 243-261.

Biegler, L. T., I. E. Grossmann and A. W. Westerberg (1997). Systematic Methods of Chemical Process Design. Upper Saddle River, NJ, Prentice Hall PTR.

Bordado, J. C. M. and J. F. P. Gomes (2001). "Characterisation of non-condensable sulphur containing gases from Kraft pulp mills." Chemosphere **44**(5): 1011-1016.

Bozell, J. J., L. Moens, D. C. Elliott, Y. Wang, G. G. Neuenscwander, S. W. Fitzpatrick, R. J. Bilski and J. L. Jarnefeld (2000). "Production of levulinic acid and use as a platform chemical for derived products." Resources, Conservation and Recycling **28**(3-4): 227-239.

Bridgwater, A. V. (2003). "Renewable fuels and chemicals by thermal procession of biomass." Chemical Engineering Journal **91**: 87-102.

Broadbelt, L. J., S. M. Stark and M. T. Klein (1994). "Computer generated reaction networks: on-the-fly calculation of species properties using computational quantum chemistry." Chemical Engineering Science **49**(24, Part 2): 4991-5010.

Broadbelt, L. J., S. M. Stark and M. T. Klein (1995). "Termination of computer-generated reaction mechanisms: species rank-based convergence criterion." Industrial and Engineering Chemistry Research **34**: 2566-2573.

Cabezas, H., J. C. Bare and S. K. Mallick (1999). "Pollution prevention with chemical process simulators: the generalized waste reduction (WAR) algorithm--full version." Computers & Chemical Engineering **23**(4-5): 623-634.

Chakraborty, A., R. Colberg and A. Linninger (2003). "Plant-Wide Waste Management 3. Long-Term Operation and Investment Planning under Uncertainty." Ind. Eng. Chem. Res.

Chakraborty, A., A. Malcolm, R. Colberg and A. Linninger (2004). "Optimal waste reduction and investment planning under uncertainty." Computers & Chemical Engineering.

Colmenares, T. R. and W. D. Seider (1987). "Heat and Power Integration of Chemical Processes." AIChE Journal **33**(6): 898-915.

D'Souza, B. and T. W. Simpson (2003). "A Genetic Algorithm based method for product family design optimization." Engineering Optimization **35**(1): 1-18.

Diwekar, U. (2003). Introduction to Applied Optimization. Dordecht, The Netherlands, Kluwer Academic Publishers.

Doman, L., J. Staub, L. Mayne, J. Barden and P. Martin (2008). International Energy Outlook, US Department of Energy.

Douglas, J. M. (1988). Conceptual Design of Chemical Processes. New York, NY, McGraw-Hill.

Dunn, R. F. and M. M. El-Halwagi (2003). "Process integration technology review: background and applications in the chemical process industry." Journal of Chemical Technology and Biotechnology **78**(9): 1011-1021.

Eden, M. R., S. B. Jørgensen, R. Gani and M. M. El-Halwagi (2000). "Reverse problem formulation based techniques for process and product synthesis and design." Computer Aided Chemical Engineering 15B. B. Chen and A. Westerberg. Amsterdam, The Netherlands, Elsevier B.V.**:** 445-450.

Eden, M. R., S. B. Jørgensen, R. Gani and M. M. El-Halwagi (2004). "A Novel Framework for Simultaneous Process and Product Design." Chemical Engineering and Processing **43**: 595-608.

El-Halwagi, M. M. (1997). Pollution Prevention through Process Integration. San Diego, CA, USA, Academic Press.

El-Halwagi, M. M. (2006). Process Integration. Boston, MA, Elsevier.

El-Halwagi, M. M., A. A. Hamad and G. W. Garrison (1996). "Synthesis of Waste Interception and Allocation Networks." AIChE Journal **42**(11): 3087-3101.

El-Halwagi, M. M. and V. Manousiouthakis (1989). "Synthesis of mass exchange networks." AIChE Journal **35**(8): 1233-1244.

El-Halwagi, M. M. and H. D. Spriggs (1998). "Solve Design Puzzles with Mass Integration." Chemical Engineering Progress **94**(8): 25-44.

Eljack, F. T., M. R. Eden, V. Kazantzi and M. M. El-Halwagi (2006). "Property clustering and group contribution for process and molecular design." Computer-Aided Chemical Engineering 21, Part 1. W. Marquardt and C. Pantelides. Amsterdam, The Netherlands, Elsevier B.V.**:** 907-912.

Fermeglia, M., G. Longo and L. Toma (2007). "A hierarchical approach for the estimation of environmental impact of a chemical process: from molecular modeling to process simulation." Computer Aided Chemical Engineering. V. Plesu and P. S. Agachi, Elsevier. **Volume 24:** 1199-1204.

Floudas, C. A., A. R. Ciric and I. E. Grossmann (1986). "Automatic Synthesis of Optimum Heat Exchanger Network Configurations." AIChE Journal **32**(2): 276-290.

Furman, K. C. and N. V. Sahinidis (2002). "A Critical Review and Annotated Bibliography for Heat Exchanger Network Synthesis in the 20th Century." Ind. Eng. Chem. Res.(41): 2335-2370.

Gadhe, J. B. and R. B. Gupta (2007). "Hydrogen production by methanol reforming in supercritical water: Catalysis by in-situ-generated copper nanoparticles." International Journal of Hydrogen Energy **32**(13): 2374-2381.

GAMS Development Corporation (2009). GAMS. Washington, DC.

Grossmann, I. E., H. Yeomans and Z. A. Kravanja (1998). "A Rigorous Disjunctive Optimization Model for Simultaneous Flowsheet Optimization and Heat Integration." Computers & Chemical Engineering **22**(Suppl.): S157-S164.

Harper, P. M. and R. Gani (2000). "A multi-step and multi-level approach for computer aided molecular design." Computers & Chemical Engineering **24**: 677-683.

Hesselmann, K. (1984). "Optimization of the Effective Profit of Heat Exchanger Networks." Journal of Heat Recovery Systems **4**(5): 351-354.

Keat, P. G. and P. K. Y. Young (2003). Managerial Economics: Economic Tools for Today's Decision Makers. Upper Saddle River, NJ, Prentice-Hall.

Konukman, A. E., M. C. Camurdan and U. Akman (1999). "Synthesis of Energy-Optimal HEN Structures with Specified Flexibility Index through Simultaneous MILP Formulation." PRES 99: 2nd Conference on Process Integration, Modelling and Optimization for Energy Saving and Pollution Reduction, Budapest, Hungarian Chemical Society.

Kovabvc-Kralj, A., P. Glavibvc and Z. Kravanja (2000). "Retrofit of Complex and Energy Intensive Processes II: Stepwise Simultaneous Superstructural Approach." Computers & Chemical Engineering **24**(1): 125-138.

Larson, E., S. Consomi and R. Katofsky (2006). "A Cost-Benefit Assessment of Biomass Gasification Power Generation in the Pulp and Paper Industry." **Volume 1: Main Report**.

Larson, E., S. Consomi and R. Katofsky (2006). "A Cost-Benefit Assessment of Biomass Gasification Power Generation in the Pulp and Paper Industry." **Volume 3: Fuel Chain and National Cost-Benefit Analysis**.

Larson, E., S. Consomi, R. Katofsky, K. Iisa and J. Frederick (2006). "Agenda 2020 CTO Committee: Cost Benefit Analysis of Gasification-Based Biorefining at U.S. Kraft Pulp Mills." Powerpoint Presentation.

Lewin, D. R., H. Wang and O. Shalev (1998). "A Generalized Method for HEN Synthesis Using Stochastic Optimization I - General Framework and MER Optimal Synthesis." Computers & Chemical Engineering **22**(10): 1503-1513.

Linnhoff, B., D. W. Townsend, D. Boland, G. F. Hewitt and B. E. A. Thomas (1994). A User Guide on Process Integration for the Efficient Use of Energy. Warwick, UK, Institution of Chemical Engineers.

Meij, R. and B. te Winkel (2004). "The emissions and environmental impact of PM10 and trace elements from a modern coal-fired power plant equipped with ESP and wet FGD." Fuel Processing Technology **85**(6-7): 641-656.

Meyer, M. H. and D. Dalal (2002). "Managing platform architectures and manufacturing processes for nonassembled products." Journal of Product Innovation Management **19**(4): 277-293.

Michalewicz, Z. (1996). Genetic Algorithms + Data Structures = Evolution Programs. New York, Springer-Verlag.

Nahmias, S. (2005). Production & Operations Analysis. New York, NY, Mcgraw-Hill.

Odjo, A., N. E. Sammons, A. Marcilla, M. R. Eden and J. Caballero (2008). "A disjunctive-genetic programming approach to synthesis of process networks." Computers & Industrial Engineering (submitted).

Parthasarathy, G. and G. Krishnagopalan (2001). "Systematic reallocation of aqueous resources using mass integration in a typical pulp mill." Advances in Environmental Research **5**(1): 61-79.

Peters, M. S., K. D. Timmerhaus and R. E. West (2003). Plant Design and Economics for Chemical Engineers. New York, NY, McGraw-Hill Professional.

Pistikopoulos, E. N., S. K. Stefanis and A. G. Livingston (1995). "A Methodology For Minimum Environmental Impact Analysis." Pollution prevention via process and product modifications. M. M. El-Halwagi and D. M. Petrides. New York, NY, American Institue of Chemical Engineers.

POLYSMART (2008). "Polygeneration in Europe - A Technical Report." European Commission within the Sixth Framework Programme (2002-2006).

Ponce-Ortega, J. M., A. Jimenez-Gutierrez and I. E. Grossmann (2008). "Optimal synthesis of heat exchanger networks involving isothermal process streams." Computers & Chemical Engineering **32**(8): 1918-1942.

Robertson, D. and K. Ulrich (1998). "Planning product platforms." Sloan Management Review **39**(4): 19-31.

Sahinidis, N. V., I. E. Grossmann, R. E. Fornari and M. Chathrathi (1989). "Optimization model for long range planning in the chemical industry." Computers & Chemical Engineering **13**(9): 1049-1063.

Sammons, N. E., M. R. Eden, H. Cullinan, E. Connor and L. Perine (2006). "A Flexible Framework for Optimal Biorefinery Product Allocation." Computer Aided Chemical Engineering **21B**: 2057-2062.

Sammons, N. E., M. R. Eden, W. Yuan, H. Cullinan and B. Aksoy (2007). "A Flexible Framework for Optimal Biorefinery Product Allocation." Journal of Environmental Progress **26**(4): 349-354.

Sammons, N. E., M. R. Eden, W. Yuan, H. Cullinan and B. Aksoy (2007). "Optimal Biorefinery Resource Utilization by Combining Process and Economic Modeling." Proceedings of 6th European Congress of Chemical Engineering.

Sammons, N. E., M. R. Eden, W. Yuan, H. Cullinan and B. Aksoy (2008). "Optimal Biorefinery Resource Utilization by Combining Process and Economic Modeling." Chemical Engineering Research and Design **86**(7): 800-808.

Sammons, N. E., M. R. Eden, W. Yuan, H. Cullinan and B. Aksoy (2008). "A Systematic Framework for Biorefinery Production Allocation." Computer Aided Chemical Engineering **25**: 1077-1082.

Schulz, H. (1999). "Short history and present trends of Fischer-Tropsch synthesis." Applied Catalysis A: General **186**(1-2): 3-12.

Seider, W. D., J. D. Seader and D. R. Lewin (2004). Product and Process Design Principles. New York, NY, John Wiley & Sons.

Shi, B. and B. H. Davis (2005). "Fischer-Tropsch synthesis: The paraffin to olefin ratio as a function of carbon number." Catalysis Today **106**(1-4): 129-131.

Shonnard, D. R. and D. S. Hiew (2000). "Comparative Environmental Assessments of VOC Recovery and Recycle Design Alternatives for a Gaseous Waste Stream." Environmental Science & Technology **34**(24): 5222-5228.

Simpson, T. W. (2004). "Product platform design and customization: Status and promise." Artificial Intelligence for Engineering Design, Analysis and Manufacturing **18**: 3-20.

Simpson, T. W., J. R. A. Maier and F. Mistree (2001). "Product platform design: method and application." Research in Engineering Design **13**(1): 2-22.

Smith, R. L., T. M. Mata, D. M. Young, H. Cabezas and C. A. V. Costa (2004). "Designing environmentally friendly chemical processes with fugitive and open emissions." Journal of Cleaner Production **12**(2): 125-129.

Solvason, C. C., N. E. Sammons, D. Bilhartz, J. A. Pack, J. Harsimran, V. Chambost, P. R. Stuart, M. R. Eden and M. M. El-Halwagi (2010). "Chemical Product Portfolio Design: A Case Study for the Forest Biorefinery." Chemical Engineering Research and Design (submitted).

Sousa, R., N. Shah and L. G. Papageorgiou (2008). "Supply chain design and multilevel planning - An industrial case." Computers & Chemical Engineering **32**: 2643-2663.

Stefanis, S. K., A. G. Livingston and E. N. Pistikopoulos (1997). "Environmental impact considerations in the optimal design and scheduling of batch processes." Computers & Chemical Engineering **21**(10): 1073-1094.

Sukumaran, S. (2008). "A Decision Support System for Biorefinery Location & Logistics." Industrial and Systems Engineering, Master's Thesis, Auburn University, AL, USA.

Theloke, J. and R. Friedrich (2007). "Compilation of a database on the composition of anthropogenic VOC emissions for atmospheric modeling in Europe." Atmospheric Environment **41**(19): 4148-4160.

Tsiakis, P. and L. G. Papageorgiou (2008). "Optimal production allocation and distribution supply chain networks." International Journal of Production Economics(111): 468-483.

Türkay, M. and I. E. Grossmann (1996). "Logic-based MINLP algorithms for the optimal synthesis of process networks." Computers & Chemical Engineering **20**(8): 959-978.

U.S. Department of Energy (2003). "How to Calculate the True Cost of Steam." Technical Report.

US-EPA. (2008). "Chemical Process Simulation for Waste Reduction: WAR Algorithm." Retrieved 09/26/2008, from http://www.epa.gov/ord/NRMRL/std/sab/war/sim_war.htm.

Vecchietti, A. and I. Grossmann (1999). "LOGMIP: a disjunctive 0-1 non-linear optimizer for process system models." Computers & Chemical Engineering **23**(4-5): 555-565.

Wang, J.-J., Y.-Y. Jing, C.-F. Zhang and J.-H. Zhao (2009). "Review on multi-criteria decision analysis aid in sustainable energy decision-making." Renewable and Sustainable Energy Reviews **13**(9): 2263-2278.

Wang, K., Y. Qian, Q. Huang and P. Yao (1999). "New Model and New Algorithm for Optimal Synthesis of Large Scale Heat Exchanger Networks without Stream Splitting." Computers & Chemical Engineering **23**(Suppl.): S149-S152.

Wang, X., Y. Li, Y. Hu and Y. Wang (2008). "Synthesis of heat-integrated complex distillation systems via Genetic Programming." Computers & Chemical Engineering **32**(8): 1908-1917.

Williams, R. H. (2000). Advanced Energy Supply Technologies. Energy and the Challenge of Sustainability, World Energy Assessment. J. Goldemberg. New York, NY, USA, United Nations Development Programme, United Nations Department of Social and Economic Affairs, and the World Energy Council**:** 273-332.

Wisner, J. D., G. K. Leong and K.-C. Tan (2005). Principles of Supply Chain Management: A Balanced Approach. Mason, OH, Thomson South-Western.

Wooley, R., M. Ruth, J. Sheehan, K. Ibsen, H. Majdeski and A. Galvez (1999). "Lignocellulosic Biomass to Ethanol Process Design and Economics Utilizing Co-Current Dilute Acid Prehydrolysis and Enzymatic Hydrolysis Current and Futuristic Scenarios." Golden, CO, USA, National Research Energy Laboratory.

Yerramsetty, K. M. and C. V. S. Murty (2008). "Synthesis of cost-optimal heat exchanger networks using differential evolution." Computers & Chemical Engineering **32**(8): 1861-1876.

Young, D. and H. Cabezas (1999). "Desigining sustainable processes with simulation: the waste reduction (WAR) algorithm." Computers & Chemical Engineering **23**: 1477-1491.

Young, D., R. Scharp and H. Cabezas (2000). "The waste reduction (WAR) algorithm: environmental impacts, energy consumption, and engineering economics." Waste Management(20): 605-615.

Yu, H., H. Fang, P. Yao and Y. Yuan (2000). "A Combined Genetic Algorithm/Simulated Annealing Algorithm for Large Scale System Energy Integration." Computers & Chemical Engineering **24**(8): 2023-2035.

Appendix A

Detailed Data For Chicken Litter Case Study

Chicken Litter to Syngas Equipment	Cost (2005 $K)
Air Separation Unit	52933
Biomass Dryer	32523
Biomass Gasifier & Tar Cracker	18320
Biomass Syngas Cooler and Filter	4998
Biomass Syngas expander	2661
Feedstock Storage Area	867
Total Fixed Cost (2005 $)	$112,302,000

Syngas to Electricity Equipment	Cost (2005 $K)
Combined Cycle Power Island (details omitted)	100091
Total Fixed Cost	$100,091,000

Syngas to Hydrogen Equipment	Cost (2005 $K)
Syngas to H2 (details omitted)	461527
Total Fixed Cost	$461,527,000

Table A.1 – Fixed cost equipment list for chicken litter biorefinery.

Litter to Syngas Cost Category	Cost (2005 $)
Utilities	$96,541
Operating Labor	$98,162
Operating Supervision	$14,724
Maintenance	$10,107,180
Operating Supplies	$1,516,077
Laboratory Charges	$14,724
Overhead	$1,361,771
Administrative	$408,531
Total Variable Cost	$13,617,710.99

Syngas to Hydrogen Cost Category	Cost (2005 $)
Utilities	$127,943,849.88
Operating Labor	$98,162
Operating Supervision	$14,724
Maintenance	$41,537,405
Operating Supplies	$6,230,611
Laboratory Charges	$14,724
Overhead	$20,211,434
Administrative	$6,063,430
Total Variable Cost	$202,114,340

Syngas to Electricity Cost Category	Cost (2005 $K)
Electricity Purchases	$5,893,707.90
Operation and Maintanance	$9,407,549.48
Total Variable Cost	$15,301,257.39

Table A.2 – Variable cost lists for chicken litter biorefinery.

Appendix B

Data for Cellulose-Based Product Portfolio Design

Starting Material	Effective % conversion	Product	Product Mass [kg per 100 kg starting material]
Cellulose	72.00%	Ethanol	40.90
Cellulose	54.00%	Succinic acid	80.00
Cellulose	40.54%	Glycerol	46.00
Cellulose	33.60%	Levulinic acid	24.10
Cellulose	40.00%	Glutamic acid	36.30
Cellulose	40.32%	2,5 furandicarboxylic acid	38.80
Cellulose	48.00%	Glucaric acid	62.20
Cellulose	38.40%	Itaconic acid	41.10
Cellulose	76.00%	Sorbitol	85.40
Cellulose	56.00%	5-HMF from glucose	43.60
Cellulose	55.00%	5-HMF from cellulose	42.80
Levulinic Acid	97.10%	Diphenolic acid	239.43
Levulinic Acid	95.00%	g-valerolactone	81.91
Levulinic Acid	63.00%	MTHF	39.12
Levulinic Acid	81.00%	Acetylacrylic acid	79.59
Levulinic Acid	74.58%	1,4-pentanediol	66.89
Levulinic Acid	51.20%	d-aminolevulinate	51.40
Levulinic Acid	80.00%	a-Angelica lactone	67.59
Levulinic Acid	90.00%	Methyl levulinate	100.87
Levulinic Acid	85.00%	Ethyl levulinate	105.53

Table B.1: Conversion percentages and mass for cellulose and levulinic acid based processes. All effective conversions taken from Solvason, Sammons et al. (2010).

	Price per mass	Price Scale-up
	$ [USD]/ kg	[--]
1,4 pentanediol	$1,125.43	Yes
2,5 furandicarboxylic acid	$14,907.86	Yes
3-Hydroxypropionic acid	$1.28	No
5-HMF	$7,655.39	Yes
A-angelica lactone	$193.10	Yes
Acetylacrylic acid	$1,968.19	Yes
Br2	$63.00	No
Cellulose	$0.27	No
D-aminolevulinate	$3,250.00	Yes
Diphenolic acid	$220.68	Yes
Ethanol	$5.83	No
Ethy levulinate	$34.48	Yes
Formamide	$31.78	No
Formic acid	$78.93	No
Glucaric acid	$291.06	Yes
Glutamic acid	$6.50	No
Glycerol	$1.78	No
G-valerolactone	$84.16	Yes
Itaconic acid	$4.00	No
Levulinic acid	$11.02	No
Methanol	$8.56	No
Methyl levulinate	$82.17	Yes
Methyltetrahydrofuran	$48.84	No
NaOMe	$20.96	No
Phenol	$33.10	No
Sorbitol	$1.15	No
Succinic acid	$4.41	No

Table B.2: Prices of chemicals of interest observed in analysis via PUB calculations.

IN			OUT			
Species	**Mass**	**Cost**	**Species**	**Mass**	**Cost**	**Absolute PUB**
[--]	**kg**	**$ [USD]**	**[--]**	**kg**	**$ [USD]**	**$ [USD]**
Cellulose	100	$27.43	2,5 furandicarboxylic acid	38.82	$578,663.85	$578,636.42
Cellulose	100	$27.43	5-HMF from glucose	43.56	$333,432.34	$333,404.91
Cellulose	100	$27.43	5-HMF from cellulose	42.78	$327,478.19	$327,450.77
Cellulose	100	$27.43	Glucaric acid	62.21	$18,106.69	$18,079.27
Cellulose	100	$27.43	Succinic acid	80	$352.74	$325.31
Cellulose	100	$27.43	Levulinic acid	24.06	$265.24	$237.81
Cellulose	100	$27.43	Ethanol	40.91	$238.55	$211.13
Cellulose	100	$27.43	Glutamic acid	36.3	$235.93	$208.51
Cellulose	100	$27.43	Itaconic acid	41.08	$164.33	$136.90
Cellulose	100	$27.43	Sorbitol	85.39	$98.16	$70.73
Cellulose	100	$27.43	Glycerol	46.05	$81.74	$54.31
Cellulose	100	$27.43	3-Hydroxypropionic acid	44.44	$56.73	$29.30
C5H8O3	100	$1,102.31	g-valerolactone	81.91	$6,893.33	$5,791.02
C5H8O3	100	$1,102.31	MTHF	39.12	$1,910.69	$808.38
C5H8O3	100	$1,102.31	Acetylacrylic acid	79.59	$156,655.81	$155,553.50
C5H8O3	100	$1,102.31	1,4-pentanediol	66.89	$75,278.46	$74,176.15
C5H8O3	100	$1,102.31	a-Angelica lactone	67.59	$13,051.12	$11,948.81
C5H8O3	100	$1,102.31	d-aminolevulinate	51.4	$167,041.70	$163,320.00
Br2	61.17	$3,853.65	formic acid	36.08	$2,847.79	
Methanol	9.2	$78.74		**SUM**	$169,889.49	
C2H2O2NNa	58.2	$1,534.79				
	SUM	$6,569.49				
C5H8O3	100	$1,102.31	Methyl levulinate	100.87	$8,288.36	$6,949.83
CH3OH	27.6	$236.22				
	SUM	$1,338.53				
C5H8O3	100	$1,102.31	Ethyl levulinate	105.54	$3,638.37	$2,304.73
CH3CH2OH	39.67	$231.33				
	SUM	$1,333.64				
C5H8O3	100	$1,102.31	Diphenolic acid	239.43	$52,838.41	$46,369.97
Phenol	162.1	$5,366.14				
	SUM	$6,468.45				

Table B.3: PUB calculations for both levels of chemical platform evaluation.

Module Number[a]	Module Name	Scaled On	Base Year CPI	Base Scale Value[b]	Base Scale Price, kS	Scale Ex-ponent[c]	Install-ation Factor[d]	Jan. 2009 CPI	Install Cost, 2009 k$
A-300	Simult. Sacc. and Fermen-tation	Mass Flow Cellulose In, kg/hr	159	27792	10,467	0.674	1.29	211	17,919
A-400	Cellulase Production	Mass Flow Cellulase Out, kg/hr	159	563	12,168	0.738	1.29	211	20,832
A-500	Product Recovery and Water Recovery	Total Broth flow, kg/hr	159	380209	7,407	0.750	1.75	211	17,201
A-600	Waste-water Treat-ment	Total Flow into An-aerobic, kg/hr	159	179346	8,417	0.643	1.24	211	13,851
A-700	Product and Feed Chemical Storage	Dehy. Ethanol flow, kg/hr	159	18565	1,169	0.681	1.56	211	2,421
A-800	Burner, Boiler, and Turbo-generator	Total Flow into Com-bustion, kg/hr	159	98957	32,227	0.717	1.40	211	59,876
A-900	Utilities	Treated Waste Water, kg/hr	159	173154	3,548	0.672	1.40	211	6,591
					Total Installed Cost, 2009$:				138,692,192

Table B.4: Capital cost for large block flow diagram converting cellulose to ethanol.

[a]In Wooley, Ruth et al. (1999), the numbering for large block modules starts at A-100, and the A-100 represents the conversion of forest-based biomass feedstock into chips, while the A-200 module represents pretreatment and detoxification resulting in a purified cellulose stream to be fed into overall process. A-100 and 200 are assumed to be identical for all processes and will be ignored in capital cost calculation.

[b]Base scale values taken from Appendix G in Wooley, Ruth et al. (1999). Specific data locations: A-300, mass flowrate of cellulose hydrolyzate entering process; A-400, total cellulase in stream 420; A-500, total flow into beer column in stream 501; A-600, total input flow into anaerobic column in stream 612; A-700, total dehydrated ethanol flow into storage in stream 515; A-800, total flow into combustion reactor in stream 803; A-900, total flow into process water tank in stream 803.

[c]From Wooley, Ruth et al. (1999), mathematical average of scale values of individual units.

[d]From Wooley, Ruth et al. (1999), installation factor for entire large block module.

Module Number[a]	Module Name	Scaled On	Base Year CPI[b]	Base Scale Value	Base Scale Price, k$	Scaling Ex-ponent	#	Install-ation Factor[c]	Jan. 2009 CPI	Install Cost, 2009 k$
A-250[d]	Levulinic Acid Reactors	Reactor size, gal	68.3	49796	103.1	0.384	5	1.29	211.1	2,056
A-400[e]	Dist-illation Column 1	Total flow into first dist. column, kg/hr	159.1	357740	1,414.9	0.750	1	1.29	211.1	2,422
A-401[f]	Dist-illation column 2	Total flow from dist. column 1 bottoms, kg/hr	159.1	30863	225.2	0.750	1	1.75	211.1	523
A-500[g]	Waste-water Treat-ment	Total Water Flow from into anaerobic, kg/hr	159.1	312628	12,032.0	0.643	1	1.24	211.1	19,800
A-600[h]	Amine Sep-aration Unit	Total Flow into Unit, kg/hr	159.1	326666	2,644.2	0.750	1	1.24	211.1	4,351
A-700[i]	Product and Feed Chemical Storage	Levulinic and Formic flow, kg/hr	159.1	27777	1,538.1	0.681	1	1.56	211.1	3,184
A-800[j]	Burner, Boiler, and Turbo-generator	Total Flow into Com-bustion, kg/hr	159.1	98957	32,227	0.717	1	1.40	211.1	59,876
A-900[k]	Utilities	Total Water Flow from into anaerobic, kg/hr	159.1	312628	5,154.2	0.672	1	1.40	211.1	9,576
					Total Installed Cost, 2009$					101,788,474

Table B.5: Capital cost for large block flow diagram converting cellulose to levulinic acid.

[a]From base case for conversion of cellulose into ethanol, several module number and name changes have been made. The dilute acid catalyzed conversion of cellulose into levulinic acid takes place in A-250, and a flashing unit is utilized to separate the vapor and liquid in A-300. The product and water recovery module has been replaced with an amine separation unit to separate formic acid and water before treating wastewater.
[b]Base Year for CPI is 1979 for module A-250, 1997 for all other modules.

[c]From Wooley, Ruth et al. (1999), mathematical average of scale values of individual units.
[d]From Wooley, Ruth et al. (1999), Appendix G, p. 114, combined flow of streams 302 (inoculum) and 304 (detoxified hydrolyzate) into CSTR train is 347,241 kg/hr. Assume same flow would enter theoretical levulinic acid reactors. Assume density close to water at 1 kg/L. From literature on reaction referenced in Solvason, Sammons et al. (2010), residence time is 2hrs, resulting in total reactor size of 754,500 L. Split into 4 parallel reactors of 188,620 L each, converted to 49,796 gal. From Peters, Timmerhaus et al. (2003), cost function for jacketed reactor is 1620*size (gal)^0.384. Assume 5th reactor needed as backup.
[e]From Wooley Ruth et al. (1999), Appendix G, p. 117, stream 501 entering distillation module has total flow rate of 380,209 kg/hr. Original distillation module scaled cost of 7,407 k$ for 2 column, 3 evaporator system. For one column, assume 1/5 of original module scaled cost of 1481 k$. Scaled down to match incoming flowrate from Aspen simulation of 788,240 lb/hr, or 357,740 kg/hr.
[f]See footnote e. Scaled down to match incoming flowrate from Aspen simulation of 68,041 lb/hr, or 30,863 kg/hr.
[g]From Wooley Ruth et al. (1999), total flow of wastewater into anaerobic digester in stream 612 is 179,346 kg/hr. Original base cost of wastewater module is 8,417 k$. Scaled up to match flowrate from amine separation unit of water-heavy stream of 689,227 lb/hr or 312,628 kg/hr.
[h]From Wooley Ruth et al. (1999), Appendix G, p. 117, stream 501 entering distillation module has total flow rate of 380,209 kg/hr. Original distillation module scaled cost of 7,407 k$ for 2 column, 3 evaporator system. Assume two columns present in amine separation unit (one for extraction, one for regeneration), 2/5 of original module scaled cost of 2963 k$. Scaled up to match incoming flowrate from Aspen simulation of 720,199 lb/hr, or 326,677 kg/hr.
[i]From Wooley Ruth et al. (1999), Appendix G, p. 124, stream 515 entering storage module has total flow rate of 18565 kg/hr. Original storage module scaled cost of 1,169 k$. Scaled up to match combined flowrates of formic acid and levulinc acid streams of 61,238 lb/hr, or 27,777 kg/hr.
[j]Assume similar flowrate and cost from base case.
[k]From Wooley Ruth et al. (1999), total flow of wastewater into anaerobic digester in stream 612 is 179,346 kg/hr. Original base cost of wastewater module is 3,548 k$. Scaled up to match flowrate from amine separation unit of water-heavy stream of 689,227 lb/hr or 312,628 kg/hr.

Module Number[a]	Module Name	Scaled On	Base Year CPI[b]	Base Scale Value	Base Scale Price, k$	Scaling Exponent	Install-ation Factor[c]	Jan. 2009 CPI	Install Cost, 2009 k$
A-300[d]	Simult. Sacc and Fer-mentation	Mass Flow Cellulose In, kg/hr	159.1	27792	10,467	0.674	1.29	211.1	17,919
A-400[e]	Cellulase Production	Mass Flow Cellulase Out, kg/hr	159.1	563	12,168	0.738	1.29	211.1	20,832
A-500[f]	Water Flash Tank	Total Broth flow, kg/hr	68.3	339072	250	0.600	1.2	211.1	927
A-550[g]	Distillation Column	Total bottoms from flash flow, kg/hr	159.1	29593	218	0.750	1.75	211.1	507
A-600[h]	Waste-water Treatment	Total Flow of water vapor from flash, kg/hr	159.1	309479	11,954	0.643	1.24	211.1	19,672
A-700[i]	Product and Feed Chemical Storage	Dehy. Ethanol flow, kg/hr	159.1	15606	1,039	0.681	1.56	211.1	2,150
A-800[j]	Burner, Boiler, and Turbo-generator	Total Flow into Combustion, kg/hr	159.1	98957	32,227	0.717	1.40	211.1	59,876
A-900[k]	Utilities	Treated Waste Water, kg/hr	159.1	339072	5,443	0.672	1.40	211.1	10,113
						Total Installed Cost:			131,996,531

Table B.6: Capital cost for large block flow diagram converting cellulose to succinic acid.

[a]From base case for conversion of cellulose into ethanol, same large blocks used with the addition of a glass-lined water flash tank.
[b]Base Year for CPI is 1979 for module A-550, 1997 for all other modules.
[c]From Wooley, Ruth et al. (1999), mathematical average of scale values of individual units.
[d]Assume same entering flowrate from base case. From Wooley, Ruth et al. (1999), Appendix G, p. 114, mass flow of cellulose in hydrolyzate going into process.
[e]Assume same exiting flowrate from base case. From Wooley, Ruth et al. (1999), Appendix G, page 115, total cellulase in stream 420.
[f]Assuming the broth is close to density of water, 3.785 kg equals one gal of water, required volume of flash tank overdesigned by 30% (due to vapor) is then 116,500 gal. Assume glass-lined steel tank, extrapolated from Peters & Timmerhaus (2003), cost is $250,000 in 1979 $.
[g]From Wooley Ruth et al. (1999), Appendix G, p. 117, stream 501 entering distillation module has total flow rate of 380,209 kg/hr. Original distillation module scaled cost of 7,407 k$ for 2 column, 3 evaporator system. For one column, assume 1/5 of original module scaled cost of 1,481 k$. Scaled down to match incoming flowrate from Aspen simulation of 29,593 kg/hr.

[h]From Wooley Ruth et al. (1999), total flow of wastewater into anaerobic digester in stream 612 is 179,346 kg/hr. Original base cost of wastewater module is 8,417 k$. Scaled up to match water flowrate from water flash tank of 309,479 kg/hr.
[i]From Wooley Ruth et al. (1999), Appendix G, p. 124, stream 515 entering storage module has total flow rate of 18,565 kg/hr. Original storage module scaled cost of 1,169 k$. Scaled down to match flowrates of succinic acid and levulinc acid streams of 15,606 kg/hr.
[j]Assume similar flowrate from base case.
[k]From Wooley Ruth et al. (1999), total flow of wastewater into anaerobic digester in stream 612 is 179,346 kg/hr. Original base cost of wastewater module is 3,548 k$. Scaled up to match exiting water flowrate from water flash tank of 339,072 kg/hr.

Module Number[a]	Module Name	Scaled On	Base Year CPI[b]	Base Scale Value	Base Scale Price	Scaling Ex-ponent	Install-ation Factor[c]	Jan. 2009 CPI	Incre-mental Install Cost, 2009 k$
A-500[d]	Wastewater Treatment	Mass Flow Levulinic In, gal/hr	159.1	325068	12,337.7	0.643	1.29	211.1	1,317
A-600[e]	Amine Separation Unit	Total Broth flow, kg/hr	159.1	355328	2,816.4	0.750	1.75	211.1	2,188
A-700[f]	Product and Feed Chemical Storage	Total Levulinic Acid, Formic Acid, and DALA, kg/hr	159.1	42808	2,000.4	0.643	1.24	211.1	107
A-900[g]	DALA Reactor	Size of reactor, gal	159.1	21919	75.2	0.384	1.24	211.1	124
A-950[h]	DALA Distillation	Exiting flow from reactor, kg/hr	159.1	18565	153.8	0.750	1.56	211.1	318
						Total Installed Cost:			4,055,285

Table B.7 - Incremental capital cost of conversion to δ-aminolevulinic acid via levulinic acid.

[a]Modules listed only include enlarged units from cellulose to levulinic acid capital cost sheet, or completely new units.
[b]Base Year for CPI is 1997 for all other modules.
[c]From Wooley, Ruth et al. (1999), mathematical average of scale values of individual units.
[d]From Wooley, Ruth et al. (1999), total flow of wastewater into anaerobic digester in stream 612 is 179,346 kg/hr. Original base cost of wastewater module is 8,417 k$. Scaled up to match flowrate flowrate from combined amine separation unit of 716,652 lb/hr or 325,068 kg/hr. Incremental cost over waste water treatment module in cellulose to levulinic acid simulation. Installation cost of the A-500 module in that simulation is 19800 k$, which is subtracted from overall installed cost total.

[e]From Wooley, Ruth et al. (1999), Appendix G, p. 117, stream 501 entering distillation module has total flow rate of 380,209 kg/hr. Original distillation module scaled cost of 7,407 k$ for 2 column, 3 evaporator system. Assume two columns present in amine separation unit (one for extraction, one for regeneration), 2/5 of original module scaled cost of 2963 k$. Incoming flowrate is entering flowrate into DALA distillation column in Excel (78,399 lb/hr) minus total DALA in entering stream that is assumed to be 100% recovered (15,212 lb/hr), which is 63,187 lb/hr, converted to 28,661 kg/hr. Combined with 326,677 kg/hr entering amine separation unit from cellulose-to-levulinic acid simulation. Incremental cost over amine separation unit in cellulose to levulinic acid simulation. Installation cost of the A-600 module in that simulation is 4,351 k$, which is subtracted from overall installed cost total.

[f]From Wooley, Ruth et al. (1999), Appendix G, p. 124, stream 515 entering storage module has total flow rate of 18,565 kg/hr. Original storage module scaled cost of 1,169 k$. Scaled up to match combined flowrates of formic acid, levulinc acid, and DALA streams of 94,375 lb/hr, or 42,808 kg/hr. Incremental cost over product and feed chemical storage unit in cellulose to levulinic acid simulation. Installation cost of the A-700 module in that simulation is 3,184 k$, which is subtracted from overall installed cost total.

[g]From Excel simulation model, combined flow of levulinic acid, recycled water, and reactants totals 91,463 lb/hr, or 41,487 kg/hr. Assume density close to water at 1 kg/L. Estimate residence time to be 2 hrs, resulting in total reactor size of 82,974 L, or 21,919 gal. From Peters, Timmerhaus et al. (2003), cost function for jacketted reactor is Cost=1620* size^0.384.

[h]From Wooley Ruth et al. (1999), Appendix G, p. 117, stream 501 entering distillation module has total flow rate of 380,209 kg/hr. Original distillation module scaled cost of 7,407 k$ for 2 column, 3 evaporator system. For one column, assume 1/5 of original module scaled cost of 1,481 k$. Scaled down to match incoming flowrate from Excel simulation of 78,399 lb/hr, or 35,561 kg/hr.

Module Number[a]	Module Name	Scaled On	Base Year CPI	Base Scale Value	Base Scale Price, k$	Scaling Exponent[b]	Install-ation Factor[c]	Jan. 2009 CPI	Incre-mental Installed Cost, 2009 k$
A-500[d]	Wastewater Treatment	Total water entering module, kg/hr	159.1	333404	12,540.2	0.643	1.24	211.1	832
A-700[e]	Product and Feed Chemical Storage	AAA, Formic Acid, and Levulinic Acid flows kg/hr	159.1	38508	1,868.8	0.643	1.56	211.1	684
A-900[f]	AAA Reactors	Size of reactor, gal	68.3	9294	54.1	0.384	1.29	211.1	216
A-950[g]	Distillation/ Separation	Total outgoing flow from reactors, kg/hr	159.1	17458	146.9	0.750	1.75	211.1	341
							Total Installed Cost:		2,073,048

Table B.8 - Incremental capital cost of conversion to acetoacrylic acid via levulinic acid.

[a]Modules listed only include enlarged units from cellulose to levulinic acid capital cost sheet, or completely new units.
[b]Base Year for CPI is 1979 for module A-900, 1997 for all other modules.
[c]From Wooley, Ruth et al. (1999), mathematical average of scale values of individual units.
[d]From Wooley, Ruth et al. (1999), total flow of wastewater into anaerobic digester in stream 612 is 179,346 kg/hr. Original base cost of wastewater module is 8,417 k$. Flowrate of water from distillation to wastewater treatment is 14,832 lb/hr. Combined with water flow from amine separation unit of 720,199 lb/hr for total of 735,031 lb/hr or 333,404 kg/hr. Incremental cost over waste water treatment module in cellulose to levulinic acid simulation. Installation cost of the A-500 module in that simulation is 19,800 k$, which is subtracted from overall installed cost total.
[e]From Wooley, Ruth et al. (1999), Appendix G, p. 124, stream 515 entering storage module has total flow rate of 18,565 kg/hr. Original storage module scaled cost of 1,169 k$. Scaled up to match combined flowrates of formic acid, levulinic acid, and AAA streams of 84,895 lb/hr, or 38,508 kg/hr. Incremental cost over product and feed chemical storage unit in cellulose to levulinic acid simulation. Installation cost of the A-700 module in that simulation is 3,184 k$, which is subtracted from overall installed cost total.
[f]From Excel simulation model, combined flow of levulinic acid and recycled water totals 38,782 lb/hr, or 17,591 kg/hr. Assume density close to water at 1 kg/L. Estimate residence time to be 2 hrs, resulting in total reactor size of 35,182 L, or 9,294 gal. From Peters, Timmerhaus et al. (2003), cost function for jacketted reactor is Cost = 1620* size^0.384.
[g]From Wooley, Ruth et al. (1999), Appendix G, p. 117, stream 501 entering distillation module has total flow rate of 380,209 kg/hr. Original distillation module scaled cost of 7,407 k$ for 2 column, 3 evaporator system. For one column, assume 1/5 of original module scaled cost of 1,481 k$. Scaled down to match incoming flowrate from Excel simulation of 38,489 lb/hr, or 17,458 kg/hr.

Module Number[a]	Module Name	Scaled On	Base Year CPI	Base Scale Value	Base Scale Price, k$	Scaling Ex-ponent[b]	Install-ation Factor[c]	Jan. 2009 CPI	Incre-mental Installed Cost, 2009 k$
A-500[d]	Wastewater Treatment	Total water entering module, kg/hr	159.1	333168	12,534.5	0.643	1.24	211.1	823
A-700[e]	Product and Feed Chemical Storage	PDO, Formic Acid, and Levulinic Acid flows kg/hr	159.1	35584	1,776.2	0.643	1.56	211.1	493
A-900[f]	PDO Reactor 1	Size of reactor, gal	68.3	9418	54.4	0.384	1.29	211.1	217
A-900[g]	PDO Reactor 2	Size of reactor, gal	68.3	13720	62.8	0.384	1.29	211.1	251
A-950[h]	Distillation/ Separation	Total outgoing flow from reactor 2, kg/hr	159.1	24168	562.6	0.750	1.75	211.1	1,306
							Total Installed Cost:		3,089,007

Table B.9 - Incremental capital cost of conversion to 1,4-pentanediol via levulinic acid.

[a]Modules listed only include enlarged units from cellulose to levulinic acid capital cost sheet, or completely new units.
[b]Base Year for CPI is 1979 for module A-900, 1997 for all other modules.
[c]From Wooley, Ruth et al. (1999), mathematical average of scale values of individual units.
[d]From Wooley, Ruth et al. (1999), total flow of wastewater into anaerobic digester in stream 612 is 179,346 kg/hr. Original base cost of wastewater module is 8,417 k$. Flowrate of water from distillation to wastewater treatment is 25,334 lb/hr. Combined with water flow from amine separation unit of 720,199 lb/hr for total of 745,533 lb/hr or 333,168 kg/hr. Incremental cost over waste water treatment module in cellulose to levulinic acid simulation. Installation cost of the A-500 module in that simulation is 19,800 k$, which is subtracted from overall installed cost total.
[e]From Wooley Ruth et al. (1999), Appendix G, p. 124, stream 515 entering storage module has total flow rate of 18,565 kg/hr. Original storage module scaled cost of 1,169 k$. Scaled up to match combined flowrates of formic acid, levulinic acid, and PDO streams of 78,449 lb/hr, or 35,584 kg/hr. Incremental cost over product and feed chemical storage unit in cellulose to levulinic acid simulation. Installation cost of the A-700 module in that simulation is 3,184 k$, which is subtracted from overall installed cost total.
[f]From Excel simulation model, combined flow of levulinic acid and acid totals 39,299 lb/hr, or 17,826 kg/hr. Assume density close to water at 1 kg/L. Estimate residence time to be 2hrs, resulting in total reactor size of 35,652 L, or 9,418 gal. From Peters, Timmerhaus et al. (2003), cost function for jacketted reactor is Cost=1620* size^0.384.
[g]From Excel simulation model, combined flow of into 2nd reactor totals 57,247 lb/hr, or 25,967 kg/hr. Assume density close to water at 1 kg/L. Estimate residence time to be 2 hrs, resulting in total reactor size of 51,934 L, or 13,720 gal.

[h]From Wooley, Ruth et al. (1999), Appendix G, p. 117, stream 501 entering distillation module has total flow rate of 380,209 kg/hr. Original distillation module scaled cost of 7,407 k$ for 2 column, 3 evaporator system. For three column system, assume 3/5 of original module scaled cost of 4,444 k$. Scaled down to match incoming flowrate from Excel simulation of 53,282 lb/hr, or 24,168 kg/hr.

Appendix C

Economic Data for Black Liquor Gasification Polygeneration

	Black Liquor through New Tomlinson Boiler	Black Liquor Gasification (common to all processes except Tomlinson)	Syngas through Combined Cycle (BLGCC)	Syngas into DME with Recycle and Back-Pressure Turbine (DMEa)	Syngas into DME with Recycle, Biomass Gasifier, and CC Turbine (DMEb)
Total Overnight Capital Cost in thousands of 2005$[a]	136154	63720	154352	188153	351975
Total Overnight Capital Cost in thousands of Nov. 2008$[b]	148093	69307	167886	204651	382838
Annualized Fixed Cost @ 8% interest over 25 years	13873	6493	15727	19171	35864
Total Variable Costs[c]	17147	2858	21964	25922	39644
Total Annual Product Costs	31020	9350	37691	45094	75508
Annual Output, Primary Product	6791112 klb Steam[d]	1.802E9 kg syngas[e]	950610 MWh[f]	69.29 mil gallons DME[g]	69.29 mil gallons DME[g]
Fixed + Variable Cost per Primary Output	$4.568/klb Steam	$5.189E-3/kg syngas	$39.65/ MWh	$0.6508/ gallon DME	$1.090/ gallon DME
Variable Cost per Output	$2.525/klb Steam	$1.586E-3/kg syngas	$23.11/ MWh	$0.3741/ gallon DME	$0.5721/ gallon DME

Table C.1 – Total cost per output for Tomlinson, gasification, BLGCC, DMEa, and DMEb in thousands of Nov. 2008$ unless otherwise noted.

[a]All data taken from Larson Consomi et al. (Vol. 1, 2006), Page 80, Table 22. New Tomlinson boiler cost is recovery boiler plus steam system modifications. Black liquor gasification is black liquor gasifier plus green liquor filter only, with 2 gasifiers operating at 50%. BLGCC, DMEa, and DMEb include all costs from table minus black liquor gasifier and green liquor filter.

[b]From Bureau of Labor Statistics, Annual Consumer Price Index for 2005 is 195.3, and for Nov. 2008 is 212.425.

[c]See Tables C.3 and C.4 for variable cost data and calculations.
[d]From Larson Consomi et al. (Vol. 1, 2006), Figure 6 on Page 16. Since cost of LP and MP steam is practically the same as seen in Table B.5, they are combined and treated equally. Multiplied by 3600 s/hr and 8330 hr/year, converted to lb and then klb.
[e]From Larson Consomi et al. (Vol. 1, 2006), Figs 23-29 on Pages 35-41. Multiplied syngas mass flowrate per second by 3600 s per hour and 8330 hours per operating year.
[f]From Larson Consomi et al. (Vol. 1, 2006), Table 29, Page 96. Since net energy production with extra O2 is greater than electricity needed for the mill and avoided electricity and exported electricity are priced differently, only avoided electricity is included as primary product.
[g]From Larson Consomi et al. (Vol. 1, 2006), Table 29, Page 96. Biofuel production in millions of gallons.

	Syngas into DME with no Recycle, Biomass Gasifier, and CC Turbine (DMEc)	Syngas into FT with Regular CC Turbine (FTa)	Syngas into FT with Large CC Turbine (FTb)	Syngas into FT with gasified biomass supplementing black liquor (FTc)	Syngas into mixed alcohols (MA)
Total Overnight Capital Cost in thousands of 2005$[a]	260046	266514	438405	401035	332495
Total Overnight Capital Cost in thousands of Nov. 2008$[b]	282848	289883	476847	436200	361650
Annualized Fixed Cost @ 8% interest over 25 years	26497	27156	44670	40863	33879
Total Variable Costs[c]	28993	30786	52811	55974	33296
Total Annual Product Costs	55490	57942	97482	96837	67175
Annual Output, Primary Product[d]	30.61 mil gallons DME	28.30 mil gallons FT fuel	28.30 mil gallons FT fuel	86.93 mil gallons FT fuel	16.76 mil gallons MA
Fixed + Variable Cost per Primary Output	$1.813/ gallon DME	$2.047/ gallon FT fuel	$3.445/ gallon FT fuel	$1.114/ gallon FT fuel	$4.008/ gallon MA
Variable Cost per Output	$0.9472/ gallon DME	$1.088 / gallon FT fuel	$1.866/ gallon FT fuel	$0.6439/ gallon FT fuel	$1.987/ gallon MA

Table C.2 - Total cost per output for DMEc, FTa, FTb, FTc, and MA in thousands of Nov. 2008$ unless otherwise noted.

[a]All data taken from Larson Consomi et al. (Vol. 1, 2006), Page 80, Table 22. DMEc, FTa, FTb, FTc, and MA include all costs from table minus black liquor gasifier and green liquor filter.
[b]From Bureau of Labor Statistics, Annual Consumer Price Index for 2005 is 195.3, and for Nov. 2008 is 212.425.
[c]See Tables C.3 and C.4 for variable cost data and calculations.
[d]From Larson Consomi et al. (Vol. 1, 2006), Table 29, Page 96. Biofuel production in millions of gallons.

	Black Liquor through New Tomlinson Boiler	Black Liquor Gasification (common to all processes except Tomlinson)	Syngas through Combined Cycle (BLGCC)	Syngas into DME with Recycle and Back-Pressure Turbine (DMEa)	Syngas into DME with Recycle, Biomass Gasifier, and CC Turbine (DMEb)
Make-up Water[a]	313	85	1879	1669	1928
Hog Fuel[b]	3096	0	2898	2898	2898
Purchased Wood Residues[b]	0	0	1451	4151	10486
Natural Gas[c]	0	0	2	0	0
Fuel Oil #6[d]	7814	0	9018	9018	9018
Total Water and Energy Utilities	11223	85	15249	17736	24331
Annual Non-fuel Operating and Maintenance[e]	5924	2772	6715	8186	15314
Total Variable (Non-FCI) Costs	17147	2858	21964	25922	39644

Table C.3 - Total variable cost for Tomlinson, gasification, BLGCC, DMEa, and DMEb.

[a]From http://www.gru.com/YourBusiness/Conservation/Water/waterCostTable.jsp the cost of water is $6.29/1000 gallons for commercial users. Multiplied by total make-up water required for each process.
[b]Annual energy values in HHV MMBTU taken from Larson, Consomi et al. (Vol. 1, 2006), Table 29, Page 96. Wood price listed in Table 26, page 90 at $1.53/MMBTU HHV.
[c]From http://bioenergy.ornl.gov/papers/misc/energy_conv.html HHV for natural gas is 1027 BTU/cf. From http://tonto.eia.doe.gov/oog/info/ngw/ngupdate.asp, average wellhead price for November 2008 is $5.97/MCF. MMBTU values in HHV given in Larson, Consomi et al. (Vol. 1, 2006), Table 29 on Page 96. Natural gas only needed for BLGCC process.

[d]From http://www.chpcentermw.org/pdfs/toolkit/7c_rules_thumb.pdf HHV of fuel oil #6 is 150,500 BTU/gal. From http://tonto.eia.doe.gov/steo_query/app/priceresult.asp, Nov 2008 spot price of Fuel Oil #6 is $1.25/gal. MMBTU values on HHV terms given in Larson, Consomi et al. (Vol. 1, 2006), Table 29 on Page 96.
[e]From Larson Consomi et al. (Vol. 1, 2006), Table 22 on page 80, assumed to be 4% of overnight capital costs.

	Syngas into DME with no Recycle, Biomass Gasifier, and CC Turbine (DMEc)	Syngas into FT with Regular CC Turbine (FTa)	Syngas into FT with Large CC Turbine (FTb)	Syngas into FT with gasified biomass supplementing black liquor (FTc)	Syngas into mixed alcohols (MA)
Make-up Water[a]	1824	1824	2058	2407	2128
Hog Fuel[b]	2898	2898	2898	2898	2898
Purchased Wood Residues[b]	3939	5452	19764	24204	4787
Natural Gas[c]	0	0	0	0	0
Fuel Oil #6[d]	9018	9018	9018	9018	9018
Total Water and Energy Utilities	17679	19191	33737	38526	18830
Annual Non-fuel Operating and Maintenance[e]	11314	11595	19074	17448	14466
Total Variable (Non-FCI) Costs	28993	30786	52811	55974	33296

Table C.4 - Total variable cost for DMEc, FTa, FTb, FTc, and MA in thousands of Nov. 2008$ unless otherwise noted.

[a]From http://www.gru.com/YourBusiness/Conservation/Water/waterCostTable.jsp the cost of water is $6.29/1000 gallons for commercial users. Multiplied by total make-up water required for each process.
[b]Annual energy values in HHV MMBTU taken from Larson, Consomi et al. (Vol. 1, 2006), Table 29, Page 96. Wood price listed in Table 26, page 90 at $1.53/MMBTU HHV.
[c]From http://bioenergy.ornl.gov/papers/misc/energy_conv.html HHV for natural gas is 1027 BTU/cf. From http://tonto.eia.doe.gov/oog/info/ngw/ngupdate.asp, average wellhead price for November 2008 is $5.97/MCF. MMBTU values in HHV given in Larson, Consomi et al. (Vol. 1, 2006), Table 29 on Page 96. Natural gas only needed for BLGCC process.
[d]From http://www.chpcentermw.org/pdfs/toolkit/7c_rules_thumb.pdf HHV of fuel oil #6 is 150,500 BTU/gal. From http://tonto.eia.doe.gov/steo_query/app/priceresult.asp, Nov 2008

spot price of Fuel Oil #6 is $1.25/gal. MMBTU values on HHV terms given in Larson, Consomi et al. (Vol. 1, 2006), Table 29 on Page 96.
[e]From Larson, Consomi et al. (Vol. 1, 2006), Table 22 on page 80, assumed to be 4% of overnight capital costs.

	MP Steam	LP Steam
Boiler fuel cost in $/MMBTU[a]	2.448	2.448
Enthalpy of high pressure steam after boiler and before turbine in BTU/lb[b]	1435.13	1435.13
Enthalpy of boiler feed water in BTU/lb[c]	1157.1	1157.1
Overall boiler efficiency, fractional[d]	0.44	0.44
High pressure steam cost in $/klb, calculated[e]	**1.547**	**1.547**
Enthalpy of low pressure steam after turbine in BTU/lb[f]	1198.5	1180.9
Electrical power cost in $/kWh[g]	0.0562	0.0562
Isentropic efficiency of steam turbine, fractional[h]	0.70	0.70
Generator efficiency, fractional[i]	0.45	0.45
Low pressure steam cost in $/klb, calculated[j]	**1.534**	**1.534**

Table C.5 – Cost of medium and low pressure steam, negligible price difference as defined in Larson, Consomi et al. (Vol. 1, 2006)

[a]Assuming $1.53/MMBTU for price of 50% moisture pulpwood is a good approximation for theoretical cost of black liquor solids, cost of 80% BLS would then be $2.448/MMBTU.
[b]From superheated steam tables at http://www.spiraxsarco.com/resources/steam-tables/superheated-steam.asp, steam at 475 deg C and 78.5 bar.
[c]From steam tables at http://www.efunda.com/materials/water/steamtable_sat.cfm, saturated liquid at 110 deg C.
[d]From Larson, Consomi et al. (Vol. 1, 2006), Table 13 on Page 55, thermal efficiency for Tomlinson boiler.
[e]From DOE publication (2003), Page 4, 2nd equation lists cost of "high pressure" before being run through a backpressure turbine.
[f]From steam tables at http://www.efunda.com/materials/water/steamtable_sat.cfm, saturated steam at 13 bar for MP steam, 4.8 bar for LP steam.
[g]From Larson, Consomi et al. (Vol. 1, 2006), Table 26 on page 90, avoided electricity purchases value based on "Tight Energy Supplies" scenario detailed in DOE's Annual Energy Outlook 2005, levelized over 25 year period from 2010-2034, based on $78/bbl world crude oil price.
[h]From http://www.massengineers.com/Documents/isentropic_efficiency.htm, typical isentropic efficiency values for steam turbines range from 70%-90%. Conservative estimate of 70%.
[i]From personal experience as employee of Oglethorpe Power Corporation, cutting-edge coal-fired plants can attain an efficiency of 45-48%. Conservative estimate of 45%.

[j]From DOE publication (2003), Page 5, 1st equation lists cost of "low pressure" taking into account the cost of generating high pressure steam and the benefit of capturing electricity through the backpressure turbine.

R01,01		
Amount of steam, both LP and MP, made from Tomlinson boiler[a]	102.75	kg/s
Amount of steam, both LP and MP, made from Tomlinson boiler	0.226	klb/s
Amount of black liquor needed for this steam[b]	39.37	kg/s
Conversion: klb of steam from kg black liquor	**5.752E-03**	
Amount of electricity generated by Tomlinson boiler steam turbine[c]	5.356E+05	MWh/yr
Amount of black liquor needed for this electricity[d]	1.181E+09	kg/yr
Conversion: MWh electricity from kg black liquor	**4.537E-04**	

R01,02		
Amount of black liquor (80% solids) going into non-Tomlinson processes[e]	35.6	kg/s
Amount of syngas produced from this amount[f]	60.1	kg/s
Conversion: kg syngas from kg black liquor	**1.688**	

R02,01		
Amount of annual syngas needed for total BLGCC process[g]	1.802E+09	kg/yr
Amount of electricity produced by BLGCC process[h]	9.506E+05	MWh/yr
Conversion: MWh electricity from kg syngas	**5.274E-04**	
Amount of steam, both LP and MP, made from BLGCC process[i]	2.907E+09	kg/yr
Amount of steam, both LP and MP, made from BLGCC process	6.408E+06	klb/yr
Conversion: klb of steam from kg syngas	**3.555E-03**	

R02,02		
Amount of syngas needed for DMEa process[j]	60.1	kg/s
Amount of DME produced from DMEa process[k]	2.311	gal/s
Conversion: gal DME from kg syngas	**3.845E-02**	
Amount of steam, both LP and MP, made from DMEa process[l]	97.0	kg/s
Amount of steam, both LP and MP, made from DMEa process	0.214	klb/s
Conversion: klb of steam from kg syngas	**3.557E-03**	
Amount of electricity generated by DMEa process[m]	4.667E+03	MWH/yr
Amount of syngas needed for DMEa electricity	1.802E+09	kg/yr
Conversion: MWh from kg syngas	**2.589E-06**	

Table C.6 – Conversion factors for Tomlinson, gasification, BLGCC, and DMEa.

[a]From Larson, Consomi et al. (Vol. 1, 2006), Figure 6 on Page 16. Since cost of LP and MP steam is practically the same, they are combined and treated equally.

[b]From Larson, Consomi et al. (Vol. 1, 2006), Table 29 on Page 96. 1,041,250 short tons of black liquor solids annually, divided by 8,330 operating hours/year and 3,600 seconds/hour, divided by 0.8 to get wet amount, multiplied by 907 kg/short ton.
[c]From Larson, Consomi et al. (Vol. 1, 2006), Table 29 on Page 96. Electricity generated per year.
[d]Multiplied black liquor per second by 3,600 s/hr and 8,330 hr/operating year.
[e]From Larson, Consomi et al. (Vol. 1, 2006), Figs 23-29 on Pages 35-41. Flowrate of 80% black liquor solids going into BL gasifier.
[f]From Larson, Consomi et al. (Vol. 1, 2006), Figs 23-29 on Pages 35-41. No syngas made in Tomlinson process. Slightly less syngas coming out of BLGCC, but conversion factor is only off by 1%.
[g]Multiplied mass flowrate per second by 3,600 s per hour and 8,330 hours per operating year.
[h]From Larson, Consomi et al. (Vol. 1, 2006), Table 29 on Page 96. Net electricity generated, with extra oxygen production.
[i]From Larson, Consomi et al. (Vol. 1, 2006), Fig 9 on page 20. LP and MP steam streams combined due to equal cost. Multiplied by 3,600 s/hr and 8,330 hr/operating year.
[j]From Larson, Consomi et al. (Vol. 1, 2006), Figs 23-29 on Pages 35-41.
[k]From Larson, Consomi et al. (Vol. 1, 2006), Table 29 on Page 96, 69.29 gallons of DME are produced annually.
[l]From Larson, Consomi et al. (Vol. 1, 2006), Fig 23 on Page 45. LP and MP steam combined. Same amount for all DME, FT, and MA processes.
[m]From Larson, Consomi et al. (Vol. 1, 2006), Table 29 on Page 96. Amount of electricity generated with extra O2 production.

R02,03		
Amount of syngas needed for DMEb process[a]	60.1	kg/s
Amount of DME produced from DMEb process[b]	2.311	gal/s
Conversion: gal DME from kg syngas	**3.845E-02**	
Amount of steam, both LP and MP, made from DMEb process	97.0	kg/s
Amount of steam, both LP and MP, made from DMEb process	0.214	klb/s
Conversion: klb of steam from kg syngas	**3.557E-03**	
Amount of electricity generated by DMEb process[c]	7.319E+05	MWH/yr
Amount of syngas needed for DMEb electricity	1.802E+09	kg/yr
Conversion: MWh from kg syngas	**4.061E-04**	

R02,04		
Amount of syngas needed for DMEc process[a]	60.1	kg/s
Amount of DME produced from DMEc process[b]	1.021	gal/s
Conversion: gal DME from kg syngas	**1.698E-02**	
Amount of steam, both LP and MP, made from DMEc process	97.0	kg/s
Amount of steam, both LP and MP, made from DMEc process	0.214	klb/s
Conversion: klb of steam from kg syngas	**3.557E-03**	
Amount of electricity generated by DMEc process[c]	7.543E+05	MWH/yr
Amount of syngas needed for DMEc electricity	1.802E+09	kg/yr
Conversion: MWh from kg syngas	**4.185E-04**	

R02,05		
Amount of syngas needed for FTa process[a]	60.1	kg/s
Amount of FT fuel produced from FTa process[b]	0.944	gal/s
Conversion: gal FT from kg syngas	**1.570E-02**	
Amount of steam, both LP and MP, made from FTa process	97.0	kg/s
Amount of steam, both LP and MP, made from FTa process	0.214	klb/s
Conversion: klb of steam from kg syngas	**3.557E-03**	
Amount of electricity generated by FTa process[c]	7.304E+05	MWH/yr
Amount of syngas needed for FTa electricity	1.802E+09	kg/yr
Conversion: MWh from kg syngas	**4.053E-04**	

Table C.7 – Conversion factors for DMEb, DMEc, and FTa.

[a]From Larson, Consomi et al. (Vol. 1, 2006), Figs 23-29 on Pages 35-41.
[b]From Larson, Consomi et al. (Vol. 1, 2006), Table 29 on Page 96, listed gallons of DME and FT produced annually for each process.
[c]From Larson, Consomi et al. (Vol. 1, 2006), Table 29 on Page 96. Amount of electricity generated with extra O_2 production for each process.

R02,06		
Amount of syngas needed for FTb process[a]	60.1	kg/s
Amount of FT fuel produced from FTb process[b]	0.944	gal/s
Conversion: gal FT from kg syngas	**1.570E-02**	
Amount of steam, both LP and MP, made from FTb process	97.0	kg/s
Amount of steam, both LP and MP, made from FTb process	0.214	klb/s
Conversion: klb of steam from kg syngas	**3.557E-03**	
Amount of electricity generated by FTb process[c]	1.907E+06	MWH/yr
Amount of syngas needed for FTb electricity	1.802E+09	kg/yr
Conversion: MWh from kg syngas	**1.058E-03**	

R02,07		
Amount of syngas needed for FTc process[a]	60.1	kg/s
Amount of FT fuel produced from FTc process[b]	2.899	gal/s
Conversion: gal FT from kg syngas	**4.823E-02**	
Amount of steam, both LP and MP, made from FTc process	97.0	kg/s
Amount of steam, both LP and MP, made from FTc process	0.214	klb/s
Conversion: klb of steam from kg syngas	**3.557E-03**	
Amount of electricity generated by FTc process[c]	6.440E+05	MWH/yr
Amount of syngas needed for FTc electricity	1.802E+09	kg/yr
Conversion: MWh from kg syngas	**3.573E-04**	

R02,08		
Amount of syngas needed for MA process[a]	60.1	kg/s
Amount of MA fuel produced from MA process[b]	0.559	gal/s
Conversion: gal MA from kg syngas	**9.299E-03**	
Amount of steam, both LP and MP, made from FTa process	97.0	kg/s
Amount of steam, both LP and MP, made from FTa process	0.214	klb/s
Conversion: klb of steam from kg syngas	**3.557E-03**	
Amount of electricity generated by DMEc process[c]	7.654E+05	MWH/yr
Amount of syngas needed for DMEc electricity	1.802E+09	kg/yr
Conversion: MWh from kg syngas	**4.247E-04**	

Table C.8 – Conversion factors for FTb, FTc, and MA.

[a]From Larson, Consomi et al. (Vol. 1, 2006), Figs 23-29 on Pages 35-41.
[b]From Larson, Consomi et al. (Vol. 1, 2006), Table 29 on Page 96, listed gallons of FT and MA produced annually for each process.
[c]From Larson, Consomi et al. (Vol. 1, 2006), Table 29 on Page 96. Amount of electricity generated with extra O_2 production for each process.

	Black Liquor through New Tomlinson Boiler	Black Liquor Gasification (common to all processes except Tomlinson)	Syngas through Combined Cycle (BLGCC)	Syngas into DME with Recycle and Back-Pressure Turbine (DMEa)	Syngas into DME with Recycle, Biomass Gasifier, and CC Turbine (DMEb)
Total Overnight Capital Cost in thousands of Nov. 2008$	148093	69307	167886	204651	382838
Annual Output, Primary Product	6791112 klb Steam	1.802E9 kg syngas	950610 MWh	69.29 mil gallons DME	69.29 mil gallons DME
FCI, $ per Primary Output	21.81	3.85E-02	176.61	2.95	5.53
	Syngas into DME with no Recycle, Biomass Gasifier, and CC Turbine (DMEc)	Syngas into FT with Regular CC Turbine (FTa)	Syngas into FT with Large CC Turbine (FTb)	Syngas into FT with gasified biomass supplementing black liquor (FTc)	Syngas into mixed alcohols (MA)
Total Overnight Capital Cost in thousands of Nov. 2008$	282848	289883	476847	436200	361650
Annual Output, Primary Product	30.61 mil gallons DME	28.30 mil gallons FT fuel	28.30 mil gallons FT fuel	86.93 mil gallons FT fuel	16.76 mil gallons MA
FCI, $ per Primary Output	9.24	10.24	16.85	5.02	21.58

Table C.9 – Linear investment factors in terms of cost per primary output. All data for overnight capital cost and annual output taken from Tables C.1 and C.2.

Appendix D

EPA WAR Score Breakdowns for Classes of Pollutants

Chemical	Normalized Scores[a]								Combined Impact Score[b]
	HTPI	TTP	HTPE	ATP	GWP	ODP	PCOP	AP	
Wood Comb-ustion VOC's[c]	2.93E-01	2.93E-01	2.66E-02	3.36E-01	1.40E-03	0.00E+00	1.26E+00	0.00E+00	2.21E+00
Gas Comb-ustion VOC's[c]	4.70E-01	4.70E-01	2.65E-01	1.64E-02	0.00E+00	0.00E+00	3.11E+00	0.00E+00	4.33E+00
CO	0.00E+00	0.00E+00	4.33E-03	0.00E+00	0.00E+00	0.00E+00	1.70E-02	0.00E+00	2.13E-02
NOx[d]	0.00E+00	0.00E+00	8.87E-03	0.00E+00	0.00E+00	0.00E+00	1.50E+00	1.07E+00	2.58E+00
PM10[e]	3.48E+00	3.48E+00	7.78E-02	1.54E-01	0.00E+00	0.00E+00	0.00E+00	0.00E+00	7.19E+00
Total Reduced Sulfur[f]	6.89E-01	6.89E-01	6.61E-03	3.43E-01	0.00E+00	0.00E+00	0.00E+00	9.17E-02	1.82E+00
SOx/SO2[g]	0.00E+00	0.00E+00	1.83E-02	0.00E+00	0.00E+00	0.00E+00	1.44E-01	9.87E-01	1.15E+00
CO2	0.00E+00	0.00E+00	2.65E-05	0.00E+00	2.44E-04	0.00E+00	0.00E+00	0.00E+00	2.71E-04
Electricity (per MWh)[h]	2.80E-01	2.80E-01	4.40E-03	9.60E-01	6.90E-01	7.40E-06	2.50E-04	2.15E+01	2.37E+01
Process steam (per klb)[i]	-6.07E-03	-6.07E-03	-9.00E-06	-1.00E-02	4.87E-02	8.00E-08	4.14E-05	1.90E-01	2.17E-01
DME, mass basis	1.77E-02	1.77E-02	0.00E+00	6.96E-05	2.44E-04	0.00E+00	2.47E-01	0.00E+00	2.83E-01
FT, mass basis[j]	8.56E-02	8.55E-02	1.71E-04	2.62E-01	6.11E-04	0.00E+00	6.95E-01	0.00E+00	1.13E+00
MOH, mass basis[k]	1.12E-01	1.12E-01	2.87E-04	5.41E-05	0.00E+00	0.00E+00	6.01E-01	0.00E+00	8.25E-01
Black liquor, mass basis[l]	4.70E-01	4.70E-01	1.74E-02	1.73E-03	0.00E+00	0.00E+00	0.00E+00	0.00E+00	9.59E-01
Syngas, mass basis[m]	1.71E-04	1.71E-04	8.28E-04	4.66E-02	6.06E-05	0.00E+00	2.25E-03	1.26E-02	6.26E-02

Table D.1 – WAR scores for categories of emissions for all processes.

[a]All scores taken from EPA WAR GUI, build 1.0.17 in 2008.
[b]All weights set to 1.
[c]See Tables D.3 and D.4 for score breakdown of VOC's for wood and gas combustion.
[d]Assume Nox is 95% NO and 5% NO2, common assumption in literature.
[e]See Table D.5 for WAR score breakdown of PM10.
[f]See Table D.6 for WAR score breakdown of total reduced sulfur.
[g]Assume SOx is primarily SO2, common assumption in literature.
[h]Determined by entering 3600 MJ/hr (1 MWh = 3600 MJ) of coal-based energy into WAR GUI and looking at energy comparison chart.
[i]See Table D.7 for WAR score breakdown of process steam.
[j]See Table D.8-9 for score breakdown of FT oil.
[k]See Table D.10 for score breakdown of mixed alcohols.
[l]See Tables D.11-12 for score calculation and breakdown of black liquor.
[m]From Larson, Consomi et al. (Vol. 1, 2006), syngas is 63.7% H2O by mass, 13.1% CO, and 13.7% H2.

Finished Product	Density, kg/m3	Density, kg/gal	Impact score, PEI per kg	Impact score, PEI per gal
DME (per gal)	668.0	2.53	2.827E-01	7.149E-01
FT (per gal)	862.0	3.26	1.129E+00	3.685E+00
MOH (per gal)	795.8	3.01	8.254E-01	2.486E+00

Table D.2 - Conversion of WAR scores for final products from mass to volumetric basis.

Chemical Species	%[b]	Normalized Scores[a] HTPI	TTP	HTPE	ATP	GWP	ODP	PCOP	AP	Total Impact Score
Methane	25.00	0.00E+00	0.00E+00	3.61E-04	0.00E+00	5.61E-03	0	4.46E-03	0	1.04E-02
Ethane	7.50	0.00E+00	0.00E+00	1.94E-04	0.00E+00	0.00E+00	0	8.51E-02	0	8.53E-02
Propane	1.13	0.00E+00	0.00E+00	1.32E-04	0.00E+00	0.00E+00	0	1.48E-01	0	1.48E-01
n-butane	0.30	2.85E-02	2.85E-02	1.00E-04	6.49E-03	0.00E+00	0	3.49E-01	0	4.13E-01
Isobutene	0.08	6.23E-01	6.23E-01	1.00E-04	0.00E+00	0.00E+00	0	3.82E-01	0	1.63E+00
other alcanes (>C4)[c]	2.25	9.39E-01	9.39E-01	8.07E-05	4.71E-02	0.00E+00	0	3.94E-01	0	2.32E+00
Ethane	22.50	0.00E+00	0.00E+00	1.04E-03	0.00E+00	0.00E+00	0	2.88E+00	0	2.88E+00
Propene	4.50	0.00E+00	0.00E+00	2.77E-04	0.00E+00	0.00E+00	0	3.81E+00	0	3.81E+00
butenes, unspecified[d]	0.38	1.45E-01	1.45E-01	0.00E+00	0.00E+00	0.00E+00	0	3.11E+00	0	3.40E+00
pentenes, unspecified[e]	1.50	3.87E-02	3.87E-02	0.00E+00	2.64E-02	0.00E+00	0	2.31E+00	0	2.41E+00
Ethyne	7.50	0.00E+00	0.00E+00	8.95E-05	0.00E+00	0.00E+00	0	3.07E-01	0	3.07E-01
Propyne	0.38	0.00E+00	0.00E+00	1.44E-04	0.00E+00	0.00E+00	0	2.19E+00	0	2.19E+00
Benzene	11.25	1.14E-01	1.14E-01	7.44E-03	1.61E-02	0.00E+00	0	2.25E-01	0	4.77E-01
Toluene	3.75	7.51E-02	7.51E-02	3.18E-04	1.13E-02	0.00E+00	0	1.27E+00	0	1.43E+00
m-xylene	0.38	7.51E-02	7.51E-02	5.48E-04	2.48E-02	0.00E+00	0	3.11E+00	0	3.29E+00
p-xylene	0.54	7.51E-02	7.51E-02	5.48E-04	1.37E-02	0.00E+00	0	1.84E+00	0	2.00E+00
o-xylene	0.55	5.74E-02	5.74E-02	5.48E-04	2.41E-02	0.00E+00	0	2.42E+00	0	2.56E+00
ethyl-benzene	0.38	1.07E-01	1.07E-01	5.48E-04	1.46E-02	0.00E+00	0	9.60E-01	0	1.19E+00
formal-dehyde	1.50	4.70E-01	4.70E-01	2.65E-01	1.64E-02	0.00E+00	0	3.11E+00	0	4.33E+00
acetal-dehyde	0.75	2.90E-01	2.90E-01	6.62E-04	1.16E-02	0.00E+00	0	2.08E+00	0	2.67E+00
other aldehydes[f]	2.25	8.17E+00	8.17E+00	9.53E-01	1.47E+01	0.00E+00	0	2.42E+00	0	3.44E+01
other olefinic aldehydes (average C4)[g]	1.50	3.38E+00	3.38E+00	0.00E+00	3.60E-02	0.00E+00	0	1.96E+00	0	8.76E+00
ketones, unspecified[h]	1.13	5.27E-02	5.27E-02	9.92E-05	4.88E-05	0.00E+00	0	1.14E-01	0	2.20E-01
Furane	3.00	2.76E-01	2.76E-01	0.00E+00	6.49E-03	0.00E+00	0	2.88E+00	0	3.44E+00
Total Impact of Wood Com-bustion VOC's:		2.93E-01	2.93E-01	2.66E-02	3.36E-01	1.40E-03	0	1.26E+00	0	2.21E+00

Table D.3: Wood conversion VOC's WAR score breakdown.

[a]All scores taken from EPA WAR GUI, build 1.0.17 in 2008. All weights set to 1.

[b]Online supplement for VOC compositions for various emission sources. Column 60 for wood combustion (Theloke and Friedrich, 2007).
[c]Modeled as pentane since percentage of total VOC's is very small.
[d]Modeled as n-butene since butenes are very small percentage of total VOC's.
[e]Modeled as n-pentene since pentenes are very small percentage of total VOC's.
[f]Modeled as acrolein, since percentage of aldehydes in VOC's is very small.
[g]Modeled as methacrolein, only known 4 carbon olefinic aldehyde.
[h]Modeled as acetone, since percentage of ketones in VOC's is very small.

		Normalized Scores								
Chemical Species	%	HTPI	TTP	HTPE	ATP	GWP	ODP	PCOP	AP	Combined Impact Score
formal-dehyde	100	4.70E-01	4.70E-01	2.65E-01	1.64E-02	0.00E+00	0.00E+00	3.11E+00	0.00E+00	4.33E+00

Table D.4: Gas conversion VOC's WAR score breakdown. Online supplement for VOC compositions for various emission sources. Column 58 for gas combustion (Theloke and Friedrich, 2007).

			Normalized Scores[a]								
Chemical Species[b]	% from lit	% norm	HTPI	TTP	HTPE	ATP	GWP	ODP	PCOP	AP	Combined Impact Score
Aluminum	14.00	27.50	3.51E+00	3.51E+00	4.76E-02	2.83E-02	0	0	0	0	7.10E+00
Calcium	2.90	5.70	2.36E+00	2.36E+00	0.00E+00	1.89E-02	0	0	0	0	4.74E+00
Chlorine	0.10	0.20	0.00E+00	0.00E+00	7.94E-02	3.96E+00	0	0	0	0	4.04E+00
Iron	5.50	10.81	1.25E-02	1.25E-02	0.00E+00	1.32E-02	0	0	0	0	3.82E-02
Potassium	1.10	2.16	2.42E+00	2.42E+00	0.00E+00	1.89E-02	0	0	0	0	4.86E+00
magnesium[c]	1.00	1.96	1.34E-01	1.34E-01	0.00E+00	1.87E-04	0	0	0	0	2.68E-01
Sodium	0.60	1.18	4.13E+00	4.13E+00	0.00E+00	3.30E-02	0	0	0	0	8.29E+00
phosphorus	0.90	1.77	1.25E+02	1.25E+02	2.38E+00	6.95E+00	0	0	0	0	2.59E+02
Silicon	24.00	47.15	1.19E-01	1.19E-01	4.76E-02	2.64E-02	0	0	0	0	3.12E-01
titanium[d]	0.80	1.57	6.14E-01	6.14E-01	0.00E+00	1.16E-02	0	0	0	0	1.24E+00
Total Impact of PM10:	50.90	100.00	3.48E+00	3.48E+00	7.78E-02	1.54E-01	0	0	0	0	7.19E+00

Table D.5: WAR score breakdown for emission category PM10.

[a]All scores taken from EPA WAR GUI, build 1.0.17 in 2008. All weights set to 1.
[b]PM10 analysis for coal-fired power plants (Meij and te Winkel, 2004). Majority of PM10 is ash from feedstock, assume same holds true for wood combustion and that ash composition is similar until better data is available. Only including elements present at greater than 0.1%, normalized to 100%.
[c]Not listed in WAR database, using data from magnesium chloride.
[d]Not listed in WAR database, using data from titanium trichloride.

			Normalized Scores[a]								Combined Impact Score
Chemical Species[b]	ppm from lit	% norm	HTPI	TTP	HTPE	ATP	GWP	ODP	PCOP	AP	
Hydrogen sulfide	2.5	4.90	0.00E+00	0.00E+00	8.51E-03	6.95E+00	0	0	0	1.87E+00	8.83E+00
Methyl mercaptan	2.5	4.90	5.08E-01	5.08E-01	1.19E-02	7.51E-04	0	0	0	0.00E+00	1.03E+00
Dimethyl sulfide	30	58.82	7.02E-01	7.02E-01	9.53E-03	1.47E-03	0	0	0	0.00E+00	1.42E+00
Dimethyl disulfide	16	31.37	7.99E-01	7.99E-01	0.00E+00	6.09E-03	0	0	0	0.00E+00	1.60E+00
Total Impact of TRS:	51	100.00	6.89E-01	6.89E-01	6.61E-03	3.43E-01	0	0	0	9.17E-02	1.82E+00

Table D.6: WAR score breakdown for emission category TRS (Total Reduced Sulfur).

[a]All scores taken from EPA WAR GUI, build 1.0.17 in 2008. All weights set to 1.
[b]Data on TRS breakdown for Kraft mills from literature (Bordado and Gomes, 2001). Data was collected at various process points throughout the mill, but not of the stack gas. Ppm's of "INCIN" exhaust stream are added up and normalized for each sulfur species, with hydrogen sulfide and methyl mercaptan assigned values of 2.5ppm since literature lists their values at <5 ppm. This is done only to approximate breakdown of total reduced sulfur into the components for environmental impact purposes.

High pressure steam before turbine	
Enthalpy of high pressure steam after boiler and before turbine in BTU/lb[a]	1435.1
Enthalpy of boiler feed water in BTU/lb[b]	1157.1
Overall boiler efficiency, fractional[c]	0.44
Total BTU needed to raise 1 lb boiler feed water to high pressure	631.9
Total MJ needed to raise 1000 lb (1 klb) boiler feed water to high pressure	666.7
Electricity savings from turbine	
Enthalpy of low pressure steam after turbine in BTU/lb[d]	1198.5
Enthalpy change in turbine in BTU/lb	236.6
Isentropic efficiency of steam turbine, fractional[e]	0.70
Generator efficiency, fractional[f]	0.45
Electricity generated in BTU/lb	74.5
Electricity generated in MJ/Klb	78.6

	Normalized Scores[g]								Combined Impact Score
	HTPI	TTP	HTPE	ATP	GWP	ODP	PCOP	AP	
High pressure steam turbine energy usage (NG-based power)[h]	3.20E-05	3.20E-05	8.70E-05	1.10E-02	6.40E-02	2.40E-07	4.70E-05	6.60E-01	7.35E-01
- Electricity savings from backpressure turbine (coal-based power)[i]	6.10E-03	6.10E-03	9.60E-05	2.10E-02	1.53E-02	1.60E-07	5.60E-06	4.70E-01	5.19E-01
Net environmental impact of process steam per klb	-6.07E-03	-6.07E-03	-9.00E-06	-1.00E-02	4.87E-02	8.00E-08	4.14E-05	1.90E-01	2.17E-01

Table D.7: WAR score breakdown for generation of process steam.

[a]From superheated steam tables at http://www.spiraxsarco.com/resources/steam-tables/superheated-steam.asp, steam at 475 deg C and 78.5 bar.
[b]From steam tables at http://www.efunda.com/materials/water/steamtable_sat.cfm, saturated liquid at 110 deg C.
[c]From Larson, Consomi et al. (Vol. 1, 2006), Table 13 on Page 55, thermal efficiency for Tomlinson boiler.
[d]From steam tables at http://www.efunda.com/materials/water/steamtable_sat.cfm, saturated steam at 13 bar.
[e]From http://www.massengineers.com/Documents/isentropic_efficiency.htm, typical isentropic efficiency values for steam turbines range from 70%-90%.
[f]From personal experience as employee of Oglethorpe Power Corporation, cutting-edge coal-fired plants can attain an efficiency of 45-48%. Conservative estimate of 45%.
[g]All scores taken from EPA WAR GUI, build 1.0.17 in 2008.

[h]Determined by entering 666.67 MJ/hr in energy field of WAR algorithm, natural gas-based power.
[i]Determined by entering 78.64 MJ/hr in energy field of WAR algorithm, coal-based power.

		Normalized Scores								Combined Impact Score
Chemical Species	Wt. Frac.	HTPI	TTP	HTPE	ATP	GWP	ODP	PCOP	AP	
methane	1.09E-01	0.00E+00	0.00E+00	3.61E-04	0.00E+00	5.61E-03	0	4.46E-03	0	1.04E-02
Ethane	1.46E-01	0.00E+00	0.00E+00	1.94E-04	0.00E+00	0.00E+00	0	8.51E-02	0	8.53E-02
propane	8.96E-02	0.00E+00	0.00E+00	1.32E-04	0.00E+00	0.00E+00	0	1.48E-01	0	1.48E-01
propene	5.71E-02	0.00E+00	0.00E+00	2.77E-04	0.00E+00	0.00E+00	0	3.81E+00	0	3.81E+00
n-butane	8.46E-02	2.85E-02	2.85E-02	1.00E-04	6.49E-03	0.00E+00	0	3.49E-01	0	4.13E-01
1-butene	4.64E-02	1.45E-01	1.45E-01	0.00E+00	0.00E+00	0.00E+00	0	3.11E+00	0	3.40E+00
n-pentane	7.45E-02	9.39E-01	9.39E-01	8.07E-05	4.71E-02	0.00E+00	0	3.94E-01	0	2.32E+00
1-pentene	3.52E-02	3.87E-02	3.87E-02	0.00E+00	2.64E-02	0.00E+00	0	2.31E+00	0	2.41E+00
n-hexane	6.27E-02	1.31E-02	1.31E-02	1.32E-04	1.58E-01	0.00E+00	0	3.68E-01	0	5.52E-01
1-hexene	2.55E-02	2.57E-02	2.57E-02	1.40E-03	1.07E-02	0.00E+00	0	1.73E+00	0	1.79E+00
n-heptane	5.11E-02	9.01E-03	9.01E-03	1.19E-04	1.13E-01	0.00E+00	0	3.14E-01	0	4.45E-01
1-heptene	1.79E-02	1.89E-02	1.89E-02	0.00E+00	8.43E-02	0.00E+00	0	1.38E+00	0	1.50E+00
n-octane	4.06E-02	8.19E-03	8.19E-03	1.01E-04	1.41E-01	0.00E+00	0	2.58E-01	0	4.15E-01
1-octene	1.22E-02	1.15E-02	1.15E-02	0.00E+00	1.16E-01	0.00E+00	0	1.02E+00	0	1.16E+00
n-nonane	3.16E-02	8.46E-03	8.46E-03	2.26E-04	4.95E-01	0.00E+00	0	2.21E-01	0	7.33E-01
1-nonene	8.19E-03	1.16E-02	1.16E-02	0.00E+00	4.71E-01	0.00E+00	0	8.08E-01	0	1.30E+00
n-decane	2.42E-02	6.86E-03	6.86E-03	0.00E+00	1.47E+00	0.00E+00	0	1.91E-01	0	1.67E+00
n-decene	5.40E-03	1.19E-02	1.19E-02	0.00E+00	1.20E+00	0.00E+00	0	6.71E-01	0	1.89E+00
n-undecane	1.83E-02	7.57E-03	7.57E-03	0.00E+00	3.30E+00	0.00E+00	0	1.69E-01	0	3.48E+00
1-undecene	3.52E-03	1.26E-02	1.26E-02	0.00E+00	1.58E+00	0.00E+00	0	5.75E-01	0	2.18E+00
n-dodecane	1.37E-02	8.44E-03	8.44E-03	0.00E+00	7.33E+00	0.00E+00	0	1.52E-01	0	7.50E+00
1-dodecene	2.26E-03	1.35E-02	1.35E-02	0.00E+00	2.08E+00	0.00E+00	0	5.50E-01	0	2.66E+00
n-tridecane	1.01E-02	1.01E-02	1.01E-02	0.00E+00	0.00E+00	0.00E+00	0	1.45E-01	0	1.65E-01
1-tridecene	1.44E-03	1.46E-02	1.46E-02	0.00E+00	0.00E+00	0.00E+00	0	4.54E-01	0	4.83E-01
n-tetradecane	7.45E-03	1.66E-02	1.66E-02	0.00E+00	0.00E+00	0.00E+00	0	1.41E-01	0	1.74E-01
1-tetradecene	9.12E-04	1.82E-02	1.82E-02	0.00E+00	0.00E+00	0.00E+00	0	4.10E-01	0	4.46E-01
n-pentadecane	5.43E-03	1.71E-02	1.71E-02	0.00E+00	0.00E+00	0.00E+00	0	1.36E-01	0	1.70E-01
1-pentadecene	5.72E-04	1.97E-02	1.97E-02	0.00E+00	0.00E+00	0.00E+00	0	3.84E-01	0	4.23E-01
n-hexadecane	3.93E-03	1.90E-02	1.90E-02	0.00E+00	0.00E+00	0.00E+00	0	1.19E-01	0	1.57E-01
1-hexadecene	3.57E-04	2.15E-02	2.15E-02	0.00E+00	0.00E+00	0.00E+00	0	0.00E+00	0	4.30E-02
n-heptadecane	2.83E-03	9.01E-02	9.01E-02	0.00E+00	0.00E+00	0.00E+00	0	1.11E-01	0	2.91E-01
1-heptadecene	2.21E-04	4.42E-02	0.00E+00	0.00E+00	0.00E+00	0.00E+00	0	0.00E+00	0	4.42E-02
n-octadecane	2.03E-03	1.19E-01	1.19E-01	0.00E+00	0.00E+00	0.00E+00	0	1.05E-01	0	3.43E-01
1-octadecene	1.36E-04	1.21E-01	1.21E-01	0.00E+00	0.00E+00	0.00E+00	0	0.00E+00	0	2.42E-01

n-nonadecane	1.45E-03	1.11E-01	1.11E-01	0.00E+00	0.00E+00	0.00E+00	0	9.96E-02	0	3.22E-01
n-eicosane (20)	1.03E-03	1.04E-01	1.04E-01	0.00E+00	0.00E+00	0.00E+00	0	9.48E-02	0	3.03E-01
n-henei-cosane (21)	7.29E-04	9.63E-02	9.63E-02	0.00E+00	0.00E+00	0.00E+00	0	9.03E-02	0	2.83E-01
n-docosane (22)	5.14E-04	8.33E-02	8.33E-02	0.00E+00	0.00E+00	0.00E+00	0	8.62E-02	0	2.53E-01
n-tricosane (23)	3.62E-04	7.81E-02	7.81E-02	0.00E+00	0.00E+00	0.00E+00	0	0.00E+00	0	1.56E-01
n-tetracosane	2.54E-04	7.50E-02	7.50E-02	0.00E+00	0.00E+00	0.00E+00	0	0.00E+00	0	1.50E-01
Total Impact of FT Crude:		8.56E-02	8.55E-02	1.71E-04	2.62E-01	6.11E-04	0	6.95E-01	0	1.13E+00

Table D.8: WAR score breakdown for Fischer-Tropsch Crude Oil. From Larson, Consomi et al. (Vol. 1, 2006), Page 37, liquid phase FTL single-pass conversion for their simulation studies is 65%. Check syngas calculation to see that 65% CO conversion results in 9.8 kg/s flow of unconverted syngas from FT island to gas turbine, very close to 9.7 kg/s value from Larson, Consomi et al., Figure 26 on Page 48. 15.5 kg/s of syngas enters FT island, resulting in 2.7 kg/s of FT liquids, and 9.7 kg/s mixture of unconverted syngas. Assume balance of 15.5 kg/s, which is 3.1 kg/s, is light gases C1-C4. This means total FT product is 3.1 kg/s + 2.7 kg/s = 5.8 kg/s. Trial and error calculations involving ASF equation show that an alpha of 0.67 is necessary to obtain a light gas flow of 3.1 kg/s, and this alpha is used to calculate the distribution of all hydrocarbons produced in FT process. See Table D.9 for ASF distribution.

Alpha =	0.67	Flow of total FT product:	5.8	Paraffin wt. frac. of carbon number	Olefin wt. frac. of carbon number	Paraffin wt. frac. of total flow	Olefin wt. frac. of total flow
Carbon number	Weight fraction[a]	Mass flow in kg/s	Paraffin/ olefin ratio[b]				
1	1.089E-01	6.316E-01		1.000	0.000	1.089E-01	0.000E+00
2	1.459E-01	8.464E-01	1.350	1.000	0.000	1.459E-01	0.000E+00
3	1.467E-01	8.506E-01	1.568	0.611	0.389	8.955E-02	5.710E-02
4	1.310E-01	7.599E-01	1.822	0.646	0.354	8.459E-02	4.642E-02
5	1.097E-01	6.364E-01	2.117	0.679	0.321	7.452E-02	3.520E-02
6	8.822E-02	5.117E-01	2.460	0.711	0.289	6.272E-02	2.550E-02
7	6.896E-02	3.999E-01	2.858	0.741	0.259	5.108E-02	1.788E-02
8	5.280E-02	3.062E-01	3.320	0.769	0.231	4.058E-02	1.222E-02
9	3.980E-02	2.308E-01	3.857	0.794	0.206	3.161E-02	8.193E-03
10	2.963E-02	1.718E-01	4.482	0.818	0.182	2.422E-02	5.405E-03
11	2.184E-02	1.266E-01	5.207	0.839	0.161	1.832E-02	3.518E-03
12	1.596E-02	9.257E-02	6.050	0.858	0.142	1.370E-02	2.264E-03
13	1.158E-02	6.719E-02	7.029	0.875	0.125	1.014E-02	1.443E-03
14	8.359E-03	4.848E-02	8.166	0.891	0.109	7.447E-03	9.119E-04
15	6.000E-03	3.480E-02	9.488	0.905	0.095	5.428E-03	5.721E-04
16	4.288E-03	2.487E-02	11.023	0.917	0.083	3.931E-03	3.567E-04
17	3.053E-03	1.771E-02	12.807	0.928	0.072	2.832E-03	2.211E-04
18	2.166E-03	1.256E-02	14.880	0.937	0.063	2.029E-03	1.364E-04
19	1.532E-03	8.883E-03	17.288	0.945	0.055	1.448E-03	8.375E-05
20	1.080E-03	6.265E-03	20.086	0.953	0.047	1.029E-03	5.123E-05
21	7.599E-04	4.407E-03	23.336	0.959	0.041	7.287E-04	3.122E-05
22	5.334E-04	3.093E-03	27.113	0.964	0.036	5.144E-04	1.897E-05
23	3.736E-04	2.167E-03	31.500	0.969	0.031	3.621E-04	1.150E-05
24	2.612E-04	1.515E-03	36.598	0.973	0.027	2.542E-04	6.947E-06

Table D.9: Distribution of Fischer-Tropsch products using ASF chain growth value of 0.67.

[a]Calculated via Anderson-Schulz-Flory equation (Schulz, 1999).
[b]Paraffin/olefin ratio is a function of carbon number n and is determined to be e^0.15n for Co catalyst. Assume similar behavior in iron slurry catalyst (Shi and Davis, 2005).

		Normalized Scores[a]								Combined Impact Score
Chemical Species[b]	Wt. Frac	HTPI	TTP	HTPE	ATP	GWP	ODP	PCOP	AP	
Methanol	1.00E-02	6.67E-02	6.67E-02	9.15E-04	1.38E-05	0	0	2.13E-01	0	3.47E-01
Ethanol	5.50E-01	4.20E-02	4.20E-02	1.25E-04	2.86E-05	0	0	4.69E-01	0	5.53E-01
Propanol[c]	4.40E-01	2.01E-01	2.01E-01	4.76E-04	8.69E-05	0	0	7.74E-01	0	1.18E+00
Total mixed alcohol scores		1.12E-01	1.12E-01	2.87E-04	5.41E-05	0	0	6.01E-01	0	8.25E-01

Table D.10: WAR score breakdown for mixed-alcohol product.

[a]All scores taken from EPA WAR GUI, build 1.0.17 in 2008. All weights set to 1.
[b]Mixed alcohol breakdown given by Larson, Consomi et al. (Vol. 1, 2006), Table 30 on Page 114. Larson notes that there is some water in the mixed alcohol product, but does not quantify how much. Assume negligible since impact scores for water are near zero.
[c]Assume 1-propanol.

1. Assume all ash/chloride bonds with K to form 1.766 mol/sec KCl				
	Mole flow, kmol/sec	Division by lowest nonwater mole flow		
C	0.781	63.613		
H	1.045	85.058		
O	0.656	53.413		
H2O	0.395	n/a		
Na	0.248	20.189		
S	0.038	3.085		
K	0.012	1.000		
2. Assume all remaining K bonds with O and H to form 12.28 mol/sec KOH				
C	0.781	20.618		
H	1.032	27.244		
O	0.644	16.988		
H2O	0.395	n/a		
Na	0.248	6.544		
S	0.038	1.000		
3. Assume all remaining S bonds with Na and H2O to form 37.89 mol/sec Na2S*9H2O				
C	0.781	4.538		
H	1.032	5.996		
O	0.994	5.776		
H2O	0.054	n/a		
Na	0.172	1.000		
4. Assume all remaining Na bonds with O to form 86.06 mol/sec Na2O				
	Mole flow, kmol/sec	Division by lowest nonwater mole flow	Multiplier	
C	0.781	1	6	6
H	1.032	1.321384215	6	7.9283
O	0.908	1.162699154	6	6.9762
H2O	0.054	n/a		
5. Assume citric acid may be used to model remaining C, H, and O at total of 130.2 mol/s C6H8O7				
Final estimation of black liquor for WAR algorithm input purposes:				
	mol/s	MW	kg/s	wt. frac.
KCl	1.77	74.55	0.132	0.0032
KOH	12.28	55.20	0.678	0.0164
Na2S* 9H2O	37.89	240.14	9.099	0.2207
Na2O	86.06	61.98	5.334	0.1294
H2O	54.00	18.01	0.973	0.0236
Citric acid (C6H8O7)	130.20	192.10	25.011	0.6067

Table D.11: Estimation of black liquor composition for determining baseline WAR scores. Work is needed to accurately determine atmospheric and toxicological data in order to assess the environmental impact of black liquor.

		Normalized Scores[a]								Combined Impact Score
Chemical Species[b]	Wt. Frac.	HTPI	TTP	HTPE	ATP	GWP	ODP	PCOP	AP	
KCl	3.19E-03	1.45E-01	1.45E-01	0.00E+00	4.50E-04	0	0	0	0	2.90E-01
KOH	1.64E-02	1.38E+00	1.38E+00	1.19E-01	4.95E-03	0	0	0	0	2.88E+00
Na2S* 9H2O	2.21E-01	1.81E+00	1.81E+00	0.00E+00	1.69E-03	0	0	0	0	3.62E+00
Na2O	1.29E-01	1.06E-01	1.06E-01	1.19E-01	3.17E-03	0	0	0	0	3.34E-01
H2O	2.36E-02	0.00E+00	0.00E+00	0.00E+00	0.00E+00	0	0	0	0	0.00E+00
Citric acid (C6H8O7)	6.07E-01	5.58E-02	5.58E-02	0.00E+00	1.43E-03	0	0	0	0	1.13E-01
Total black liquor scores		4.70E-01	4.70E-01	1.74E-02	1.73E-03	0	0	0	0	9.59E-01

Table D.12: WAR score breakdown of black liquor in particular case study.

[a]All scores taken from EPA WAR GUI, build 1.0.17 in 2008.
[b]Atomic breakdown of black liquor given in Larson, Consomi et al. (Vol. 1, 2006). See Table D.11 for approximation of weight fractions.

Appendix E

Impact and Pareto-Optimal Data for Black Liquor Gasification

New Tomlinson Process	lb pollutant/ MMBTU HHV input into bark boiler[a]	*HHV in MMBTU/lb of wood[b]	lb pollutant / lb wood input (or kg)	Wood input into bark boiler, lb/s[c]	lb/s pollutant out of bark boiler
VOC	0.0130	4.300E-03	5.590E-05	15.74	8.799E-04
CO	0.6000	4.300E-03	2.580E-03	15.74	4.061E-02
NOx	0.2200	4.300E-03	9.460E-04	15.74	1.489E-02
PM10	0.0540	4.300E-03	2.322E-04	15.74	3.655E-03
SOx	0.0698	4.300E-03	3.001E-04	15.74	4.724E-03
CO2	213	4.300E-03	9.159E-01	15.74	1.442E+01
TRS	0.0000	4.300E-03	0.000E+00	15.74	0.000E+00

New Tomlinson Process	lb pollutant/ MMBTU HHV input into Tomlinson[a]	*HHV in MMBTU/lb of black liquor solids[b]	lb pollutant / lb BLS input (or kg)	BLS input into Tomlinson boiler, lb/s[d]	lb/s pollutant out of Tomlinson boiler	Total lb/s pollutant out of Tomlinson process
VOC	0.0134	0.005974	8.005E-05	69.44	5.559E-03	6.439E-03
CO	0.0940	0.005974	5.616E-04	69.44	3.900E-02	7.961E-02
NOx	0.1544	0.005974	9.224E-04	69.44	6.405E-02	7.895E-02
PM10	0.0477	0.005974	2.850E-04	69.44	1.979E-02	2.344E-02
SOx	0.0215	0.005974	1.284E-04	69.44	8.920E-03	1.364E-02
CO2	205	0.005974	1.225E+00	69.44	8.505E+01	9.946E+01
TRS	0.0034	0.005974	2.031E-05	69.44	1.411E-03	1.411E-03

New Tomlinson Process	Primary output: klb steam per second[e]	lb/s pollutant per klb/s steam	kg/s pollutant per klb/s steam	WAR scores of pollutants, PEI/kg[f]	PEI per klb/s steam
VOC	0.2260	2.849E-02	1.292E-02	4.331E+00	5.598E-02
CO	0.2260	3.522E-01	1.598E-01	2.133E-02	3.408E-03
NOx	0.2260	3.493E-01	1.584E-01	2.579E+00	4.086E-01
PM10	0.2260	1.037E-01	4.705E-02	7.194E+00	3.385E-01
SOx	0.2260	6.037E-02	2.738E-02	1.149E+00	3.147E-02
CO2	0.2260	4.401E+02	1.996E+02	2.705E-04	5.400E-02
TRS	0.2260	6.241E-03	2.831E-03	1.819E+00	5.149E-03
	Total emissions of PEI generated per klb/s steam:				0.8971

Table E.1: PEI of emissions generated per klb/s steam for new Tomlinson boiler.

[a]From Larson, Consommi et al. (Vol 3, 2006), Table 1 on page 2. Lime kiln left out of all factor calculations since this equipment is common to all processes and has the same impact regardless of what is being made.
[b]From Larson, Consommi et al. (Vol. 1, 2006), Table 5 on Page 15.
[c]From Larson, Consommi et al. (Vol. 1, 2006), Table 5 on Page 15, 340 bone dry short tons hog fuel enter Tomlinson process bark boiler every day. At 50% moisture, converted to 680 wet tons/day. Converted to 2000 lb/short ton and divided 24*60*60 seconds per day.
[d]From Larson, Consommi et al. (Vol. 1, 2006), Table 5 on Page 15, 6 million lb/day of black liquor solids enter Tomlinson boiler every day. Divided 24*60*60 seconds per day.
[e]From Table C.6.
[f]From Table D.1.

BLGCC	lb pollutant /MMBTU HHV input into barkboiler[a]	*HHV in MMBTU/lb of wood[b]	lb pollutant / lb wood input (or kg)	Wood input into bark boiler, lb/s[c]	total lb/s pollutant out of bark boiler
VOC	0.0130	4.300E-03	5.590E-05	1.468E+01	8.204E-04
CO	0.6000	4.300E-03	2.580E-03	1.468E+01	3.786E-02
NOx	0.2200	4.300E-03	9.460E-04	1.468E+01	1.388E-02
PM10	0.0540	4.300E-03	2.322E-04	1.468E+01	3.408E-03
SOx	0.0698	4.300E-03	3.001E-04	1.468E+01	4.405E-03
CO2	213	4.300E-03	9.159E-01	1.468E+01	1.344E+01
TRS	0.0000	4.300E-03	0.000E+00	1.468E+01	0.000E+00

Humidified syngas breakdown[d]	CO	H2	H2O	
Mass Fraction[e]	3.406E-01	3.559E-01	3.035E-01	Total
HHV in MMBTU/lb	2.215E-02	2.966E-01	0.000E+00	1.131E-01

Humidified syngas + natural gas breakdown	Syngas	Natural Gas	
Mass Fraction[f]	8.646E-01	1.354E-01	Total
HHV in MMBTU/lb	1.131E-01	2.360E-02	1.010E-01

BLGCC	lb pollutant /MMBTU HHV NG-syngas blend input into duct burner[a]	HHV in MMBTU/lb of natural gas-syngas blend	lb pollutant per lb NG-syngas blend	lb/s NG-syngas blend input into duct burner[g]	total lb/s pollutant coming out of duct burner
VOC	0.0054	0.1010	5.453E-04	4.263	2.325E-03
CO	0.0818	0.1010	8.261E-03	4.263	3.522E-02
Nox	0.0974	0.1010	9.836E-03	4.263	4.193E-02
PM10	0.0074	0.1010	7.473E-04	4.263	3.186E-03
SOX	0.0004	0.1010	4.039E-05	4.263	1.722E-04
CO2	169	0.1010	1.707E+01	4.263	7.276E+01
TRS	0.0000	0.1010	0.000E+00	4.263	0.000E+00

BLGCC	lb pollutant /MMBTU HHV input into gas turbine[a]	HHV in MMBTU/lb of humidified syngas	lb pollutant per lb humid syngas	lb/s syngas input into gas turbine[h]	total lb/s pollutant coming out of gas turbine	total lb/s pollutant out of BLGCC process
VOC	0.0021	0.1131	2.375E-04	65.55	1.557E-02	1.872E-02
CO	0.0330	0.1131	3.732E-03	65.55	2.447E-01	3.178E-01
Nox	0.0897	0.1131	1.015E-02	65.55	6.651E-01	7.209E-01
PM10	0.0066	0.1131	7.465E-04	65.55	4.894E-02	5.553E-02
SOX	0.0000	0.1131	0.000E+00	65.55	0.000E+00	4.577E-03
CO2	221	0.1131	2.500E+01	65.55	1.639E+03	1.725E+03
TRS	0	0.1131	0.000E+00	65.55	0.000E+00	0.000E+00

BLGCC	Primary output: MWh electricity generated per second[i]	lb/s pollutant per MWh/s electricity	kg/s pollutant per MWh/s electricity	WAR scores of pollutants, PEI/kg[j]	PEI per MWh/s electricity
VOC	0.0317	5.904E-01	2.678E-01	4.331E+00	1.160E+00
CO	0.0317	1.002E+01	4.547E+00	2.133E-02	9.698E-02
NOx	0.0317	2.274E+01	1.032E+01	2.579E+00	2.660E+01
PM10	0.0317	1.752E+00	7.946E-01	7.194E+00	5.716E+00
SOx	0.0317	1.444E-01	6.549E-02	1.149E+00	7.527E-02
CO2	0.0317	5.441E+04	2.468E+04	2.705E-04	6.676E+00
TRS	0.0317	0.000E+00	0.000E+00	1.819E+00	0.000E+00
	Total emissiosn of PEI generated per MWh/s electricity:				40.33

Table E.2: PEI of emissions generated per MWh/s steam for BLGCC process.

[a]From Larson, Consommi et al. (Vol. 3, 2006), Table 2 on page 2. Lime kiln left out of all factor calculations since this equipment is common to all processes and has the same impact regardless of what is being made.
[b]From Larson, Consommi et al. (Vol. 1, 2006), Table 5 on Page 15.

[c]From Larson, Consommi et al. (Vol. 1, 2006), Table 5 on Page 15, 317 bone dry short tons hog fuel enter Polysulfide BLGCC bark boiler every day. At 50% moisture, converted to 634 wet tons/day. Converted to 2000 lb/short ton and divided 24*60*60 seconds per day.
[d]From Larson, Consommi et al. (Vol. 1, 2006), Figure 9 on Page 20, syngas is humidified before entering gas turbine and duct burner.
[e]Assume H2/CO ratio from Larson, Consommi et al. (Vol. 1, 2006) of 1.045 holds for dry syngas. From Larson, Consommi et al. (Vol. 1, 2006), Figure 9 on page 20, the Saturator unit adds 9.5 kg/s of water to dry syngas for a total clean wet syngas flow of 31.3 kg/s.
[f]From Larson, Consommi et al. (Vol. 1, 2006), Figure 9 on Page 20, mass flow rates into duct burner.
[g]From Larson, Consommi et al. (Vol. 1, 2006), Figure 9 on Page 20, 1.92 kg/s total fuel flow into duct burner converted to lb/s.
[h]From Larson, Consommi et al. (Vol. 1, 2006), Figure 9 on Page 20, 29.73 kg/s total fuel flow into gas turbine converted to lb/s.
[i]See Table C.6.
[j]See Table D.1.

Dry syngas breakdown	CO	H2	
Mass Fraction[a]	4.890E-01	5.110E-01	Total
HHV in MMBTU/lb	2.215E-02	2.966E-01	1.624E-01

Syngas + Hog Fuel breakdown[b]	Syngas	Hog Fuel	
Mass Fraction[c]	6.983E-01	3.017E-01	Total
HHV in MMBTU/lb	1.624E-01	4.300E-03	1.147E-01

DMEa	lb pollutant /MMBTU HHV input into bark boiler[d]	*HHV in MMBTU/lb of syngas + hog fuel[e]	lb pollutant / lb wood + syngas input (or kg)	Wood + syngas input into bark boiler, lb/s[f]	total lb/s pollutant out of bark boiler
VOC	0.0130	0.1147	1.491E-03	51.16	7.628E-02
CO	0.6000	0.1147	6.882E-02	51.16	3.521E+00
NOx	0.2200	0.1147	2.523E-02	51.16	1.291E+00
PM10	0.0540	0.1147	6.193E-03	51.16	3.169E-01
SOx	0.1141	0.1147	1.309E-02	51.16	6.695E-01
CO2	265	0.1147	3.039E+01	51.16	1.555E+03
TRS	0.0000	0.1147	0.000E+00	51.16	0.000E+00

DMEa	Primary output: gal/s of DME[g]	lb/s pollutant per gal/s DME	kg/s pollutant per gal/s DME	WAR scores of pollutants, PEI/kg[h]	Total PEI per gal/s DME
VOC	2.3110	3.301E-02	1.497E-02	4.331E+00	6.485E-02
CO	2.3110	1.523E+00	6.910E-01	2.133E-02	1.474E-02
NOx	2.3110	5.586E-01	2.534E-01	2.579E+00	6.534E-01
PM10	2.3110	1.371E-01	6.219E-02	7.194E+00	4.474E-01
SOx	2.3110	2.897E-01	1.314E-01	1.149E+00	1.510E-01
CO2	2.3110	6.728E+02	3.052E+02	2.705E-04	8.256E-02
TRS	2.3110	0.000E+00	0.000E+00	1.819E+00	0.000E+00
	Total emissions of PEI generated per gal/s DME:				1.414

Table E.3: PEI of emissions generated per gal/s DME for DMEa process.

[a]Assume H2/CO ratio from Larson, Consommi et al. (Vol. 1, 2006) of 1.045 holds for dry syngas. From Larson, Consommi et al. (Vol. 1, 2006), Figure 9 on page 20, the Saturator unit adds 9.5 kg/s of water to dry syngas for a total clean wet syngas flow of 31.3 kg/s.
[b]From Larson, Consommi et al. (Vol. 1, 2006), Figure 23 on Page 45, unconverted syngas is combined with hog fuel for input into bark boiler.
[c]From Larson, Consommi et al. (Vol. 1, 2006), Figure 23 on Page 45, from mass flow rates into bark boiler for syngas and biomass.
[d]From Larson, Consommi et al. (Vol. 3, 2006), Table 3 on page 2. Lime kiln left out of all factor calculations since this equipment is common to all processes.

[e]From Larson, Consommi et al. (Vol. 1, 2006), Table 5 on Page 15.
[f]From Larson, Consommi et al. (Vol. 1, 2006), Figure 23 on Page 45, from mass flow rates into bark boiler for syngas and biomass. Converted from kg/s to lb/s.
[g]See Table C.6.
[h]See Table D.1.

DMEb	lb pollutant/MMBTU HHV syngas input into duct burner[a]	HHV in MMBTU/lb of syngas[b]	lb pollutant per lb syngas	lb/s syngas input into duct burner[c]	total lb/s pollutant coming out of duct burner
VOC	0.0054	0.1624	8.769E-04	16.320	1.431E-02
CO	0.0818	0.1624	1.328E-02	16.320	2.168E-01
NOx	0.0974	0.1624	1.582E-02	16.320	2.581E-01
PM10	0.0074	0.1624	1.202E-03	16.320	1.961E-02
SOx	0.0000	0.1624	0.000E+00	16.320	0.000E+00
CO2	474	0.1624	7.698E+01	16.320	1.256E+03
TRS	0.0000	0.1624	0.000E+00	16.320	0.000E+00

DMEb	lb pollutant/MMBTU HHV input into gas turbine[a]	HHV in MMBTU/lb of syngas[b]	lb pollutant per lb syngas	lb/s syngas input into gas turbine[d]	total lb/s pollutant coming out of gas turbine	total lb/s pollutant out of DMEb process
VOC	0.0021	0.1624	3.410E-04	71.00	2.421E-02	3.852E-02
CO	0.0330	0.1624	5.359E-03	71.00	3.805E-01	5.973E-01
NOx	0.0897	0.1624	1.457E-02	71.00	1.034E+00	1.292E+00
PM10	0.0066	0.1624	1.072E-03	71.00	7.610E-02	9.571E-02
SOX	0.0895	0.1624	1.453E-02	71.00	1.032E+00	1.032E+00
CO2	240	0.1624	3.897E+01	71.00	2.767E+03	4.023E+03
TRS	0	0.1624	0.000E+00	71.00	0.000E+00	0.000E+00

DMEb	Primary output: gal/s of DME[e]	lb/s pollutant per gal/s DME	kg/s pollutant per gal/s DME	WAR scores of pollutants, PEI/kg[f]	PEI per gal/s DME
VOC	2.3110	1.667E-02	7.561E-03	4.331E+00	3.275E-02
CO	2.3110	2.585E-01	1.172E-01	2.133E-02	2.501E-03
NOx	2.3110	5.592E-01	2.537E-01	2.579E+00	6.542E-01
PM10	2.3110	4.142E-02	1.879E-02	7.194E+00	1.351E-01
SOx	2.3110	4.465E-01	2.025E-01	1.149E+00	2.328E-01
CO2	2.3110	1.741E+03	7.897E+02	2.705E-04	2.136E-01
TRS	2.3110	0.000E+00	0.000E+00	1.819E+00	0.000E+00
	Total emissions of PEI generated per gal/s DME:				1.271

Table E.4: PEI of emissions generated per gal/s DME for DMEb process.

[a]From Larson, Consommi et al. (Vol. 3, 2006), Table 4 on page 3. Lime kiln left out of all factor calculations since this equipment is common to all processes and has the same impact regardless of what is being made.
[b]See Table E.3.
[c]From Larson, Consommi et al. (Vol. 1, 2006), Figure 24 on Page 46, 7.4kg/s total fuel flow into duct burner converted to lb/s.
[d]From Larson, Consommi et al. (Vol. 1, 2006), Figure 24 on Page 46, 32.2 kg/s total fuel flow into gas turbine converted to lb/s.
[e]See Table C.6.
[f]See Table D.1.

DMEc	lb pollutant/MMBTU HHV syngas input into duct burner[a]	HHV in MMBTU/lb of syngas[b]	lb pollutant per lb syngas	lb/s syngas input into duct burner[c]	total lb/s pollutant coming out of duct burner
VOC	0.0054	0.1624	8.769E-04	8.159	7.154E-03
CO	0.0818	0.1624	1.328E-02	8.159	1.084E-01
NOx	0.0974	0.1624	1.582E-02	8.159	1.290E-01
PM10	0.0074	0.1624	1.202E-03	8.159	9.804E-03
SOx	0.0000	0.1624	0.000E+00	8.159	0.000E+00
CO2	237	0.1624	3.849E+01	8.159	3.140E+02
TRS	0.0000	0.1624	0.000E+00	8.159	0.000E+00

DMEc	lb pollutant/MMBTU HHV input into gas turbine[a]	HHV in MMBTU/lb of syngas[b]	lb pollutant per lb syngas	lb/s syngas input into gas turbine[d]	total lb/s pollutant coming out of gas turbine	total lb/s pollutant out of DMEc process
VOC	0.0021	0.1624	3.410E-04	56.23	1.918E-02	2.633E-02
CO	0.0330	0.1624	5.359E-03	56.23	3.013E-01	4.097E-01
NOx	0.0897	0.1624	1.457E-02	56.23	8.191E-01	9.481E-01
PM10	0.0066	0.1624	1.072E-03	56.23	6.026E-02	7.007E-02
SOx	0.0895	0.1624	1.453E-02	56.23	8.172E-01	8.172E-01
CO2	240	0.1624	3.897E+01	56.23	2.191E+03	2.505E+03
TRS	0	0.1624	0.000E+00	56.23	0.000E+00	0.000E+00

DMEc	Primary output: gal/s of DME[e]	lb/s pollutant per gal/s DME	kg/s pollutant per gal/s DME	WAR scores of pollutants, PEI/kg[f]	PEI per gal/s DME
VOC	1.0210	2.579E-02	1.170E-02	4.331E+00	5.067E-02
CO	1.0210	4.013E-01	1.820E-01	2.133E-02	3.882E-03
NOx	1.0210	9.286E-01	4.212E-01	2.579E+00	1.086E+00
PM10	1.0210	6.863E-02	3.113E-02	7.194E+00	2.239E-01
SOx	1.0210	8.004E-01	3.631E-01	1.149E+00	4.173E-01
CO2	1.0210	2.454E+03	1.113E+03	2.705E-04	3.011E-01
TRS	1.0210	0.000E+00	0.000E+00	1.819E+00	0.000E+00
	Total emissions of PEI generated per gal/s DME:				2.083

Table E.5: PEI of emissions generated per gal/s DME for DMEc process.

[a]From Larson, Consommi et al. (Vol. 3, 2006), Table 5 on page 3. Lime kiln left out of all factor calculations since this equipment is common to all processes and has the same impact regardless of what is being made.
[b]See Table E.3.
[c]From Larson, Consommi et al. (Vol. 1, 2006), Figure 25 on Page 47, 3.7 kg/s total fuel flow into duct burner converted to lb/s.

[d]From Larson, Consommi et al. (Vol. 1, 2006), Figure 25 on Page 47, 25.5 kg/s total fuel flow into duct burner converted to lb/s.
[e]See Table C.6.
[f]See Table D.1.

FTa	lb pollutant /MMBTU HHV syngas input into duct burner[a]	HHV in MMBTU/lb of syngas[b]	lb pollutant per lb syngas	lb/s syngas input into duct burner[c]	total lb/s pollutant coming out of duct burner
VOC	0.0054	0.1624	8.769E-04	2.205	1.934E-03
CO	0.0818	0.1624	1.328E-02	2.205	2.929E-02
NOx	0.0974	0.1624	1.582E-02	2.205	3.488E-02
PM10	0.0074	0.1624	1.202E-03	2.205	2.650E-03
SOx	0.0956	0.1624	1.552E-02	2.205	3.423E-02
CO2	325	0.1624	5.278E+01	2.205	1.164E+02
TRS	0.0000	0.1624	0.000E+00	2.205	0.000E+00

FTa	lb pollutant /MMBTU HHV input into gas turbine[a]	HHV in MMBTU/lb of syngas[b]	lb pollutant per lb syngas	lb/s syngas input into gas turbine[d]	total lb/s pollutant coming out of gas turbine	total lb/s pollutant out of FTa process
VOC	0.0021	0.1624	3.410E-04	63.95	2.181E-02	2.374E-02
CO	0.0330	0.1624	5.359E-03	63.95	3.427E-01	3.720E-01
NOx	0.0897	0.1624	1.457E-02	63.95	9.315E-01	9.664E-01
PM10	0.0066	0.1624	1.072E-03	63.95	6.854E-02	7.119E-02
SOx	0.1069	0.1624	1.736E-02	63.95	1.110E+00	1.144E+00
CO2	272	0.1624	4.417E+01	63.95	2.825E+03	2.941E+03
TRS	0	0.1624	0.000E+00	63.95	0.000E+00	0.000E+00

FTa	Primary output: gal/s of FT[e]	lb/s pollutant per gal/s FT	kg/s pollutant per gal/s FT	WAR scores of pollutants, PEI/kg[f]	PEI per gal/s FT
VOC	0.9440	2.515E-02	1.141E-02	4.331E+00	4.941E-02
CO	0.9440	3.940E-01	1.787E-01	2.133E-02	3.812E-03
NOx	0.9440	1.024E+00	4.643E-01	2.579E+00	1.197E+00
PM10	0.9440	7.541E-02	3.420E-02	7.194E+00	2.461E-01
SOx	0.9440	1.212E+00	5.498E-01	1.149E+00	6.319E-01
CO2	0.9440	3.115E+03	1.413E+03	2.705E-04	3.822E-01
TRS	0.9440	0.000E+00	0.000E+00	1.819E+00	0.000E+00
	Total emissions of PEI generated per gal/s FT:				2.511

Table E.6: PEI of emissions generated per gal/s FT oil for FTa process.

[a]From Larson, Consommi et al. (Vol. 3, 2006) Table 6 on page 3. Lime kiln left out of all factor calculations since this equipment is common to all processes and has the same impact regardless of what is being made.
[b]See Table E.3.
[c]From Larson, Consommi et al. (Vol. 1, 2006), Figure 26 on Page 48, 1.0 kg/s total fuel flow into duct burner converted to lb/s.
[d]From Larson, Consommi et al. (Vol. 1, 2006), Figure 26 on Page 48, 29.0 kg/s total fuel flow into duct burner converted to lb/s.
[e]See Table C.6.
[f]See Table D.1.

FTb	lb pollutant /MMBTU HHV input into gas turbine[a]	HHV in MMBTU/lb of syngas[b]	lb pollutant per lb syngas	lb/s syngas input into gas turbine[c]	total lb/s pollutant coming out of gas turbine
VOC	0.0021	0.1624	3.410E-04	143.10	4.880E-02
CO	0.0330	0.1624	5.359E-03	143.10	7.669E-01
NOx	0.0897	0.1624	1.457E-02	143.10	2.085E+00
PM10	0.0066	0.1624	1.072E-03	143.10	1.534E-01
SOx	0.1319	0.1624	2.142E-02	143.10	3.065E+00
CO2	259	0.1624	4.206E+01	143.10	6.019E+03
TRS	0	0.1624	0.000E+00	143.10	0.000E+00

FTb	Primary output: gal/s of FT[d]	lb/s pollutant per gal/s FT	kg/s pollutant per gal/s FT	WAR scores of pollutants, PEI/kg[e]	PEI per gal/s FT
VOC	0.9440	5.170E-02	2.345E-02	4.331E+00	1.016E-01
CO	0.9440	8.124E-01	3.685E-01	2.133E-02	7.860E-03
NOx	0.9440	2.208E+00	1.002E+00	2.579E+00	2.583E+00
PM10	0.9440	1.625E-01	7.370E-02	7.194E+00	5.302E-01
SOx	0.9440	3.247E+00	1.473E+00	1.149E+00	1.693E+00
CO2	0.9440	6.376E+03	2.892E+03	2.705E-04	7.823E-01
TRS	0.9440	0.000E+00	0.000E+00	1.819E+00	0.000E+00
	Total PEI of emissions generated per gal/s FT:				5.698

Table E.7: PEI of emissions generated per gal/s FT oil for FTb process.

[a]From Larson, Consommi et al. (Vol. 3, 2006), Table 7 on page 3. Lime kiln left out of all factor calculations since this equipment is common to all processes and has the same impact regardless of what is being made.
[b]See Table E.3.
[c]From Larson, Consommi et al. (Vol. 3, 2006), Figure 27 on Page 49, 64.9 kg/s total fuel flow into duct burner converted to lb/s.
[d]See Table C.6.
[e]See Table D.1.

Humidified syngas breakdown[a]	CO	H2	H2O	
Mass Fraction[b]	3.566E-01	3.727E-01	2.707E-01	Total
HHV in MMBTU/lb	2.215E-02	2.966E-01	0.000E+00	1.184E-01

FTc	lb pollutant /MMBTU HHV input into gas turbine[c]	HHV in MMBTU /lb of humid syngas	lb pollutant per lb syngas	lb/s syngas input into gas turbine[d]	total lb/s pollutant coming out of gas turbine
VOC	0.0021	0.1184	2.487E-04	87.98	2.188E-02
CO	0.0330	0.1184	3.908E-03	87.98	3.439E-01
NOx	0.0897	0.1184	1.062E-02	87.98	9.347E-01
PM10	0.0066	0.1184	7.817E-04	87.98	6.877E-02
SOx	0.0000	0.1184	0.000E+00	87.98	0.000E+00
CO2	322	0.1184	3.814E+01	87.98	3.355E+03
TRS	0	0.1184	0.000E+00	87.98	0.000E+00

FTc	Primary output: gal/s of FT[e]	lb/s pollutant per gal/s FT	kg/s pollutant per gal/s FT	WAR scores of pollutants, PEI/kg[f]	PEI per gal/s FT
VOC	2.8990	7.548E-03	3.424E-03	4.331E+00	1.483E-02
CO	2.8990	1.186E-01	5.380E-02	2.133E-02	1.148E-03
NOx	2.8990	3.224E-01	1.462E-01	2.579E+00	3.772E-01
PM10	2.8990	2.372E-02	1.076E-02	7.194E+00	7.741E-02
SOx	2.8990	0.000E+00	0.000E+00	1.149E+00	0.000E+00
CO2	2.8990	1.157E+03	5.250E+02	2.705E-04	1.420E-01
TRS	2.8990	0.000E+00	0.000E+00	1.819E+00	0.000E+00
	Total emissions of PEI generated per gal/s FT:				0.613

Table E.8: PEI of emissions generated per gal/s FT oil for FTc process.

[a]From Larson, Consommi et al. (Vol. 1, 2006), Figure 28 on Page 50, syngas is humidified before entering gas turbine.
[b]Assume H2/CO ratio of 1.045 holds for dry syngas. From Larson, Consommi et al. (Vol. 1, 2006), Figure 28 on page 50, the Saturator unit adds 10.8 kg/s of water to dry syngas for a total clean wet syngas flow of 39.9 kg/s.
[c]From Larson, Consommi et al. (Vol. 3, 2006), Table 8 on page 4. Lime kiln left out of all factor calculations since this equipment is common to all processes and has the same impact regardless of what is being made.
[d]From Larson, Consommi et al. (Vol. 1, 2006), Figure 28 on Page 50, 39.9 kg/s total fuel flow into gas turbine converted to lb/s.
[e]See Table C.6.
[f]See Table D.1.

MA	lb pollutant /MMBTU HHV syngas input into duct burner[a]	HHV in MMBTU/lb of dry syngas[b]	lb pollutant per lb syngas	lb/s syngas input into duct burner[c]	total lb/s pollutant coming out of duct burner
VOC	0.0021	0.1624	3.410E-04	6.174	2.106E-03
CO	0.0330	0.1624	5.359E-03	6.174	3.309E-02
NOx	0.0897	0.1624	1.457E-02	6.174	8.994E-02
PM10	0.0066	0.1624	1.072E-03	6.174	6.617E-03
Sox	0.1667	0.1624	2.707E-02	6.174	1.671E-01
CO2	259	0.1624	4.206E+01	6.174	2.597E+02
TRS	0.0000	0.1624	0.000E+00	6.174	0.000E+00

Humidified Syngas breakdown[d]	CO	H2	H2O	
Mass Fraction[e]	3.833E-01	4.006E-01	2.161E-01	Total
HHV in MMBTU/lb	2.215E-02	2.966E-01	0.000E+00	1.273E-01

MA	lb pollutant /MMBTU HHV input into gas turbine[a]	HHV in MMBTU/lb of humid syngas	lb pollutant per lb syngas	lb/s syngas input into gas turbine[f]	total lb/s pollutant coming out of gas turbine	total lb/s pollutant out of MA process
VOC	0.0021	0.1273	2.673E-04	84.67	2.264E-02	2.474E-02
CO	0.0330	0.1273	4.201E-03	84.67	3.557E-01	3.888E-01
NOx	0.0897	0.1273	1.142E-02	84.67	9.669E-01	1.057E+00
PM10	0.0066	0.1273	8.402E-04	84.67	7.114E-02	7.776E-02
Sox	0.0000	0.1273	0.000E+00	84.67	0.000E+00	1.671E-01
CO2	303	0.1273	3.857E+01	84.67	3.266E+03	3.526E+03
TRS	0	0.1273	0.000E+00	84.67	0.000E+00	0.000E+00

MA	Primary output: gal/s of MA[g]	lb/s pollutant per gal/s MA	kg/s pollutant per gal/s MA	WAR scores of pollutants, PEI/kg[h]	lb/s of env impact per gal/s MA
VOC	0.5590	4.426E-02	2.008E-02	4.331E+00	8.696E-02
CO	0.5590	6.955E-01	3.155E-01	2.133E-02	6.729E-03
NOx	0.5590	1.890E+00	8.575E-01	2.579E+00	2.211E+00
PM10	0.5590	1.391E-01	6.309E-02	7.194E+00	4.539E-01
Sox	0.5590	2.990E-01	1.356E-01	1.149E+00	1.559E-01
CO2	0.5590	6.307E+03	2.861E+03	2.705E-04	7.739E-01
TRS	0.5590	0.000E+00	0.000E+00	1.819E+00	0.000E+00
	Total PEI of emissions generated per gal/s MA:				3.689

Table E.9: PEI of emissions generated per gal/s mixed alcohol for MA process.

[a]From Larson, Consommi et al. (Vol. 3, 2006), Table 9 on page 4. Lime kiln left out of all factor calculations since this equipment is common to all processes and has the same impact regardless of what is being made.
[b]See Table E.3.
[c]From Larson, Consommi et al. (Vol. 1, 2006), Figure 29 on Page 51, 2.8 kg/s total fuel flow into duct burner converted to lb/s.
[d]From Larson, Consommi et al. (Vol. 1, 2006), Figure 29 on Page 51, syngas is humidified before entering gas turbine.
[e]Assume H2/CO ratio of 1.045 holds for dry syngas. From Larson, Consommi et al. (Vol. 1, 2006), Figure 29 on page 51, the Saturator unit adds 8.3 kg/s of water to dry syngas for a total clean wet syngas flow of 38.4 kg/s.
[f]From Larson, Consommi et al. (Vol. 1, 2006), Figure 29 on Page 51, 38.4 kg/s total fuel flow into duct burner converted to lb/s.
[g]See Table C.6.
[h]See Table D.1.

Opt. Run	Optimized Product Flow	Change from previous runs	GP, $/s	PEI/s	PEI norm
1	FTc: 2.898 gal/s FT fuel, .214 Klb/s steam, .021 MWh/s electricity	N/A	1.338	-21.707	0
2	FTb: 0.943 gal/s FT fuel, .214 Klb/s steam, .064 MWh/s electricity	No FTc	0.487	-25.41	-3.703
3	DMEb: 2.311 gal/s DME fuel, 0.214 Klb/s steam, 0.024 MWh/s electricity	No FTc or FTb	0.024	-29.581	-7.874
4	DMEa: 2.311 gal/s DME fuel, 0.214 Klb/s steam, neg electricity	No FTc, FTb, or DMEb	-0.22	-29.193	-7.486
5	FTa: 0.943 gal/s FT fuel, 0.214 Klb/s steam, 0.024 MWh/s electricity	No FTc, FTb, DMEb, or DMEa	-0.23	-28.324	-6.617
6	DMEc: 1.020 gal/s DME fuel, 0.214 Klb/s, 0.025 MWh/s electricity	No FTc, FTb, DMEb, DMEa, or FTa	-0.55	-31.317	-9.61
7	BLGCC: 0.214 Klb/s steam, 0.032 MWh/s electricity	No FTc, FTb, DMEb, DMEa, FTa, or DMEc	-0.62	-32.909	-11.2
8	NewTom: 0.205 Klb/s steam, 0.016 MWh/s electricity	No FTc, FTb, DMEb, DMEa, FTa, DMEc, or BLGCC	-0.81	-33.968	-12.26
9	MA: 0.559 gal/s MA fuel, 0.214 Klb/s steam, 0.026 MWh/s electricity	No FTc, FTb, DMEb, DMEa, FTa, DMEc, BLGCC, or NewTom	-0.95	-30.722	-9.015

Table E.10: Data for single process solution pareto curve of PEI versus profitability.

Opt. Run	Optimized Product Flow	Change from previous runs	GP, $/s	PEI/s	PEI norm
1	FTc: 2.898 gal/s FT fuel, .214 Klb/s steam, .021 MWh/s electricity	N/A	1.310	-21.71	0.00
2	FTb: 0.094 gal/s FT fuel, 0.021 Klb/s steam, 0.006 MWh/s electricity FTc: 2.608 gal/s FT fuel, 0.192 Klb/s steam, 0.019 MWh/s electricity	Cap FTc FT fuel at 90% of Run 1 value: 2.608	1.243	-22.08	-0.37
3	DMEa: 0.076 gal/s DME, .007 Klb/s steam, neg electricity FTb: 0.158 gal/s FT fuel, 0.036 Klb/s steam, 0.011 MWh/s electricity FTc: 2.318 gal/s FT fuel, 0.171 Klb/s steam, 0.017 MWh/s electricity	Cap FTc FT fuel at 80% of Run 1 value: 2.318	1.144	-22.57	-0.87
4	DMEa: 0.229 gal/s DME, .021 Klb/s steam, neg electricity FTb: 0.189 gal/s FT fuel, 0.043 Klb/s steam, 0.013 MWh/s electricity FTc: 2.029 gal/s FT fuel, 0.150 Klb/s steam, 0.015 MWh/s electricity	Cap FTc FT fuel at 70% of Run 1 value: 2.029	1.013	-23.19	-1.49
5	DMEa: 0.383 gal/s DME, .035 Klb/s steam, neg electricity FTb: 0.221 gal/s FT fuel, 0.050 Klb/s steam, 0.015 MWh/s electricity FTc: 1.739 gal/s FT fuel, 0.128 Klb/s steam, 0.013 MWh/s electricity	Cap FTc FT fuel at 60% of Run 1 value: 1.739	0.881	-23.82	-2.11
6	DMEa: 0.536 gal/s DME, .050 Klb/s steam, neg electricity FTb: 0.253 gal/s FT fuel, 0.057 Klb/s steam, 0.017 MWh/s electricity FTc: 1.449gal/s FT fuel, 0.107 Klb/s steam, 0.011 MWh/s electricity	Cap FTc FT fuel at 50% of Run 1 value: 1.449	0.749	-24.44	-2.73
7	DMEa: 0.690 gal/s DME, 0.064 Klb/s steam, neg electricity FTb: 0.284 gal/s FT fuel, 0.064 Klb/s steam, 0.019 MWh/s electricity FTc: 1.159 gal/s FT fuel, 0.085 Klb/s steam, 0.009 MWh/s electricity	Cap FTc FT fuel at 40% of Run 1 value: 1.159	0.617	-25.06	-3.35
8	DMEa: 0.843 gal/s DME, .078 Klb/s steam, neg electricity FTb: 0.316 gal/s FT fuel, 0.072 Klb/s steam, 0.021 MWh/s electricity FTc: 0.869 gal/s FT fuel, 0.064 Klb/s steam, 0.006 MWh/s electricity	Cap FTc FT fuel at 30% of Run 1 value: 0.869	0.485	-25.68	-3.97
9	DMEa: 0.996 gal/s DME, 0.092 Klb/s steam, neg electricity FTb: 0.348 gal/s FT fuel, 0.079 Klb/s steam, 0.023 MWh/s electricity FTc: 0.580 gal/s FT fuel, 0.043 Klb/s steam, 0.004 MWh/s electricity	Cap FTc FT fuel at 20% of Run 1 value: 0.580	0.354	-26.30	-4.59
10	DMEa: 1.150 gal/s DME, .106 Klb/s steam, neg electricity FTb: 0.380 gal/s FT fuel, 0.086 Klb/s steam, 0.026 MWh/s electricity FTc: 0.290 gal/s FT fuel, 0.021 Klb/s steam, 0.002 MWh/s electricity	Cap FTc FT fuel at 10% of Run 1 value: 0.290	0.222	-26.92	-5.22
11	DMEa: 1.303 gal/s DME, 0.121 Klb/s steam, neg electricity FTb: 0.411 gal/s FT fuel, 0.093 Klb/s steam, 0.028 MWh/s electricity	No FTc	0.09	-27.54	-5.84
12	DMEa: 0.978 gal/s DME, 0.090 Klb/s steam, neg electricity DMEb: 0.527 gal/s DME fuel, 0.049 Klb/s steam, 0.006 MWh/s electricity FTb: 0.329 gal/s FT fuel, 0.075 Klb/s steam, 0.022 MWh/s electricity	No FTc, cap FTb FT fuel at 80% of Run 5 value: .329	0.083	-27.96	-6.25
13	DMEa: 0.653 gal/s DME, 0.060 Klb/s steam, neg electricity DMEb: 1.052 gal/s DME fuel, 0.097 Klb/s steam, 0.011 MWh/s electricity FTb: 0.247 gal/s FT fuel, 0.056 Klb/s steam, 0.017 MWh/s electricity	No FTc, cap FTb FT fuel at 60% of Run 5 value: .247	0.077	-28.38	-6.67
14	DMEa: 0.325 gal/s DME, 0.030 Klb/s steam, neg electricity DMEb: 1.584 gal/s DME fuel, 0.147 Klb/s steam, 0.017 MWh/s electricity FTb: 0.164 gal/s FT fuel, 0.037 Klb/s steam, 0.011 MWh/s electricity	No FTc, cap FTb FT fuel at 40% of Run 5 value: .164	0.071	-28.80	-7.10
15	DMEb: 2.109 gal/s DME fuel, 0.195 Klb/s steam, 0.022 MWh/s electricity FTb: 0.082 gal/s FT fuel, 0.019 Klb/s steam, 0.006 MWh/s electricity	No FTc, cap FTb FT fuel at 20% of Run 5 value: .082	0.064	-29.22	-7.51
16	DMEb: 2.311 gal/s DME fuel, 0.214 Klb/s steam, 0.024 MWh/s electricity	No FTc or FTb	0.009	-29.58	-7.87
17	DMEb: 1.849 gal/s DME fuel, 0.171 Klb/s steam, 0.020 MWh/s electricity FTa: 0.188 gal/s FT fuel, 0.043 Klb/s steam, 0.005 MWh/s electricity	No FTc or FTb, cap DMEb fuel at 80% of Run 11 value: 1.849	-0.035	-29.33	-7.62
18	DMEb: 1.387 gal/s DME fuel, 0.128 Klb/s steam, 0.015 MWh/s electricity FTa: 0.377 gal/s FT fuel, 0.085 Klb/s steam, 0.010 MWh/s electricity	No FTc or FTb, cap DMEb fuel at 60% of Run 11 value: 1.387	-0.091	-29.08	-7.37

19	DMEb: 0.924 gal/s DME fuel, 0.085 Klb/s steam, 0.010 MWh/s electricity FTa: 0.566 gal/s FT fuel, 0.128 Klb/s steam, 0.015 MWh/s electricity	No FTc or FTb, cap DMEb fuel at 40% of Run 11 value: 0.924	-0.141	-28.83	-7.12
20	DMEb: 0.462 gal/s DME fuel, 0.043 Klb/s steam, 0.005 MWh/s electricity FTa: 0.755 gal/s FT fuel, 0.171 Klb/s steam, 0.015 MWh/s electricity	No FTc or FTb, cap DMEb fuel at 20% of Run 11 value: 0.462	-0.191	-28.58	-6.87
21	FTa: 0.943 gal/s FT fuel, 0.214 Klb/s steam, 0.024 MWh/s electricity	No FTc, FTb, or DMEb	-0.241	-28.32	-6.62
22	DMEa: 2.311 gal/s DME fuel, 0.214 Klb/s steam, neg electricity	No FTc, FTb, DMEb, or FTa	-0.339	-29.19	-7.49

Table E.11: Data for split process solution pareto curve of PEI versus profitability.